12-2023

Quantifying impacts of climate change on headwater streamflow regime in Robinson Forest: Insights from 35-years of data collection.

Lauren Brown
University of Louisville

QUANTIFYING IMPACTS OF CLIMATE CHANGE ON HEADWATER STREAMFLOW REGIME IN ROBINSON FOREST: INSIGHTS FROM 35-YEARS OF DATA COLLECTION

By Lauren Brown

B.S. Civil & Environmental Engineering, 2022

A Thesis or Dissertation Submitted to the Faculty of the

J.B. Speed School of Engineering of the University of Louisville

In Partial Fulfillment of the Requirements For the Degree of

Master of Engineering In Civil & Environmental Engineering

Department of Civil & Environmental Engineering

University of Louisville

Louisville, Kentucky

December 2023

ACKNOWLEDGEMENTS

This research was only made possible through the help of several people. First and foremost, I would like to thank my Thesis Chair, Dr. Tyler Mahoney, for his constant support, encouragement, and guidance. Without Dr. Mahoney, this thesis would not have been written. I would also like to thank my Thesis Committee: Dr. Mark French and Dr. Andrew Day for their advice and assistance in my research. I would like to thank the University of Louisville's Department of Civil and Environmental Engineering for years of educational support as well as the USGS Annual Base Grant program for funding this research. I would also like to thank Steve, Michele, Carlea, and Lavender Brown as well as John Stumpf for their unwavering encouragement and support. Finally, I would like to thank Taylor Alison Swift for teaching me that anything is possible.

ABSTRACT

Climate change may shift patterns of streamflow permanence in headwater systems by altering the frequency, magnitude, duration, timing, and rate of change of surface streamflow, impacting both local ecosystems as well as regional water budgets and availability. While much uncertainty surrounds modeling-based methods to quantify the impacts of climate change on water budgets, long-term hydrologic data collected from headwaters in experimental research forests serve as critical evidence to reduce such uncertainty. The objective of this study is to quantify shifts in frequency, magnitude, duration, timing, and rate of change of streamflow in two headwater catchments with relatively little recent disturbance on the Cumberland Plateau using a suite of emerging hydrological statistics and trend analyses. This study determined that each catchment resulted in different streamflow permanence trends over time. Climate and evapotranspiration (ET) may have a significant impact on processes impacting streamflow permanence in each catchment as the major structural differences between the two catchments are slope and aspect.

KEYWORDS:

streamflow permanence, climate change, hydrology, Cumberland Plateau, headwater stream ecosystems

TABLE OF CONTENTS

LIST OF TABLES

LIST OF FIGURES

CHAPTER 1 INTRODUCTION AND MOTIVATION

1.1 The importance of headwater systems

Headwater streams – defined here as distinctive small streams which form the start of river networks (e.g., (Wohl, 2018)) – are well-recognized to perform vital ecosystem services. For example, studies have emphasized the significance of headwater streams with respect to nutrient retention and turnover ((Alexander et al., 2007); (Birgand et al., 2007)), to lifecycles of amphibians, fish, and macroinvertebrates ((Price et al., 2012); (Drayer & Richter, 2016); (Koundouri et al., 2017)), for bioremediation and water supply ((Meyer et al., 2003); (Hill et al., 2014)), and for complementing ecosystem services of nearby higher order streams (Datry et al., 2018).

Headwater streams frequently comprise the majority of total stream network length in most river systems across the United States ((Nadeau & Rains, 2007); (Lane et al., 2022)), and this is particularly true on the Cumberland Plateau in eastern Kentucky, which is the focus of this study. Recent estimates indicate that nearly 80% of total river network length consists of headwater streams on the Cumberland Plateau ((Strahler, 1957); (Villines et al., 2015); (Williamson et al., 2015)). The prevalence of such streams has been attributed to the region's humid climate and physiography, which consists of steep, well-dissected hillslopes, shallow, well-drained soils, and narrow valleys (e.g., (Sloan et al., 1983); (Fritz et al., 2008)).

Headwater streams are also recognized to impact and frequently control the quantity and quality of downstream waters in many regions of the US (Alexander et al., 2007; Datry et al., 2018). For example, prior studies indicate that headwater streams control the rate of subsurface recharge and residence times of water and nitrogen across many downstream landscapes (Alexander et al., 2007). Furthermore, recent studies estimate that nearly 40% of total flow volume delivered to the outlet of watersheds is contributed by headwater reaches throughout the Cumberland Plateau Mahoney et al., 2023. Taken together – these studies underscore the widespread and ubiquitous importance of headwaters to downstream water bodies and larger ecosystems throughout the US. Headwater streams are also recognized to impact and frequently control the quantity and quality of downstream waters in many regions of the US ((Alexander et al., 2007); (Datry et al., 2018)). For example, prior studies indicate that headwater streams control the rate of subsurface recharge and residence times of water and nitrogen across many downstream landscapes (Alexander et al., 2007). Furthermore, recent studies estimate that nearly 40% of total flow volume delivered to the outlet of watersheds is contributed by headwater reaches throughout the Cumberland Plateau (Mahoney et al., 2023). Taken together – these studies underscore the widespread and ubiquitous importance of headwaters to downstream water bodies and larger ecosystems throughout the US.

1.2 The vulnerability of headwater streams

Despite the recognized importance of such streams, headwater systems are currently classified in the US as “vulnerable,” meaning that they are particularly susceptible to degradation and alteration (Johnson et al., 2010; Creed et al., 2017). This

vulnerability is primarily associated with the nonperennial nature of many headwater streams and the lack of protection that such streams receive under current Federal US policy (e.g., the Waters of the US [WOTUS] Rule and Clean Water Act [CWA]). Non-perennial streams contain surface streamflow seasonally or only after storm events (e.g., (Shanafield et al., 2021)). A recent supreme court ruling in *Sackett v. Environmental Protection Agency* has specified that nonperennial systems generally would not be considered under the WOTUS rule, dictating that such waters refer only to geographical features with a "continuous surface connection" to downstream water bodies (*Sackett v. Environmental Protection Agency*, 21-454, U.S., 2023).

The vulnerability of headwater systems can be attributed to the limited knowledge surrounding hydrologic processes which control headwater streamflow–which intrinsically manifests from a lacking inventory of the spatial extent of headwater streams (Svec et al., 2005) and from the scarcity of hydrologic data collected on such systems (Poff et al., 2006) throughout the US. Specifically, while 1st and 2nd order streams (Strahler, 1957) make up nearly 75% of river network length across the US, less than 5% of all USGS gages monitor such networks (Poff et al., 2006). This fraction is not expected to increase in coming years, as the USGS has shifted its focus on monitoring for water supply and flood control purposes near cities and population centers (Hodgkins et al., 2019; Hammond et al., 2021). Furthermore, recent studies indicate that observations of hydroperiod across the continental US (CONUS) generated from the *Gages II* dataset compare poorly to perennial and non-perennial classifications from the National Hydrography Dataset Plus V2 (NHDPlusV2; U.S. Geological Survey, 2019), which serves as the nation's primary inventory of headwater streams. This suggests that the

existing inventories of headwater streams poorly capture the hydrologic regimes of such systems. The vulnerability of headwater systems can be attributed to the limited knowledge surrounding hydrologic processes which control headwater streamflow–which intrinsically manifests from a lacking inventory of the spatial extent of headwater streams (Svec et al., 2005) and from the scarcity of hydrologic data collected on such systems (Poff et al., 2006) throughout the US. Specifically, while 1st and 2nd order streams (Strahler, 1957) make up nearly 75% of river network length across the US, less than 5% of all USGS gages monitor such networks (Poff et al., 2006). This fraction is not expected to increase in coming years, as the USGS has shifted its focus on monitoring for water supply and flood control purposes near cities and population centers ((Hodgkins et al., 2019); (Hammond et al., 2021)). Furthermore, recent studies indicate that observations of hydroperiod across the continental US (CONUS) generated from the *Gages II* dataset compare poorly to perennial and non-perennial classifications from the National Hydrography Dataset Plus V2 (NHDPlusV2; (U.S. Geological Survey, 2019)), which serves as the nation's primary inventory of headwater streams. This suggests that the existing inventories of headwater streams poorly capture the hydrologic regimes of such systems.

On the Cumberland Plateau, disturbance of headwater streams is pervasive. In eastern Kentucky – like much of central Appalachia – extraction of natural resources is an important component of the region's economy. However, previous studies have recognized the impact of resource extraction on the degradation of headwater resources (e.g., (Dyer & Curtis, 1977); (Arthur et al., 1998); (U.S. EPA, 2011); (Witt et al., 2016)). Surface mining processes and valley fills cause low-order non-perennial and perennial

reaches to be permanently lost as a result of burial under overburden (U.S. EPA, 2011). Further, surface mining processes degrade water quality in headwaters by elevating conductivity and selenium concentrations, amongst other pollutants, which has caused documented toxic effects in aquatic organisms, birds, and people who rely upon such streams for water supply (e.g., (U.S. EPA, 2011); (Sena et al., 2014)).

Timber harvest is also associated with degradation of headwater resources in Kentucky Arthur et al., 1998. Timber harvest reduces rates of evapotranspiration (ET) and interception of rainfall on hillslopes surrounding headwater streams, causing an increase in overland runoff generation, soil loss, and nutrient export to downstream water bodies (Witt et al., 2016). Streamside management zones (SMZs) are a common best management practice to mitigate the impacts of timber harvest on water quality by regulating the width and density of uncut trees surrounding a stream, yet current policy in Kentucky does not require SMZs surrounding intermittent and ephemeral stream reaches. Taken together, shifts in policy surrounding protection of headwater streams coupled with the prevalence of resource extraction in the region increase the vulnerability of headwater stream systems in Kentucky, suggesting that now is a critical time for better understanding hydrological processes that control streamflow in headwater systems. Timber harvest is also associated with degradation of headwater resources in Kentucky (Arthur et al., 1998). Timber harvest reduces rates of evapotranspiration (ET) and interception of rainfall on hillslopes surrounding headwater streams, causing an increase in overland runoff generation, soil loss, and nutrient export to downstream water bodies (Witt et al., 2016). Streamside management zones (SMZs) are a common best management practice to mitigate the impacts of timber harvest on water quality by

regulating the width and density of uncut trees surrounding a stream, yet current policy in Kentucky does not require SMZs surrounding intermittent and ephemeral stream reaches. Taken together, shifts in policy surrounding protection of headwater streams coupled with the prevalence of resource extraction in the region increase the vulnerability of headwater stream systems in Kentucky, suggesting that now is a critical time for better understanding hydrological processes that control streamflow in headwater systems.

1.3 Impacts of climate and physiography on streamflow regime in headwater systems

Streamflow regime – here defined as the frequency, magnitude, duration, timing, and rate of change of surface streamflow presence – plays a critical role in the structure of headwater ecosystems (Poff et al., 1997). For example, intermittent rivers which transition between wet and dry hydroperiods provide refugia for both aquatic and terrestrial organisms ((Costigan et al., 2016); (Hammond et al., 2021)). Streamflow regime is also a common measure of the "permanence" of streamflow in headwater systems. Federal agencies have recently used streamflow permanence to classify stream reaches as perennial, intermittent, and ephemeral (Fritz et al., 2013), which has also been an important factor when determining the federal jurisdiction over such streams (Williamson et al., 2015).Streamflow regime – here defined as the frequency, magnitude, duration, timing, and rate of change of surface streamflow presence – plays a critical role in the structure of headwater ecosystems (Poff et al., 1997). For example, intermittent rivers which transition between wet and dry hydroperiods provide refugia for both aquatic and terrestrial organisms ((Costigan et al., 2016); (Hammond et al., 2021)). Streamflow regime is also a common measure of the "permanence" of streamflow in

headwater systems. Federal agencies have recently used streamflow permanence to classify stream reaches as perennial, intermittent, and ephemeral (Fritz et al., 2013), which has also been an important factor when determining the federal jurisdiction over such streams (Williamson et al., 2015).

Recent studies indicate that, across CONUS, climate is the dominant driver of streamflow regime in headwater systems. For example, Hammond et al. (2021) found that the ratio of precipitation to potential evapotranspiration was the strongest predictor of streamflow regime across CONUS. In this regard, changes to climate, which may manifest as increasing annual temperatures and alterations to precipitation amounts and intensities, may significantly alter streamflow regime in headwater systems in coming years (Williamson and Barton, (2020)). This poses as a particular concern with respect to the vulnerability of headwater systems, given that current regulation defines protection of headwaters based on the continuity of surface streamflow. Conceivably, decreased precipitation and increased ET may cause significant decreases in streamflow permanence, which could result in decreased protection such streams receive from the federal government. Notwithstanding changes in policy and protection of headwater streams, shifts in climate (and concomitant shifts in hydrologic regime) may also have important impacts on headwater refugia and taxa, given that wet and dry hydroperiods may also shift in parallel.

Structural watershed properties are also recognized to regulate components of streamflow regime regionally throughout the US ((Hammond et al., 2021); (Price et al., 2021)), albeit with lesser significance compared to climate drivers. For example, depth to bedrock controls the amount of water that can be stored in the subsurface of watersheds,

which may influence the rate of streamflow wetting/drying ((Costigan et al., 2016); (Shanafield et al., 2021)). Shallow depths to bedrock often promote rapid transport of water through the subsurface, and thus such systems frequently experience greater degrees of drying compared to catchments with larger depths to bedrock ((Addor et al., 2018); (Shanafield et al., 2021)).

1.4 Motivation of this research

This research is primarily motivated by the need to better understand the impacts of climate change on streamflow regime in headwater systems. Common methods to quantify the impacts of climate change on streamflow regime include the use of general circulation models which are used to project precipitation and temperature in space and time ((Ward et al., 2020); (Al Aamery et al., 2021)). Such models are critical to our understanding of future climate impacts on hydrologic processes, however such models are frequently applied at coarse spatial resolutions ((Liang-Liang et al., 2022)) which may be inadequate for understanding hydrologic regime in small headwater streams which often have contributing areas less than 1 km^2. This research aims to overcome this limitation by using historical data collected in headwater catchments situated in a research forest on the Cumberland Plateau over the last four decades to quantify trends in climate and streamflow regime.

We further emphasize that there have been few studies of streamflow permanence published in the central Appalachian region of the US (e.g., (Williamson et al., 2015), (Jensen et al., 2017), (Jensen et al., 2019); (Mahoney et al., 2023)), especially with respect to those that monitor climate change (Zipper et al., 2021). This paucity of studies gives credence to conducting this study in central Appalachia, given the importance of

Appalachian headwaters for structuring habitats and biodiversity ((Price et al., 2012); (Drayer & Richter, 2016)), and the enhanced vulnerability that such systems face due to widespread land use change from surface mining and timber harvest ((Zégre et al., 2013); (Witt et al., 2016)). Developing methods to investigate long-term streamflow permanence trends in headwater stream networks is expected to enhance both the understanding of headwater function and the protection of such systems under the Clean Water Act.

1.5 Contents of thesis

Chapter 1 of this thesis discusses the importance and vulnerability of headwater streams. The drivers of streamflow regime in headwater systems are presented, with emphasis given to the impacts of climate change on hydrologic processes controlling hydroperiod and streamflow permanence. The motivation of this research is presented here.

Chapter 2 provides a literature review of methods used to characterize hydrologic regime in previous studies. These are divided into field-based methods and statistical methods. Methods used to understand shifts in hydrologic regime due to climate change are highlighted. The objectives of this study are also presented.

Chapter 3 provides information on the study sites, which are located on the Cumberland Plateau in eastern Kentucky. The study sites consist of two headwater catchments with little disturbance in the last 100 years, which are situated within the Robinson Forest Environmental Monitoring Network.

Chapter 4 describes the methods used to analyze climate and streamflow regime in headwater catchments. We provide details regarding trend analysis and statistical tests used to quantify trends.

Chapter 5 provides the results of the trend analyses for various metrics used to quantify climate and streamflow regime.

Chapter 6 discusses the results within the context of other studies that have investigated the impacts of climate change on streamflow regime. We also discuss limitations of this study and future work.

Chapter 7 concludes the study.

CHAPTER 2 LITERATURE REVIEW AND OBJECTIVES

Streamflow regime is a critical component of ecosystem structure and integrity ((Koundouri et al., 2017); (Colvin et al., 2019)). The flow regime paradigm, defined by Poff et al. (1997) as the frequency, magnitude, duration, timing, and rate of change of streamflow, is now widely used to connect streamflow regime to ecosystem function. Briefly, *frequency* here refers to the number of times a discharge of a given magnitude occurs over a defined timescale, *magnitude* refers to the volumetric flow rate of water moving past a fixed point over a defined timescale, *duration* refers to the period associated with a specific flow condition over a defined time scale, *timing* refers to the regularity with which flow of a given magnitude occurs during a specific timescale, and *rate of change* refers to degree to which flow changes from one magnitude to another ((Poff & Ward, 1989); (Poff et al., 1997)).

The individual components of the natural flow regime uniquely support different ecosystem functions. For example, the duration of no flow is a critical component for aquatic species that are sensitive to streambed moisture saturation ((Price et al., 2021; Price et al., 2012)). Further, the seasonal timing of low flow is important for providing cues to aquatic organisms regarding life cycle transition, such as spawning and migration (e.g., (Montgomery et al., 1983); (Poff et al., 1997)). In the built environment, flow magnitude controls water supply and flooding.

The components of streamflow regime have been quantified through three primary methods: 1) field-based quantification of streamflow regime (e.g., (Prancevic & Kirchner, 2019)), 2) inference of streamflow regime using hydrologic signatures (e.g., (Hammond et al., 2021)), and 3) investigation of streamflow regime with process-based models ((Ward et al., 2018); (Mahoney et al., 2023)). Herein, we provide a brief review of field-based methods and hydrologic signatures used to quantify flow regime. Process-based models are increasingly being used to project streamflow regime in space and time where observations may not be available. However, this study primarily focuses on understanding shifts in streamflow regime based on observation given that verifying the fidelity of process-based models is increasingly difficult at sub-reach spatial scales (Stadnyk et al., 2013). We additionally review several of the most prominent studies that have quantified shifts in streamflow regime due to climate change.

2.1 Quantification of streamflow regime

2.1.1 Field-based methods to quantify streamflow regime

Field-based studies have made significant strides in characterizing the mechanisms controlling streamflow regime in headwater and non-perennial systems Senatore et al., 2021. These studies include the use of biological and physical indicators as surrogate measures of surface streamflow frequency (e.g., perennial, intermittent, ephemeral; see review in Fritz et al., 2020), repeated mapping of the flowing extent of the stream network to determine expansion and contraction rates of non-perennial streams (e.g., (Godsey and Kirchner, 2014); (Whiting and Godsey, 2016); (Zimmer and McGlynn, 2017); (Senatore et al., 2021)), and implementation of highly instrumented networks of flow-state sensors ((Goulsbra et al., 2014; Jensen et al., 2019); (Botter et al.,

2021)) to understand the timing of streamflow permanence in reaches of varying order (Prancevic and Kirchner, 2019). While such methods are the most reliable measures of streamflow regime, especially in low-order reaches where little hydrologic data are available (e.g., Jensen et al., 2018), they face logistical challenges given that repeated field surveys and extensive networks of flow state sensors are time and cost prohibitive. Field-based studies have made significant strides in characterizing the mechanisms controlling streamflow regime in headwater and non-perennial systems (Senatore et al., 2021). These studies include the use of biological and physical indicators as surrogate measures of surface streamflow frequency (e.g., perennial, intermittent, ephemeral; see review in (Fritz et al., 2020)), repeated mapping of the flowing extent of the stream network to determine expansion and contraction rates of non-perennial streams (e.g., (Godsey & Kirchner, 2014); (Whiting & Godsey, 2016); (Zimmer & McGlynn, 2017); (Senatore et al., 2021)), and implementation of highly instrumented networks of flow-state sensors ((Goulsbra et al., 2014); (Jensen et al., 2019); (Botter et al., 2021)) to understand the timing of streamflow permanence in reaches of varying order (Prancevic & Kirchner, 2019). While such methods are the most reliable measures of streamflow regime, especially in low-order reaches where little hydrologic data are available (e.g., (Jensen et al., 2018)), they face logistical challenges given that repeated field surveys and extensive networks of flow state sensors are time and cost prohibitive.

2.1.2 Hydrologic signatures to quantify streamflow regime

Recent studies have used *hydrologic signatures* to quantify streamflow regime in headwater and non-perennial systems (e.g., Hammond et al., 2021). Hydrologic signatures are defined as metrics that quantify aspects of streamflow regime (McMillan,

2021), and typically are derived from components of a hydrograph. Hydrologic signatures can generally be calculated relatively quickly wherever discharge data is present, overcoming some of the logistical limitations of field-based methods to quantify streamflow regime. Recent studies have used *hydrologic signatures* to quantify streamflow regime in headwater and non-perennial systems (e.g., (Hammond et al., 2021)). Hydrologic signatures are defined as metrics that quantify aspects of streamflow regime (McMillan, 2021), and typically are derived from components of a hydrograph. Hydrologic signatures can generally be calculated relatively quickly wherever discharge data is present, overcoming some of the logistical limitations of field-based methods to quantify streamflow regime.

Dozens, if not hundreds, of hydrologic signatures have been developed in recent years to quantify various hydrologic processes (McMillan et al., 2017). Recent studies have provided guidance with respect to choosing hydrologic signatures to represent the various components of hydrologic regimes in headwater and non-perennial systems. For example, the most widely used metric to represent the frequency of streamflow presence in a headwater or non-perennial stream is the *no-flow fraction*, which represents fraction of days in a year with a discharge of zero (e.g., Hammond et al., 2021; Sauquet et al., 2021; Zipper et al., 2021). To represent the magnitude of streamflow regime, several researchers have simply identified flow associated with various exceedance probabilities derived from a flow duration curve, including the minimum and maximum flows over each period of analysis (e.g., Hirsch and De Cicco, 2015; Sauquet et al., 2021). *No-flow duration*, defined as the length of consecutive no-flow days, has commonly been used to define the duration of both flow and drying regimes (Price et al., 2021). The *no-flow start*

date, defined as the date of first no flow in a stream, is commonly used to quantify the timing of streamflow regime (Hammond et al., 2021; Zipper et al., 2021). Recent studies quantify rate of change using the *midpoint of the flow duration curve* (McMillan, 2021).Dozens, if not hundreds, of hydrologic signatures have been developed in recent years to quantify various hydrologic processes (McMillan et al., 2017). Recent studies have provided guidance with respect to choosing hydrologic signatures to represent the various components of hydrologic regimes in headwater and non-perennial systems. For example, the most widely used metric to represent the frequency of streamflow presence in a headwater or non-perennial stream is the *no-flow fraction*, which represents fraction of days in a year with a discharge of zero (e.g., (Hammond et al., 2021); (Sauquet et al., 2021); (Zipper et al., 2021)). To represent the magnitude of streamflow regime, several researchers have simply identified flow associated with various exceedance probabilities derived from a flow duration curve, including the minimum and maximum flows over each period of analysis (e.g., (Hirsch & De Cicco, 2015); (Sauquet et al., 2021)). *No-flow duration*, defined as the length of consecutive no-flow days, has commonly been used to define the duration of both flow and drying regimes (Price et al., 2021). The *no-flow start date*, defined as the date of first no flow in a stream, is commonly used to quantify the timing of streamflow regime ((Hammond et al., 2021); (Zipper et al., 2021)). Recent studies quantify rate of change using the *midpoint of the flow duration curve* ((McMillan, 2021)).

Recent studies have calculated hydrologic signatures in non-perennial streams at the CONUS scale with the intent of identifying the controlling structural and functional processes for streamflow regime regionally ((Hammond et al., 2021); (Price et al.,

2021)). In such studies, random forest models are used to predict hydrologic signatures using a suite of climate and structural watershed variables. Statistical analyses then identify the most important predictors of various hydrologic signatures, which facilitates inference of the controls of the components of streamflow regime. These studies suggest that climate, typically characterized by the ratio of annual precipitation divided by the annual potential evapotranspiration, controls components of flow regime throughout many regions of CONUS, whereas physiography and land use control the rate and duration of streamflow drying regionally (Hammond et al., 2021; Price et al., 2021).

Typically, these and analogous studies (Sauquet et al., 2021; Zipper et al., 2021) utilize data collected from GAGES-II USGS sites which have at least 30 years of data (Falcone, 2011). While these gages represent the most extensive publicly available discharge data collected on headwater and non-perennial streams, seldom have headwaters in central Appalachia been represented in such studies ((Hammond et al., 2021); (Price et al., 2021); (Sauquet et al., 2021);(Zipper et al., 2021)), which can be attributed to the lack of USGS gages on small streams in this region Falcone, 2011. Further, the smallest contributing area of catchments analyzed therein throughout the Eastern Forests ecoregion was 3.5 km^2. Notably, streams with drainage area less than 1 km^2 in central Appalachia have been classified as perennial in previous studies ((Cherry, 2006); (Mahoney et al., 2023)), suggesting that closer analysis of headwater flow regime on the central Appalachian Plateau is warranted. ((Hammond et al., 2021); (Price et al., 2021); (Sauquet et al., 2021); (Zipper et al., 2021)), which can be attributed to the lack of USGS gages on small streams in this region (Falcone, 2011). Further, the smallest contributing area of catchments analyzed therein throughout the Eastern Forests

ecoregion was 3.5 km^2. Notably, streams with drainage area less than 1 km^2 in central Appalachia have been classified as perennial in previous studies ((Cherry, 2006); (Mahoney et al., 2023)), suggesting that closer analysis of headwater flow regime on the central Appalachian Plateau is warranted.

2.2 Methods to quantify climate change impacts on flow regime

Recent studies suggest that by the year 2050, average daily temperature on the Cumberland Plateau may increase by nearly 2.4° C, thus increasing potential evapotranspiration within soils by a factor of nearly 1.15 (Williamson and Barton, 2020). Consequently, possible increased soil evaporation rates may decrease hydrologic connectivity between the saturated zone and stream network during low-flow periods, thus increasing the frequency and duration of streamflow intermittency (Datry et al., 2018; Ward et al., 2020). Recent studies suggest that by the year 2050, average daily temperature on the Cumberland Plateau may increase by nearly 2.4° C, thus increasing potential evapotranspiration within soils by a factor of nearly 1.15 (Williamson & Barton, 2020). Consequently, possible increased soil evaporation rates may decrease hydrologic connectivity between the saturated zone and stream network during low-flow periods, thus increasing the frequency and duration of streamflow intermittency ((Datry et al., 2018); (Ward et al., 2020)).

Several studies have predicted that the extent of non-perennial streams and rivers will increase due to climate change across both watershed and regional scales ((Jaeger et al., 2014); (Ward et al., 2020)). This has been corroborated by several CONUS and global scales studies which have analyzed changes in hydrologic signatures using the GAGES-II dataset, although increased streamflow drying is not ubiquitous across all non-

perennial stream systems ((Sauquet et al., 2021); (Zipper et al., 2021)). Typically, trends in streamflow regime are quantified using some combination of statistical tests (e.g., Mann-Kendall tests, Mann-Whitney tests; (Zipper et al., 2021)) coupled with analyses to quantify slopes of trend lines (e.g., linear regression, Sen's Slopes; (Ward et al., 2020) (Sauquet et al., 2021); (Tramblay et al., 2021)) Several studies have predicted that the extent of non-perennial streams and rivers will increase due to climate change across both watershed and regional scales ((Jaeger et al., 2014); (Ward et al., 2020)). This has been corroborated by several CONUS and global scales studies which have analyzed changes in hydrologic signatures using the GAGES-II dataset, although increased streamflow drying is not ubiquitous across all non-perennial stream systems ((Sauquet et al., 2021); (Zipper et al., 2021)). Typically, trends in streamflow regime are quantified using some combination of statistical tests (e.g., Mann-Kendall tests, Mann-Whitney tests; (Zipper et al., 2021)) coupled with analyses to quantify slopes of trend lines (e.g., linear regression, Sen's Slopes; (Ward et al., 2020) (Sauquet et al., 2021); (Tramblay et al., 2021)). These studies generally indicate that the frequency of no-flow has tended to increase over time in the eastern US. However, small streams in central Appalachia have not been extensively incorporated into these analyses.

2.4 Objectives

Our objective was to characterize the frequency, magnitude, duration, timing, and rate of change of streamflow regime in central Appalachian headwater streams and investigate shifts in climate and streamflow regime in such systems. We carry out this objective by investigating hydrologic regime in two well-monitored catchments on the Cumberland Plateau. The two catchments analyzed herein have been relatively

undisturbed over the last 100 years and are classified as second growth forests (Williamson et al., 2015). We chose these study catchments to isolate the impact of climate on streamflow regime because landscape disturbance is well-documented to alter hydrologic processes in headwaters (U.S. EPA, 2011), and thus attributing shifts in hydrologic regime due to climate change versus land use alteration may prove to be exceedingly complex in disturbed watersheds.

While climate is recognized as the primary driver of streamflow regime, we also aim to investigate the role of structural watershed properties, including watershed configuration and contributing area, in controlling streamflow regime. Studies comparing the structural controls of hydrologic regime are currently lacking (Hammond et al., 2021). Given the proximity of the catchments, the analysis should also offer insight into the structural controls of streamflow permanence on the Cumberland Plateau.

CHAPTER 3 STUDY WATERSHED

3.1 Overview of eastern KY and the Cumberland Plateau

Our study catchments are located in the Clemons Fork watershed (14.5 km^2), which is situated in Robinson Forest on the Cumberland Plateau (see Fig. 3.1 and Fig. 3.2). The Cumberland Plateau is located within the central Appalachian Mountain Range, and includes sections of eastern Kentucky, Tennessee, northern Alabama, and northwest Georgia. This region is characterized by narrow valleys, steep ridges, and dissected stream networks (Woods, 2002). The Cumberland Plateau's geology consists of limestone, shale, and sandstone developed during the Mississippian and Pennsylvanian periods (Simpson and Florea, 2009). Natural weathering over the past 350 million years has enriched soils, and much of the natural vegetation in the area consists of mixed mesophytic forest (Woods, 2002). Soils on the plateau are generally shallow and well-drained (Fritz et al., 2008). is characterized by narrow valleys, steep ridges, and dissected stream networks (Woods, 2002). The Cumberland Plateau's geology consists of limestone, shale, and sandstone developed during the Mississippian and Pennsylvanian periods (Simpson & Florea, 2009). Natural weathering over the past 350 million years has enriched soils, and much of the natural vegetation in the area consists of mixed mesophytic forest (Woods, 2002). Soils on the plateau are generally shallow and well-drained (Fritz et al., 2008).

Large deposits of coal and densely forested areas made the region a hotbed for coal mining and timber harvest during the Industrial Revolution, operations which have largely persisted into the early 21st century (Jones, 1992). Large deposits of coal and densely forested areas made the region a hotbed for coal mining and timber harvest during the Industrial Revolution, operations which have largely persisted into the early 21st century (Jones, 1992). In recent years, shifts in environmental policies, mining practices, and alternative energy sources have caused resource extraction from the region to become less profitable (Jones, 1992), stunting the growth of many logging and mining communities in the region. In recent years, shifts in environmental policies, mining practices, and alternative energy sources have caused resource extraction from the region to become less profitable (Jones, 1992), stunting the growth of many logging and mining communities in the region. Currently, most residents of the Cumberland Plateau reside in small communities that are often located in floodplains given that these areas are largely the only available flat land suitable for community development (Smith, 2023). Consequently, these communities are prone to flash flooding throughout the year ((Crysler et al., 1980); (Guttman and Ezell 1980)), as intense convective storms during the summer, rain on snow during the winter, and steep slopes with shallow, well-drained soils transport water quickly to streams (Christian et al., 2023). Flash flooding within the Cumberland Plateau has impacted the local economy and safety of residents. In 2022, flash flooding killed 39 residents of eastern Kentucky and caused extensive damage to infrastructure (Christian et al., 2023). as intense convective storms during the summer, rain on snow during the winter, and steep slopes with shallow, well-drained soils transport water quickly to streams (Christian et al., 2023). Flash flooding within the

Cumberland Plateau has impacted the local economy and safety of residents. In 2022, flash flooding killed 39 residents of eastern Kentucky and caused extensive damage to infrastructure (Christian et al., 2023).

3.2 Overview of the Robinson Forest Environmental Monitoring Network

Robinson Forest is a 5,983-ha research forest managed through the University of Kentucky (Sena, 2021; see Fig. 3.2). In the early 1900s, the Mowbray-Robinson Lumber Company purchased and leased thousands of acres of land throughout 29 Kentucky Counties for timber harvesting and surface mining (Overstreet,1984). Within these tracts of land, the company clearcut much of what is now known as Robinson Forest. By 1923, E.O. Robinson, co-founder of the Mowbray-Robinson Lumber Company, deeded the Robinson Forest Trust to the University of Kentucky for the demonstration of reforestation. The forest is currently being developed as a teaching, research, and extension facility.

Since the early 1970's, environmental data has been collected in various locations throughout the forest through the US Department of Forestry and the UK College of Agriculture, which is today termed the Robinson Forest Environmental Monitoring Network (Sena, 2021). The research forest consists of several second growth forests with limited disturbance since the 1920s, as well as forests that have been cut with varying degrees of streamside management (Arthur et al., 1998). A base camp and several access roads have been developed to assist with monitoring (Sena, 2021). (Arthur et al., 1998). A base camp and several access roads have been developed to assist with monitoring (Sena, 2021).

The Robinson Forest Environmental Monitoring Network consists of 12 weirs and 9 bulk deposition and precipitation collection systems which are located throughout the forest. Environmental data has been collected continuously since 1971 in several catchments on stripcharts except for periods of extreme flooding and equipment failure until 2009 when the stripcharts were replaced with pressure transducers and electronic data loggers. Stripcharts recorded data whenever a significant shift in the parameter was detected, with a minimum timestep of one day. Data loggers implemented in 2009 recorded once every fifteen minutes. Parameters monitored with the stripcharts and data loggers included flow depth (converted to volumetric flow rate with depth-discharge curves), water temperature, precipitation, and air temperature. Weekly grab samples were used to monitor water quality including chloride, nitrate, sulphate, ammonium, pH, alkalinity, calcium, magnesium, potassium, sodium, conductivity, total organic carbon, phosphate, and turbidity. In sum, the forest has recorded daily streamflow, daily precipitation, daily temperature, and weekly stream-water chemistry for over 40 years from catchments representing a range of contributing areas and timber harvest management strategies, including several second-growth forests. Several other datasets, including precipitation bulk-deposition chemistry data and water temperature data have supported these measurements (Sena, 2020).

The topography of the Robinson Forest consists of long, rectilinear side slopes cut into a horizontally bedded substrate of shale, sandstone, coal, and siltstone classified as part of the Breathitt Formation ((Hinrichs,1978); (McDowell, 1985)). Soil descriptions from recent studies identified the soil of footslopes to be Kimper series Humic

Dystropepts, sideslopes to be Cloverlick series Humic Dystrudepts, and ridgetop to be Gilpin series Typic Hapludalts (Williamson & Barton, 2020). The naturally well-drained soils in the forest and minimally permeable geology allow for subsurface flow to quickly respond to precipitation (Coltharp & Springer, 1980). While Robinson Forest's natural geology remains intact, many surrounding properties that were once owned by the Mowbray-Robinson Lumber Company have been subject to surface mining. The vegetation of Robinson Forest is typical of the mixed mesophytic forest region, with oak (*Quercus sp*.), hickory (*Carya sp*.), yellow-poplar (*Liriodendrontulipifera*), and American beech (*Fagus grandifolia*) as dominant overstory species and eastern hemlock (*Tsuga canadensis*) common in riparian areas (Williamson & Barton, 2020).

The climate of Robinson Forest is classified as temperate-humid-continental with warm and humid summers and cool winters. Precipitation is distributed throughout the year, but there is generally heavier precipitation in the spring and summer months with drier autumns. Mean annual precipitation across Robinson Forest from 1971 to 2018 was 1121 mm (Sena, 2021). Most years, short duration-flooding occurs with several higher-intensity flood events occurring in 1981 and 2009 (Sena et al., 2020). Streamflow is generally highest during Winter and Spring months during leaf-off periods (Abney et al., 2022). As the growing season begins, streamflow beings to decrease with surface streamflow decreasing in late summer and autumn months as precipitation rates decline. (Abney et al., 2022). As the growing season begins, streamflow beings to decrease with surface streamflow decreasing in late summer and autumn months as precipitation rates decline.

3.3 Overview of Falling Rock and Little Millseat

While many catchments have been monitored in Robinson Forest, we investigate shifts in streamflow regime and climate in two second growth headwater catchments located within Clemons Fork (see Fig. 3.2, 3.3, and 3.5): Falling Rock (88 ha) and Little Millseat (79 ha). We specifically investigate these catchments for several reasons. First, these catchments have received little landscape disturbance since initial logging in the 1920s, which should better isolate potential shifts in streamflow regime due to changes in climate. Second, while both catchments are second-growth forests, we hypothesize that the study catchments may also elucidate differences in streamflow regime related to structural watershed properties given their unique physiography and aspects.

While both the Falling Rock and Little Millseat catchments have similar contributing areas and land uses, Falling Rock has a dendritic drainage pattern and flows from east to west (Fig. 3.3 and 3.4). Little Millseat is characterized by a trellis-like drainage pattern that flows from west to east (Fig. 3.6 and 3.7). Falling Rock is on the eastern edge of the Clemons Fork Basin and has an even distribution of aspect angle between the four cardinal directions (Fig. 3.5) with elevations between 294 and 459 m above sea level (Sena, 2021). Little Millseat is on the western edge of the Clemons Fork Basin and has an aspect angle split primarily between North and South with smaller portions facing East and West (Fig. 3.8) and with elevations between 303 and 462 m above sea level (Sena, 2021). The soil profile for both watersheds consists of Cloverlick-Shelocta-Kimper, Matewan-Gilpin-Marrowbone, and Handshoe-Fedscreek-Shelocta consisting of steep slopes and stony to rocky texture (Fig. 3.4 and Fig. 3.6). Both Falling Rock and Little Millseat consist of first order streams, as classified by the NHD High Res

V2 mapping (Fig. 3.3 and Fig. 3.5). However, previous studies that have mapped the stream networks based on the locations of head cuts identified each stream as third order at the outlet of each catchment ((Cherry, 2006); (Fritz et al., 2006); (Mahoney et al., 2023)).

3.4 Materials

We used the following datasets collected from Falling Rock and Little Millseat to assess shifts in climate and streamflow regime: 1) minimum daily discharge, 2) mean daily discharge, 3) maximum daily discharge, 4) total daily precipitation, 5) minimum daily temperature, 6) mean daily temperature, and 7) maximum daily temperature. A summary of data used herein is shown in Table 3.1. Data were QAQC'd and published on the USGS Science Base platform through a partnership between the UK Department of Forestry and Natural Resources and the USGS Ohio-Kentucky-Indiana Water Science Center (see data release from Sena et al., 2020). While most data exists from 1971 until 2018, we analyzed a subset of data between 1980 and 2018, where available, which is a similar date range used by analogous studies which investigate shifts in non-perennial streamflow and drought due to climate change throughout CONUS ((Price et al., 2021); (Hammond et al., 2022); (Zipper et al., 2021)).

Discharge data were collected from v-notch weirs at the outlet of each catchment (Sena et al., 2020). Precipitation gages were located at the ridge and base of each catchment, and a fifth gage was located at weather station near the Robinson Forest base camp, termed the Camp Weather Station (CWS; see Fig. 3.2). To ensure each catchment's precipitation dataset was the best representation of the local climate trends, the precipitation data recorded at the base of each catchment was prioritized for analysis.

This data was given precedence given that 1) the precipitation gage was placed at the outlet of each catchment near where the respective flow exits into Clemons Fork and 2) typically these gages had the longest period of record. For any gaps in data collected at the base of each catchment, the ridge precipitation data was substituted in. The ridge data is the next best data source as it is closest to the base gage, resulting in similar precipitation measurements, but often the record was much shorter. In the scenario where there was no data available for either base or ridge, the CWS gage was used. This data was prioritized last given that the weather station is 2.5 km southwest of Falling Rock's outlet and 1.5 km south of Little Millseat's outlet. Air temperature data has only been QAQC'd and published from the CWS gage.

This procedure produced a relatively continuous record of precipitation, air temperature, and discharge in Falling Rock and Little Millseat; however, there were still some notable gaps in the published ScienceBase data. We developed a script to determine the number of days each year with no data. To ensure partial years did not skew the dataset, any year with less than 85% of data was excluded from the analysis. Table 3.1 shows the years that were eliminated from analysis for each catchment. The most notable disruption in discharge data occurred in Little Millseat from 1994-1999. For most analyses, at least 30 years of data are used, which is typically considered a minimum standard for climate analyses ((World Meteorological Organization, 1989); (Sauquet et al., 2021); (Tramblay et al., 2021))

All analyses were carried out using the open-source programming language *R*. *R* and *Rstudio* can be downloaded through the Comprehensive R Archive Network (CRAN; https://posit.co/download/rstudio-desktop/). We generated all plots using the base *plot*

functions and the package *ggplot2*. We used the following *R* packages to quantify streamflow regime and carry out trend analysis: *hydroTSM*, *trend*, *lubridate*, *dplyr*, *scales*, *trend*, *EGRET*, *TTR*, *tidyquant*, *tidyr*, *ggridges*, *robslopes*, *Kendall*, *zyp*, and *gridExtra*. All code is published to Github for public download and may be retrieved at: https://github.com/tyler-mahoney.

Table 3.1 Summary of unique years excluded from data analysis for each catchment.

	Minimum Discharge	Mean Discharge	Maximum Discharge	Precipitation	Minimum Air Temperature	Mean Air Temperature	Maximum Air Temperature
Falling Rock Date Range of Data Analyzed	1/1/1980-12/31/2015	1/1/1980-12/31/2015	1/1/1980-12/31/2015	1/1/1980-12/31/2018	1/1/1980-12/31/2015	1/1/1980-12/31/2015	1/1/1980-12/31/2015
Little Millseat Date Range of Data Analyzed	1/1/1980-12/31/2018	1/1/1980-12/31/2018	1/1/1980-12/31/2018	1/1/1980-12/31/2015	1/1/1980-12/31/2015	1/1/1980-12/31/2015	1/1/1980-12/31/2015
Falling Rock Excluded Years	2014	2014	2014	NA	2007, 2009	2007, 2009	2007, 2009
Little Millseat Excluded Years	1994,1995, 1996,1997, 1998, 1999	1994,1995, 1996,1997, 1998, 1999	1994,1995, 1996,1997, 1998, 1999	NA	2007, 2009	2007, 2009	2007, 2009

Figure 3.1 Appalachian Mountain Region

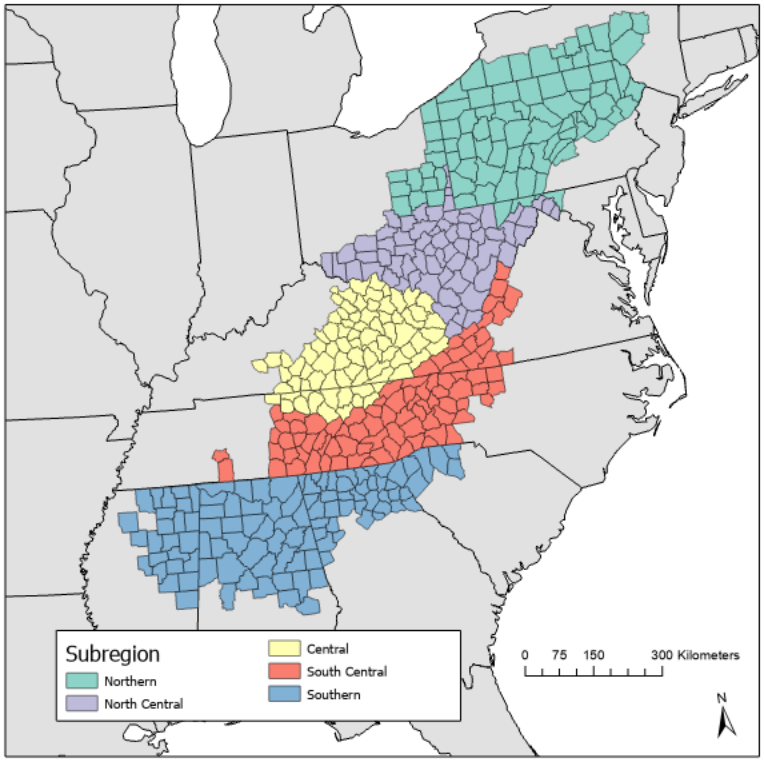

Figure 3.2 Study catchments used to evaluate impacts of climate change on flow regime.

Clemons Fork (14.5 km2) is situated within the Robinson Forest Environmental Monitoring Network. Weirs are installed at the outlets of each catchment analyzed herein, including the Falling Rock catchment (88 ha) and the Little Millseat Catchment (78 ha). Rain gages have been installed at the base and ridge of each catchment. A fifth weather station is located at the outlet of Clemons Fork near the Robinson Forest Camp site. The NHD High Res V2 stream network is plotted for Clemons Fork, which is classified as 4th order at the outlet of the watershed.

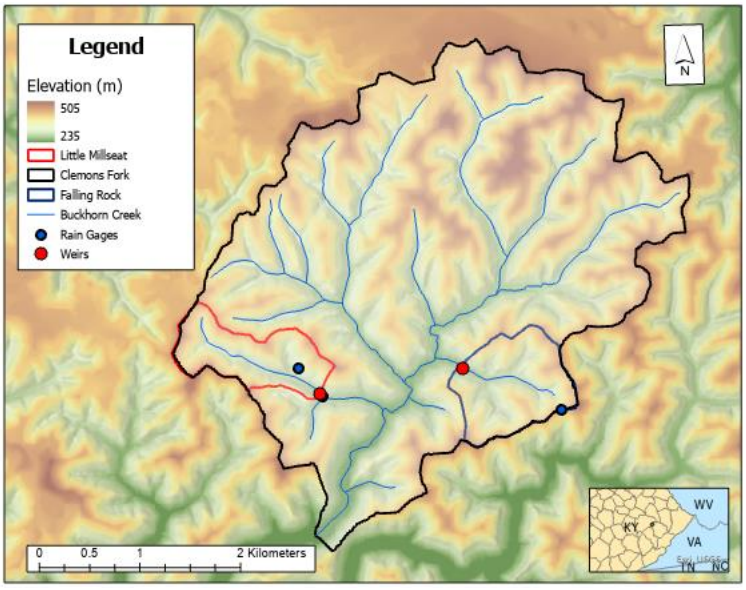

Figure 3.3 Falling Rock Catchment (88ha).

The catchment is a second-growth forest that has not been disturbed since 1923. Two rain gages exist at the head and base of the catchment. Flow is monitored at the outlet of the catchment with a V-notch weir.

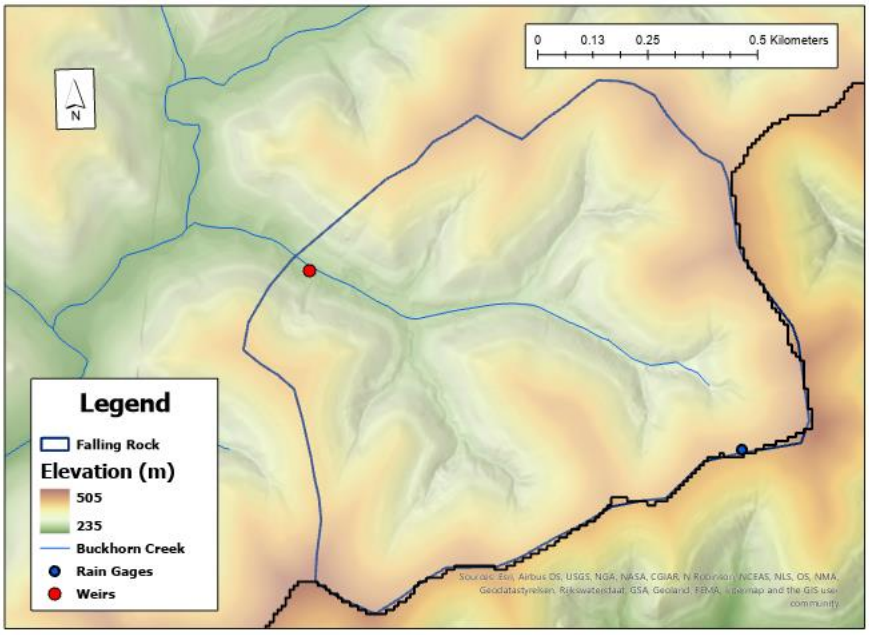

Figure 4 Falling Rock Catchment soils data.

The soils consist of Cloverlick-Shelocta-Kimper (uCskF), Matewan-Gilpin-Marrowbone (uMgmF), and Handshoe-Fedscreek-Shelocta (uHfsF) consisting of steep slopes and stony to rocky texture.

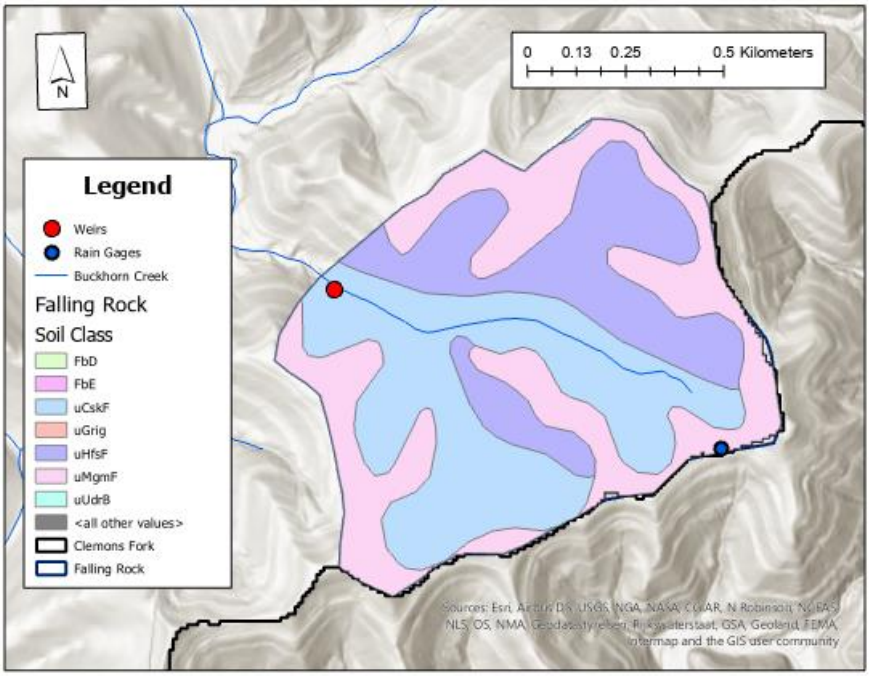

Figure 3.5 Falling Rock aspect direction.

The aspect of the catchment is split between North (315.01°-45°), East (45.01°-135°), South (135.01°-225°), and West (225.01°-315°). The aspect of Falling Rock is distributed evenly between the four cardinal directions.

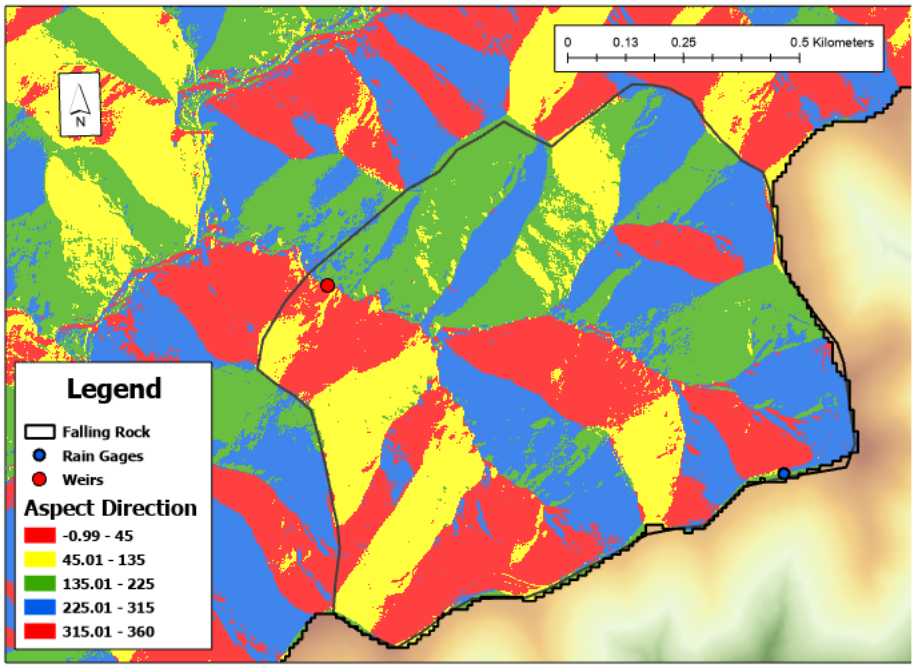

Figure 3.6 Little Millseat Catchment (79ha).

The catchment is a second-growth forest that has not been disturbed since 1923. Two rain gages exist at the head and base of the catchment. Flow is monitored at the outlet of the catchment with a V-notch weir.

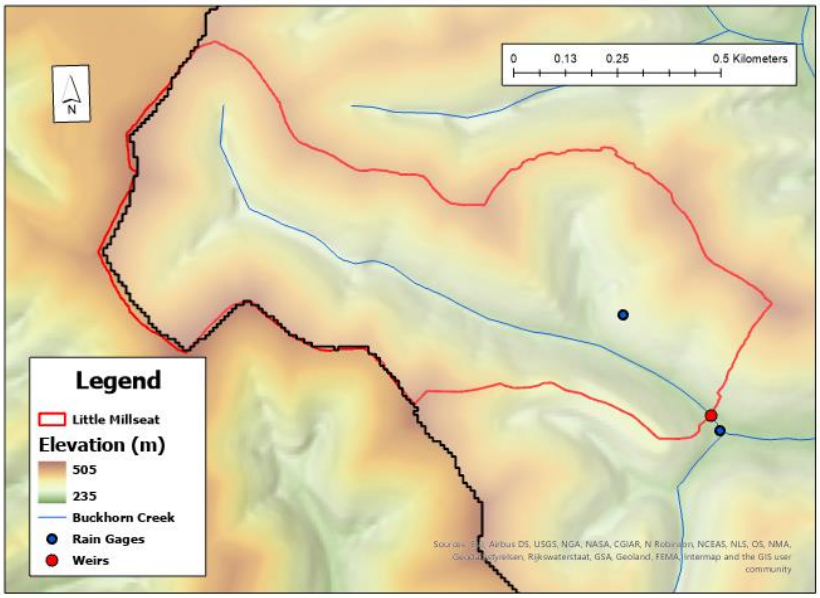

Figure 3.7 Little Millseat Catchment Soils data.

The soil of the catchment consists of Cloverlick-Shelocta-Kimper (uCskF), Matewan-Gilpin-Marrowbone (uMgmF), and Handshoe-Fedscreek-Shelocta (uHfsF) consisting of steep slopes and stony to rocky texture

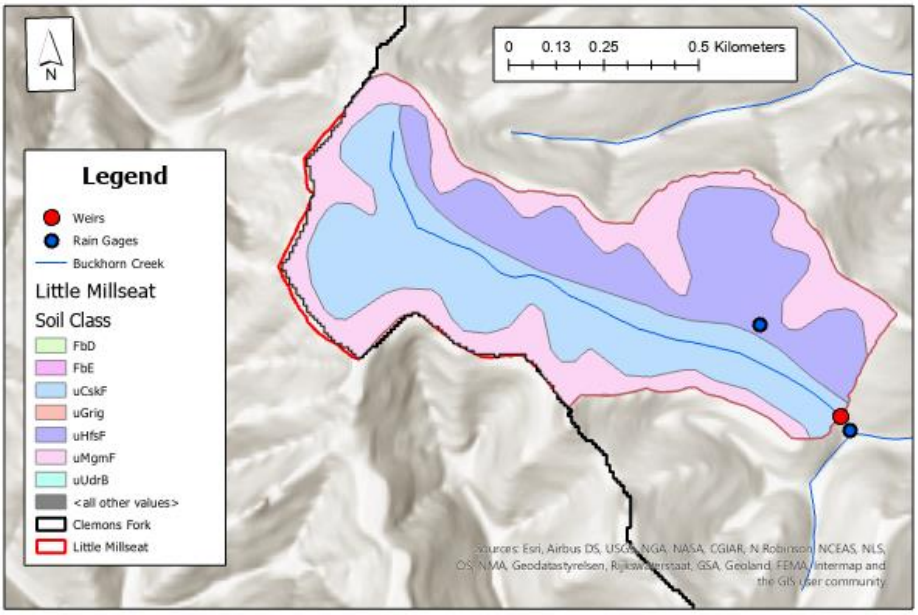

Figure 8 Little Millseat aspect direction.

The aspect of the catchment is split between North (315.01°-45°), East (45.01°-135°), South (135.01°-225°), and West (225.01°-315°). The aspect of Little Millseat is distributed primarily between North and South with smaller portions of East and West facing slopes.

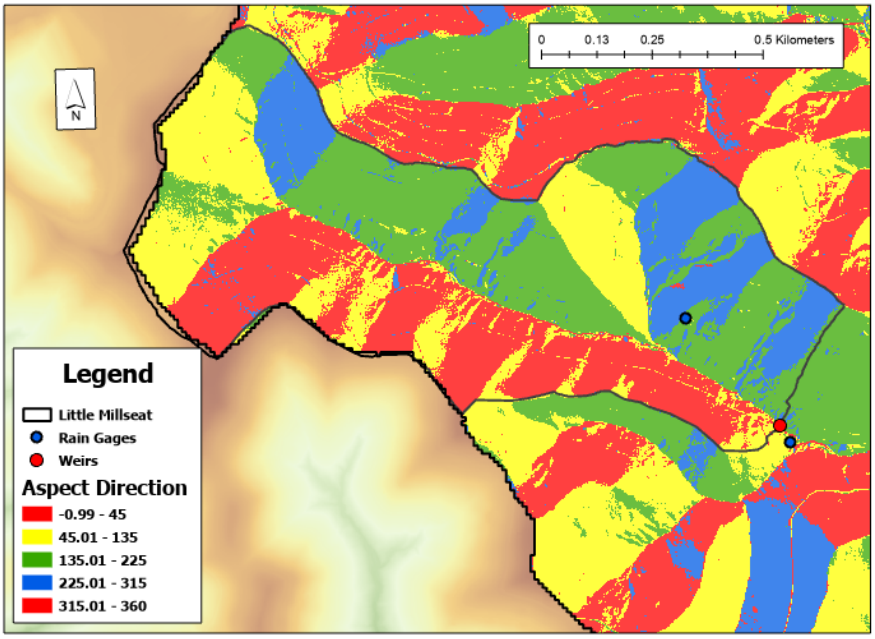

CHAPTER 4 METHODS

We investigated shifts in climate and hydrologic regime by conducting trend analysis on datasets described in section 3.4 and on hydrologic signatures derived from discharge hydrographs, as described below. Hydrologic signatures are defined as metrics that quantify aspects of streamflow response, and have been widely used to assess both the flow regime and drying regime of headwater and non-perennial streams (e.g., ; (McMillan, 2021); (Price et al., 2021); (Sauquet et al., 2021)).

Recent studies have found shifts in climate change and discharge to be pronounced over seasonal and monthly timescales (e.g., (Eisner et al., 2017); (Ward et al., 2020)). For this reason, we analyzed climate, discharge, and hydrologic signatures over various timescales, including: 1) half-decadal, 2) yearly, 3) seasonal, and 4) monthly. Yearly timescales are divided by climate year (1 April to 31 March), water year (1 October to 30 September), and calendar year. Recent studies have analyzed trends by both climate year (e.g., (Hammond et al., 2021)) and by water year (e.g., (Ward et al., 2020)), and we aimed to reduce uncertainty surrounding time series discretization on trend analysis by including results for each period.

A summary of the climate metrics, discharge metrics, and hydrologic signatures and the timescales over which trends are evaluated herein is shown in Table 4.1. We describe climate metrics, discharge metrics, hydrologic signatures, and trend analyses employed herein in subsequent sections.

4.1 Characterizing Climate

The climate metrics analyzed herein include minimum, mean, and maximum air temperature, precipitation, and minimum, mean, and maximum water temperature. These variables were analyzed at the half-decadal, yearly, seasonal, and monthly time scales. Air temperature was only available at Camp Weather Station whereas precipitation was available at the base and ridge of each catchment. Water temperature was available at the outlet of each catchment, but data only existed for approximately 15 years. We then conducted trend analyses of each climate metric to determine the magnitude of change occurring at each site, as described in section 4.3.

4.2 Characterizing Streamflow permanence in headwater system

We used various discharge metrics and hydrologic signatures to characterize streamflow regime in Falling Rock and Little Millseat. Our objectives were to characterize the frequency, duration, timing, magnitude, and rate of change of surface streamflow in each catchment. Dozens, if not hundreds, of hydrologic signatures have historically been used to characterize various components of streamflow hydrographs (e.g., (McMillan et al., 2017); (McMillan, 2020); (McMillan, 2021)). We chose to analyze a subset of hydrologic signatures which are commonly used to quantify streamflow and drying regimes (e.g., (Hammond et al., 2021); (Price et al., 2021); (Sauquet et al., 2021)), as described in the subsequent sections.

4.2.1 Frequency

We defined *frequency* as the number of times a discharge of a given magnitude occurred over a defined timescale (e.g., (Poff et al., 1997)). We used several hydrologic

signatures to investigate shifts in the frequency in Falling Rock and Little Millseat ((McMillan, 2020)).

To evaluate the frequency of low flows, we quantified the number of no-flow days during a given period, defined as any given day when the mean discharge was 0 cfs, as well as the number of days during a given period when discharge was less than flows exceeded 90%, 75%, and 50% of the time, as calculated from a flow duration curve over the entire study period. Trends representing shifts in the frequency of low flows were evaluated at the half-decadal, yearly, seasonal, and monthly timescales. An increasing trend in any of these signatures indicated an increase in the frequency of low flow days over the time scale (Ekström et al., 2018).

To evaluate the frequency of high flows, we quantified the number of days during a given period when discharge was greater than flows exceeded 25%, 5%, and 1% of the time, as calculated from a flow duration curve over the entire study period. Trends representing shifts in the frequency of high flows were evaluated at the half-decadal, yearly, seasonal, and monthly timescales. An increasing trend in any of these signatures indicated an increase in the frequency of high flow days over the time scale.

We calculated flow duration curves over the entire time series for Falling Rock and Little Millseat to determine the 90%, 75%, 50%, 25%, 5%, and 1% exceeded flows in each catchment. To determine the flow duration curves, discharge timeseries data from each catchment were sorted from highest flows to lowest and ranked from 1 (highest flow) to n (lowest flow). The probability of exceedance was calculated for each data point using the following equation:

$$P = 100 * \frac{M}{n+1} \quad \text{(Eq. 4.1)}$$

where *P* is the probability that a given flow will be equaled or exceeded, *M* is the ranked position of given flow in the list, and n is the number of events in a period of record. We opted to use flow exceedance probabilities as thresholds (rather than predefined discharge values) to represent shifts in the frequency of low and high flows since this approach normalizes flow thresholds over the cumulative flow duration curve for each catchment.

4.2.2 Duration

We defined *duration* as the period associated with a specific flow condition over a defined time scale (Poff et al., 1997). Given that this study is concerned with determining shifts in the degree of streamflow permanence in headwater catchments, we quantified shifts specifically in the duration of low flow periods in each catchment (as opposed to the duration of high flow periods). This was carried out by determining the longest consecutive period of no flow in both Falling Rock and Little Millseat over half-decadal, annual, seasonal, and monthly timescales. To do this, we classified each day with recorded discharge as being a *flow day* (i.e., mean daily discharge > 0.00 cfs) or a *no flow day* (i.e., mean daily discharge = 0.00 cfs). We then added the consecutive no flow days until a flow day occurred. The largest consecutive *no flow* period was then used to conduct trend analysis. If the duration of no flow was found to be increasing over time, this would indicate that the stream became drier over the period. Decreases in largest no-flow period would indicate that the stream became wetter over time (Ekström et al., 2018).

Since we were primarily concerned with understanding shifts in periods when stream drying occurred, this study only calculated the duration of low flow events. Quantifying the duration of high-flow events would likely aid in understanding shifts in sustained high flows in each catchment, for example due to flooding, however this is outside the scope of this research.

4.2.3 Timing

We defined *timing* as the regularity with which a flow of a given magnitude occurs during a specific timescale (Poff et al., 1997). To determine the shifts in low flow timing, the first no-flow day of each year was used to analyze if no flow days occurred sooner or later from year to year (Hammond et al., 2021). The timing of the first no flow day was determined as follows. Each calendar date was given a numeric value between 1 (January 1st) and 365 (December 31st) during non-leap years, or a value between 1 and 366 during leap years. Then, the numeric date of the first no flow day was recorded for each year. If the trend of the first no flow day is positive, this indicates stream drying occurs later in the calendar year, and thus the stream may be carrying water for longer periods before it runs dry. Conversely, if the first no flow day occurs earlier in the year, the stream may be carrying less water before drying.

4.2.4 Magnitude

We defined *magnitude* as the volumetric flow rate of water moving past a fixed point in the catchment over a defined timescale (Poff et al., 1997). Three hydrologic signatures were used to calculate the magnitude of streamflow, including the minimum, mean, and maximum daily flow for each time period. Decreasing minimum discharge values may indicate that the system is drying over time (Ekström et al., 2018). On the other

hand, increasing peak discharge values can indicate that the system is becoming wetter or that there may be more intense precipitation events occurring over time (Ekström et al., 2018). Minimum, mean, and maximum daily discharges were calculated over half-decadal, yearly, seasonal, and monthly timescales. We defined *magnitude* as the volumetric flow rate of water moving past a fixed point in the catchment over a defined timescale (Poff et al., 1997). Three hydrologic signatures were used to calculate the magnitude of streamflow, including the minimum, mean, and maximum daily flow for each time period. Decreasing minimum discharge values may indicate that the system is drying over time (Ekström et al., 2018). On the other hand, increasing peak discharge values can indicate that the system is becoming wetter or that there may be more intense precipitation events occurring over time (Ekström et al., 2018). Minimum, mean, and maximum daily discharges were calculated over half-decadal, yearly, seasonal, and monthly timescales.

4.2.5 Rate of Change

We defined *rate of change* as the degree to which flow changes from one magnitude to another in each catchment. We used the slope of the midpoint of the flow duration curve to determine shifts in the rate of change in each catchment. The slope of the flow duration curve is indicative of how quickly or slowly the system drains (Rosburg et al., 2017). Typically, systems with steep slopes of the midpoints of the flow duration curve are classified as flashy, whereas systems with mild slopes are classified as less flashy (McMillan, 2020). To calculate the slope of the midpoint of the flow duration curve, the following equation was used: Typically, systems with steep slopes of the midpoints of the flow duration curve are classified as flashy, whereas systems with mild slopes are classified

as less flashy (McMillan, 2020). To calculate the slope of the midpoint of the flow duration curve, the following equation was used:

$$s = \frac{Q_{20} - Q_{70}}{50} \quad \text{(Eq. 4.2)}$$

where s is the slope of flow duration curve, Q_{20} is the discharge value where flow is exceeded 20% of the time for a specified temporal scale, and Q_{70} is the discharge value where flow is exceeded 70% of the time for a specified temporal scale. The slope of the midpoint of the flow duration curve was calculated for half decadal, yearly, seasonal, and monthly to understand shifts in drainage in each catchment.

We also calculated an annual water budget to assess shifts in the rate of change in each catchment. The water budget is used to quantify the amount of precipitation that converts into streamflow and the amount of precipitation lost to ET and deep aquifer storage in a catchment (NASA, 2022). The water budget is estimated as:

$$P = ET + \Delta S + Q_{out} \quad \text{(Eq. 4.3)}$$

where P is precipitation, ET is evapotranspiration, ΔS is change in storage, and Q_{out} is flow out of the catchment over a defined timescale. Q_{in} is not explicitly considered herein as all flow into the catchment is assumed to come from precipitation and we assume that groundwater follows the topography of the catchment. We determined water budgets over an annual time scale.

To calculate the water budget, the mean daily discharge was used to estimate the daily discharge volume transported in each catchment. We then estimated the annual volume of discharge by summing daily discharge over the calendar year. Afterwards, the

volume of precipitation falling on the catchment was estimated by multiplying the daily precipitation depth occurring in each catchment times the catchment area.

We then estimated the percent of precipitation that leaves the system as streamflow, f_P, as:

$$f_P = \frac{Q_{out}}{P} * 100 \quad \text{(Eq. 4.4)}$$

If f_P increases over time, it is likely that increasing amounts of precipitation become streamflow rather than being lost to ET. If the f_P decreases, it is likely that increasing amounts precipitation are being lost in the system to ET or storage, rather than converted into streamflow.

4.3 Trend analysis

We used multiple timescales to understand trends in streamflow regime at different intervals. A range of long-term (half decadal) and short-term (seasonal) trend cycles were evaluated to understand shifts in climate and streamflow regime. The half-decadal timestep was leveraged to investigate any trends from weather patterns such as El Nino and La Nina. We used calendar year, climate year, and water year discretization to evaluate yearly trends in climate and streamflow regime between 1980 and 2015. We then discretized years into seasons and months to evaluate trends in climate and streamflow regime that might occur, for example only during the fall across each year.

The Mann-Kendall test and Sen's slope were used to conduct the trend analyses in Falling Rock and Little Millseat. These techniques are commonly used to evaluate trends in hydrologic regime ((Ward et al., 2020); (Zipper et al., 2021)). These tests work in tandem

to determine the statistical significance and slope of a given monotonic trend. The Mann-Kendall trend test is a hypothesis test to determine if a null hypothesis can be accepted or rejected with a certain level of confidence. The Mann-Kendall test is beneficial to use if the data is not normally distributed as it is a non-parametric test ((Kendall, 1938); (Mann, 1945)). The Mann-Kendall test uses the sign of the difference between earlier and later pairs of data to determine if a trend is occurring. The later data points are compared to all earlier data points. This results in $n(n-1)/2$ pairs of data, where n is the number of data points. If any values are missing or recorded as N/A, the point is not included in analysis, which is useful for non-continuous datasets like some of the data available from the Robinson Forest Environmental Monitoring Network, as there were some interruptions to data collected, as described in Table 3.1. The test uses the assumption that any data value is greater than, less than, or equal to another value, that data are independent, and that the data distribution remains constant (Helsel and Hirsch 1992). The Mann-Kendall test can also be applied to log transformed data, which is particularly useful for analyzing low flow trends (Mahoney et al., 2023).

To begin, the difference between later measured values (y_j) and earlier measured values (y_i) is calculated and the difference is given an integer value of 1, 0, or -1 corresponding to if the difference is positive, zero, or negative. The test statistic is then calculated as:

$$S = \sum_{i=1}^{n-1} \sum_{j=i+1}^{n} sign(y_j - y_i) \qquad \text{(Eq. 4.5)}$$

where $sign(y_j - y_i)$, is equal to $+1$, 0, or -1 as indicated above.

If S is positive, it indicates an upward trend as later values are larger than earlier values. When S is negative, it indicates a negative trend as later values are smaller than earlier values. If S is near zero, no trend is indicated. The test statistic τ is computed as follows:

$$\tau = \frac{S}{n(n-1)/2} \quad \text{(Eq. 4.6)}$$

which has a range of –1 to +1 and is the correlation coefficient in regression analysis. The null hypothesis of no trend is rejected when S and τ are not zero. If a significant trend is found, the rate of change can be calculated using the Sen's slope estimator (Helsel and Hirsch 1992). Sen's slope determines the linear rate of change for a dataset and the corresponding confidence interval (Sen, 1968). Sens slope can be calculated using:

$$Sen's\ Slope = median\left(\frac{x_j - x_i}{j-i} : i < j\right) \quad \text{(Eq. 4.7)}$$

$$S = median\left(x_j - x_i\right) \quad \text{(Eq. 4.8)}$$

A 1–α confidence interval for Sen's slope can be calculated as (*lower*, *upper*) as:

$$\mathrm{N} = \mathrm{C}(\mathrm{n}, 2) \quad \text{(Eq. 4.9)}$$

$$\mathrm{k} = \mathrm{se} \cdot \mathrm{z}_{\mathrm{crit}} \quad \text{(Eq. 4.10)}$$

$$\mathrm{lower} = \mathrm{m}_{\frac{\mathrm{N-k}}{2}} \quad \text{(Eq. 4.11)}$$

$$\mathrm{upper} = \mathrm{m}_{\frac{\mathrm{N+k}}{2}+1} \quad \text{(Eq. 4.12)}$$

where N is the number of pairs of time series elements (x_i, x_j) where i < j and se = the standard error for the Mann-Kendall test. Also m_h is the h^{th} smallest in the set $\frac{x_j - x_i}{j - i}$ for $i < j$ and z_{crit} is the $1 - \frac{\alpha}{2}$ critical value for the normal distribution. Here, we report results as significant for α values of both 0.05 and 0.1.

The *sens.slope* and *zyp* packages in R were used to determine the Sen's Slope and corresponding confidence interval values for all climate metrics, discharge metrics, and hydrologic signatures evaluated herein. These packages compute both the slope (i.e. linear rate of change) and confidence levels according to Sen's method. Further, the packages compute the upper and lower confidence limits for Sen's slope both with no consideration of autocorrelation (*Sens.slope: Sen's slope. RDocumentation*) and consideration of autocorrelation (Bronaugh et al., 2009). and consideration of autocorrelation (Bronaugh et al., 2009). Sen's slope is useful for non-parametric data and can be computed even if there are gaps or missing values in the dataset (Helsel and Hirsch 1995, page 371). We compute Sen's slope both considering autocorrelation and not considering autocorrelation given that some hydrologic processes may be relevant on an annual basis whereas others may not (Hirsch & De Cicco, 2015).

Three additional packages in R were necessary to complete trend analysis, including *trend*, *robslopes*, and *Kendall* packages. We used a combination of the three packages to compute the Sen's slope, intercept, Kendall-P value, and Zhang Yue-Pilon P value. The P-Value determines the statistical significance of the trend. With a 95% confidence interval, a P-value of 0.05 or smaller returns a statistically significant trend.

We also denote a weak statistically significant trend as any P-value between 0.05 and 0.1, which has a 90% confidence interval.

We also computed the trend of each climate, discharge, and hydrologic signature using linear regression as:

$$Y = \beta_0 + \beta_1 X + \varepsilon \quad \text{(Eq. 4.14)}$$

where β_1 is the slope of the relationship between the climate, discharge, or hydrologic signature, Y calculated at a certain timestep, X is the timestep, β_0 is the intercept, and ε is the error term. The *trend* package in R is used to determine the linear trendline. By using the *stat_smooth* function on the dataset, the trendline is calculated and displayed on the graph. It is recommended to also compute the slope of a linear trendline in addition to Sen's slope for variables that have many zero values, as Sen's slope may return a null trend slope during these instances ((Hammond et al., 2021); (Zipper et al., 2021)). This is particularly important for evaluating near-zero flows.

Finally, we created *Quantile-Kendall* plots to visualize shifts in discharge in Falling Rock and Little Millseat (Hirsch & De Cicco, 2015). Each point plotted on a Quantile-Kendall plot represents the trend line of flow for a given order statistic calculated from a non-exceedance curve over consecutive years. The flow from each day is ordered from 1 to 365 for every year over the period of record, where 1 represents the lowest flow of the year and 365 represents the largest flow of the year. The first order statistic, which is presented furthest left on the Quantile-Kendall plot, represents the trend line of the lowest flow of each year. The next point to the right represents the second order statistic, moving

upward in rank, until the final point, which represents the 365^{th} order statistic (i.e., the annual maximum daily discharge). The color of each point represents the p-value for the Mann-Kendall test for the trend. Red indicates a trend with significance at $\alpha = 0.05$, green indicates a trend with significance at $0.05 < \alpha < 0.1$, and blue indicates the p-value is greater than 0.1. We generated Quantile-Kendall plots for Falling Rock and Little Millseat for water year. This is another measure of shifts in streamflow magnitude over the study period.

Table 4. 1 Summary of climate metrics, discharge metrics, and hydrologic signatures and respective time scales analyzed herein.

Signature	Timescale						
	Half-decadal	Calendar Year	Water Year	Climate Year	Seasonal	Monthly	
Minimum Air Temperature	x	x	x	x	x	x	Climate
Mean Air Temperature	x	x	x	x	x	x	
Maximum Air Temperature	x	x	x	x	x	x	
Total Precipitation	x	x	x	x	x	x	
Minimum flow	x	x	x	x	x		Magnitude
Minimum flow (logarithmic scale)	x	x	x	x	x		
Mean flow	x	x	x	x	x		
Mean flow (logarithmic scale)	x	x	x	x	x		
Maximum flow	x	x	x	x	x		
Maximum flow (logarithmic scale)	x	x	x	x	x		
Days with flow less than 90% exceeded flow	x	x	x	x	x	x	Frequency
Days with flow less than 75% exceeded flow	x	x	x	x	x	x	
Days with flow less than 50% exceeded flow	x	x	x	x	x	x	

Days with flow greater than 25% exceeded flow	x	x	x	x	x	x	
Days with flow greater than 5% exceeded flow	x	x	x	x	x	x	
Days with flow greater than 1% exceeded flow	x	x	x	x	x	x	
No flow days	x	x	x	x	x	x	
Longest consecutive no flow period		x	x	x			Duration
First no-flow day		x					Timing
Slope of the flow duration curve midpoint	x	x	x	x	x	x	Rate of Change
Water budget		x	x	x			

CHAPTER 5 RESULTS

Table 5.1 and 5.2 show the summary statistics from running Mann Kendall tests and Sen's slopes for all climate parameters and hydrologic signatures in Falling Rock and Little Millseat. Dark orange cells represent negative trends with a confidence level of α = 0.05, light orange cells represent negative trends at a confidence level of $0.05 < \alpha < 0.1$, grey cells represent parameters with non-significant confidence levels, light green cells represent positive trends at a confidence level of $0.05 < \alpha < 0.1$, and dark green cells represent positive trends at a confidence level of α = 0.05. The value of Sen's Slope for each parameter is recorded in the cells. Mann Kendall tests and Sen's Slope were not calculated for cells with "---". Trends with Sen's slope of 0 have also been denoted as grey.

We also display P-values and Sen's Slopes for each parameter analyzed herein as individual tables in the Supplementary Information section found at the end of this thesis. In addition, we have generated box plots and bar charts that show changes in each parameter over yearly timescales and overlay Sen's slope values and slopes derived from linear models. We do not display these tables and figures in the main body of the thesis to enhance readability. We present summary figures for magnitude (Fig. 5.1) and streamflow regime (Fig. 5.2) at the end of this chapter.

5.1 Shifts in climate and precipitation in Robinson Forest

5.1.1 Shifts in total precipitation in Falling Rock and Little Millseat

We observed statistically significant trends in total precipitation recorded at the Falling Rock rain gage in February and November with significance of 0.05 and 0.1, respectively (Table S.1 and Fig. 5.1). Both months exhibited decreasing slopes over the duration of the study period, indicating that total monthly precipitation declined over the study period in February and November. No significant trends were observed at the half-decadal, yearly, or season time scales in Falling Rock.

We also observed statistically significant trends in total precipitation recorded at the Little Millseat rain gage in February and November with significance of 0.03 and 0.09, respectively (Table S.2 and Fig. S.2). Both months exhibited decreasing slopes over the duration of the study period, indicating that total monthly precipitation amounts declined over the study period in February and November. No significant trends were observed at the half-decadal, yearly, or season time scales.

Taken together, our results indicate little change in total precipitation amounts over the period of record between 1980 and 2015 in both catchments. Slopes of trend lines in both Falling Rock and Little Millseat during months with statistically significant shifts in precipitation (February and November) are approximately on the same order of magnitude, which suggests that both catchments received similar amounts of precipitation over the period of record.

5.1.2 Shifts in air temperature in Robinson Forest

We observed statistically significant trends in minimum air temperature in Robinson Forest at the half decadal scale with significance of 0.03 (Table S.3 and Fig. S.3). There were also statistically significant trends at the calendar, water, and climate yearly scales, during the spring season, and in the months of April, May, June, and December with significance of 0.01, 0.05, 0.01, 0.01, 0.07, 0.08, and 0.01 respectively. All time periods exhibited increasing slopes in temperature over the duration of the study period, indicating that air temperature increased over the study period.

We observed statistically significant trends in mean air temperature in Robinson Forest at the half decadal scale with significance of 0.05 (Table S.4 and Fig. S.4). There were also statistically significant trends at the calendar, water, and climate year time scales, during the spring season, and in the months of April, May, and June with significance of 0.01, 0.08, 0.01, 0.03, 0.02, 0.09, and 0.05 respectively. All time periods exhibited increasing slopes over the duration of the study period, indicating that mean air temperature increased over the study period.

There were statistically significant trends in maximum air temperature in Robinson Forest at the calendar and climate year time scales, and in the month of April with significance of 0.03, 0.03, and 0.10 respectively (Table S.5 and Fig. S.5). All time periods exhibited increasing slopes over the duration of the study period, indicating that max air temperatures increased over the study period.

Taken together, minimum, mean, and maximum temperatures each demonstrated statistically significant increasing trends over various time scales. Sen's Slopes ranged

between 0.08 °F/yr and 0.15°F/yr, indicating that temperature increased in the forest between approximately 2.8°F and 5.25°F over the period of record. This has important implications for hydrologic processes and streamflow regime in the catchments given that increased temperature may cause increased potential evapotranspiration on forest hillslopes (Williamson and Barton, 2020) as well as increased water holding capacity in the atmosphere above the forest, given that an approximately 1.8°F increase in atmospheric temperature can increase water holding capacity by nearly 7% (O'Gorman and Muller, 2010), which may affect precipitation intensities. (Williamson & Barton, 2020) as well as increased water holding capacity in the atmosphere above the forest, given that an approximately 1.8 °F increase in atmospheric temperature can increase water holding capacity by nearly 7% (O'Gorman & Muller, 2010), which may affect precipitation intensities.

5.2 Shifts in discharge magnitude in Robinson Forest

5.2.1 Shifts in minimum discharge in Falling Rock and Little Millseat

We observed statistically significant trends in minimum discharge in Falling Rock during the summer season and the months of July, August, and September with significance of 0.06, 0.04, 0.01, and 0.07 respectively (Table S.6 and Fig. S.6). While there were statistically significant trends, the only period with a Sen's slope greater than zero was the month of August with a slope of 0.02. This indicates that minimum streamflow increased in Falling Rock during the month of August. No significant trends were observed at the half-decadal or yearly time scales.

We observed statistically significant trends in minimum discharge in Little Millseat during the water year, winter, and spring seasons with significance of 0.08, 0.06, and 0.05

respectively (Table S.7 and Fig. S.7). The seasonal timescales exhibited decreasing slopes over the duration of the study period, indicating that minimum discharge rates declined over the study period in the winter and spring. No significant trends were observed at the half-decadal or monthly time scales.

One potential reason for differences in trend direction of minimum discharge in Falling Rock and Little Millseat is the aspect of each watershed. Little Millseat's aspect has a higher predominance of south-facing slopes compared to Falling Rock, which may increase the rate of evapotranspiration, as south-facing slopes are recognized to have higher ET rates compared to north-east facing hillslopes (Donaldson et al., 2023). Within the northern hemisphere, southwest facing slopes experience the highest ET rates as they experience peak solar radiation at the hottest point in the day, in the afternoon. Northeastern facing aspects experience less evapotranspiration as they are shaded during the afternoon and early evening (Bennie et al., 2008). Studies show that soils with north/northeast facing aspects are moister and have the capability to absorb more runoff, in-turn reducing the velocity of water entering streams whereas south facing slopes have higher runoff velocities. Additionally, north facing aspects have the capability of growing woody vegetation like Oak trees whereas south facing slopes are better equipped to grow less dense vegetation like grasses (Donaldson et al., 2023). The increased capability for ground cover and moister soils in combination with lower velocities can have a large impact on the permanence of headwater streams. This result is particularly relevant to streamflow permanence because declines in minimum flow may cause streamflow expansion/contraction rates to decrease over time (Mahoney et al., 2023), which may particularly impact ecosystems that are sensitive to changes in streamflow wetting/drying

(e.g., Price et al., 2012). We further discuss implications of structural differences in the catchments in more detail in Section 6 of this thesis. (Mahoney et al., 2023), which may particularly impact ecosystems that are sensitive to changes in streamflow wetting/drying (e.g., (Price et al., 2012)). We discuss implications of structural differences in the catchments in more detail in Section 6 of this thesis.

5.2.2 Shifts in mean discharge in Falling Rock and Little Millseat

We observed statistically significant trends in the mean discharge in Falling Rock during the calendar and water year time scales, winter, and summer seasons, and the months of July, August, October, and December with significance of 0.04, 0.10, 0.07, 0.02, 0.01, 0.02, 0.09, and 0.07 respectively (Table S.8 and Fig. S.8). The winter and month of December had positive slopes. All other time periods had a Sen's slope of 0. This indicates a positive trend in mean discharge for Falling Rock in particular for winter flows. No significant trends were observed at the half-decadal or yearly time scales.

We observed statistically significant trends in mean discharge in Little Millseat during the half decadal, Calendar, Water, and Climate year time scales (Table S.9 and Fig. S.9). Additionally, we observed significant trends for the winter season, and the months of January, August, and September with significance of 0.03, 0.05, 0.00, 0.07, 0.02, 0.04, 0.06, and 0.09 respectively. All statistically significant trends had a positive slope, indicating increasing mean discharge in Little Millseat.

5.2.3 Shifts in maximum discharge in Falling Rock and Little Millseat

We observed statistically significant trends in maximum discharge in Falling Rock during the Water Year, Winter and Spring seasons, and months of January, March, April, July, and December with significance of 0.04, 0.03, 0.04, 0.02, 0.06, 0.08, 0.05, and 0.1

respectively (Table S.10 and Fig. S.10). All statistically significant trends had a positive slope. This indicates a positive increase in maximum discharge for Falling Rock. No significant trends were observed at the half-decadal or yearly time scales.

We observed statistically significant trends in maximum discharge in Little Millseat during the half decadal, calendar, water, and climate year, winter and summer seasons, and the months January, September, October, and December with significance of 0.03, 0.04, 0.02, 0.00, 0.01, 0.03, 0.02, 0.08, 0.09, and 0.02 respectively (Table S.11 and Fig. S.11). All statistically significant trends have a positive slope. This indicates a positive increase in maximum discharge for Little Millseat.

Both Falling Rock and Little Millseat demonstrated statistically significant increases in mean and maximum discharge over the period of record at various timescales. Meanwhile, minimum flows in Little Millseat decreased over the period of record, suggesting that in some catchments large flows increased while small flows decreased, whereas in other catchments like Falling Rock all flows increased. We interpret this to mean that during low flows periods, when the ratio of precipitation to actual evapotranspiration is also low, structural watershed properties, such as aspect and drainage pattern, control trends in discharge magnitude. However, during storm events, when potential evapotranspiration limits actual evapotranspiration because the ratio of precipitation to potential evapotranspiration is high, structural watershed properties control daily streamflow magnitude to a lesser degree.

We found no significant trends with respect to increasing precipitation amounts over the period of record. However, we also observed significantly increasing trends for mean and maximum discharge in both Little Millseat and Falling Rock. It is plausible that

increased temperature may increase water holding capacity of the atmosphere above the forest, which may thus increase the intensities of storm events over the period of record.

5.2.4 Trends in discharge magnitude revealed by Quantile-Kendall plots

Quantile-Kendall plots indicate that statistically significant shifts in discharge extend beyond just the minimum, mean, and maximum flows in each catchment (Fig. 5.1). In Little Millseat, we observed statistically significant increases in several high flow values (i.e., those exceeded less than 5% of the water year) at a rate of nearly 2-3% (Fig. 5.1a, 5.1b, 5.1c). Additionally, max daily discharge values exceeded 50% of the water year were observed to have statistically significant increases at a rate of nearly 2%. In Falling Rock, we observed statistically significant increases in flow across the flow duration curve, with significant increases in both high flows (i.e., those exceeded less than 10% of the water year) at a rate of nearly 2-3% and low flows (i.e., those exceeded between 75% and 95% of the water year) at a rate of nearly 3-5%. Additionally, we observed statistically significant increases in max daily discharge values exceeded approximately 50% of the water year at a rate of 2.5%. Taken together we find that not only are high flows increasing in both catchments, but also a range of flows surrounding the median of each flow duration curve are increasing in both catchments.

5.3 Shifts in frequency of streamflow regime

5.3.1 Shifts in the frequency of no flow days in Falling Rock and Little Millseat

We observed statistically significant trends in no flow days in Falling Rock during the summer and autumn seasons, and the months June, July, August, September, and October with significance of 0.00, 0.02, 0.02, 0.01, 0.00, 0.03, 0.05, and 0.04 respectively (Table S.12 and Fig. S.12). All statistically significant trends had a negative slope. This indicates

a decrease in the number of no flow days for Falling Rock, which implies that the catchment is becoming wetter with time. This is corroborated by the observed increases in low flow magnitude in Falling Rock as increasing magnitude of flows likely decreases the number of no-flow days occurring in the catchment.

We observed statistically significant trends in no flow days in Little Millseat in the winter season, and the months October and November with significance of 0.08, 0.02, and 0.08 respectively (Table S.13 and Fig. S.13). However, all statistically significant trends were found to have a Sen's slope of zero, which suggests that there were no trends in the number of no flow days in Little Millseat.

5.3.2 Shifts in the frequency of low flow days in Falling Rock and Little Millseat

Shifts in the frequency of low flow days in Falling Rock and Little Millseat are recorded in Tables S.14, S.15, S.16, and S.17 and Figs. S.14, S.15, S.16, and S.17.

We observed statistically significant trends in days with average flow less than Q_{90} in Falling Rock during the calendar, water, and climate year, summer and autumn seasons, and the months June, July, August, September, October, and November with significance of 0.01, 0.00, 0.03, 0.00, 0.03, 0.05, 0.01, 0.00, 0.04, 0.04, and 0.04 respectively. All statistically significant trends were found to have negative slopes. We observed statistically significant trends in days with average flow less than Q_{75} in Falling Rock during the calendar and water year, winter, spring, and autumn seasons, and the months, July, August, September, and November with significance of 0.05, 0.02, 0.01, 0.05, 0.06, 0.01, 0.02, 0.03, and 0.09 respectively. The yearly and monthly trends have negative slopes whereas the seasonal trends have a positive slope. In general, we find that there is a decrease in the

frequency of low-flow days in Falling Rock over the period of record, which is consistent with the increasing magnitude of low flows observed in Falling Rock.

We observed several statistically significant trends in days with average flow less than Q_{90} and in days with average flow less than Q_{75}, however all trends were found to have a slope at or near zero, which indicates that little changes in the frequency of low-flow days have occurred over the period of record.

Interestingly, few statistically significant trends in the frequency of no flow regimes and low flow regimes were observed in Little Millseat, suggesting that the frequency of flow regime in Little Millseat is relatively stable. This is seemingly in contrast to the decreases in minimum flow magnitude observed in the catchment. One potential reason why frequency of streamflow regime is relatively stable in the catchment is that surface streamflow may be sustained at the outlet of the catchment perennially from springs (Williamson et al., 2015), which may contribute a small amount of streamflow for most times of the year, and this may maintain the frequency with which low and no flow occurs in the catchment. (Williamson et al., 2015), which may contribute a small amount of streamflow for most times of the year and only dry during prolonged drought periods, and this may maintain the frequency with which low and no flow occurs in the catchment. Furthermore, slight increases in ET over time due to aspect may not significantly impact median and maximum flow events. During low flow events, drier soils from South facing aspects may be more susceptible to streambed drying (Bennie, 2008) which could explain the stability of median and high flow events and variation in low flow events.

5.3.3 Shifts in the frequency of high flow days in Falling Rock and Little Millseat

Shifts in the frequency of high flow days in Falling Rock and Little Millseat are recorded in Tables S.18, S.19, S.20, S.21, S.22, S.23, S.24, and S.25 and Figs. S.18, S.19, S.20, S.21, S.22, S.23, S.24, and S.25.

In Falling Rock, we observed significant trends in the number of days with average flow less than Q_{50} during the calendar and water year, winter and spring seasons, and the months May, July, and December. All trends were found to have a negative slope, indicating that the number of days with average flow less than Q_{50} decreased over the period of record. We also found significant trends in Falling Rock for the number of days with average flow greater than Q_{25}, Q_5, and Q_1 at several timescales, including half decadal, calendar and climate year, seasonal, and monthly timescales. We observed significant trends in spring and summer seasons and in the months of January, May, July, September, and December. All trends calculated for these metrics were found to be positive, indicating that the number of days with high flows increased in Falling Rock over the period of record.

In Little Millseat, we observed significant negative trends in the number of days with average flow less than Q_{50} during the calendar year and in the month of August. We also found significant trends in days with average flow greater than Q_{25} and Q_5 in Little Millseat at several timescales, including climate year, and during the month of May. Trends for the number of days with average flow greater than Q_{25} and Q_5 were positive, indicating that the number of days with high flows increased in Little Millseat over the period of record.

In sum, our results indicate that more frequent high flows occurred in both Falling Rock and Little Millseat over the period of analysis, however trends were less frequently observed in Little Millseat.

5.4 Shifts in timing of first no flow day

Trends in the timing of first no flow in Falling Rock and Little Millseat are recorded in Tables S.26 and S.27 and Fig. S.26 and S.27, however, we did not observe statistically significant trends in the timing of the first no flow day for both Falling Rock and Little Millseat. Future studies might investigate the median date of no flow as opposed to the first no flow day to further assess shifts in the timing of no flow in the forest.

5.5 Shifts in duration of no flow period

We observed statistically significant trends in no flow duration, as represented by the longest consecutive no flow period during a timescale, in Falling Rock during the calendar and water years, summer season, and the months June, July, August, September, and December with significance of 0.02, 0.02, 0.00, 0.06, 0.01, 0.00, and 0.03 respectively (Table S.28 and Fig. S.28). All statistically significant trends have negative slopes, which indicates a decrease in no flow duration in Falling Rock over the period of record, suggesting that the catchment becomes wetter over the period of record.

We observed statistically significant trends in no flow duration in Little Millseat during the water and climate years, winter, spring, and autumn seasons, and the months January, February, May, June, October, and November with significance of 0.05, 0.08, 0.00, 0.01, 0.02, 0.02, 0.03, 0.05, 0.02, 0.00, and 0.00 respectively (Table S.29 and Fig. S.29). The water year and autumn both displayed statistically significant positive trends, whereas other timescales had a Sen's slope of 0. This indicates a slight positive trend in no

flow duration in Little Millseat, which suggests that the length of consecutive no flow periods is increasing over the period of record.

5.6 Shifts in rate of change

5.6.1 Shifts in slope of the midpoint of flow duration curve in Falling Rock and Little Millseat

We observed statistically significant trends in the slope of the midpoint of the flow duration curve in Falling Rock during the calendar year, and the months of January, February, March, July, August, and December with significance of 0.05, 0.06, 0.03, 0.10, 0.03, 0.06, and 0.01 respectively (Table S.30 and Fig. S.30). All statistically significant trends have a positive slope except for February which has a negative slope. This indicates the slope of the midpoint of the flow duration curve increased over the period of record for Falling Rock.

We observed statistically significant trends in the slope of the midpoint of the flow duration curve in Little Millseat during the calendar and water years, winter season, and the months of July, August, and December with significance of 0.06, 0.03, 0.08, 0.04, 0.08, and 0.03 respectively (Table S.31 and Fig. S.31). All statistically significant trends have positive slopes. This indicates the slope of the midpoint of the flow duration curve increased over the period of record for Little Millseat.

5.6.2 Shifts in water budget in Falling Rock and Little Millseat

We observed statistically significant trends in the fraction of precipitation converted into runoff (f_P) in Falling Rock in the calendar, water, and climate years, winter, spring, summer, and autumn seasons, and the months of February, March, May, July, August, and October with significance of 0.02, 0.07, 0.08, 0.03, 0.03, 0.02, 0.10, 0.04, 0.00,

0.01, 0.00, 0.01, and 0.10 respectively (Table S.32 and Fig. S.32). All statistically significant trends have a positive slope or slope of zero. This indicates an increasing trend in the fraction of precipitation converted into runoff over the period of record for Falling Rock, which implies that more runoff is generated in the catchment over time.

We observed statistically significant trends in the fraction of precipitation converted into runoff (f_P) in Little Millseat during winter, and the months of January and April with significance of 0.05, 0.04, and 0.01 respectively. Winter had a slope of 0.00, while January and April each had positive trends, indicating an increasing fraction of precipitation was converted into runoff over the period of record for Little Millseat.

We interpret the increased slope of the midpoint of the flow duration curve and the increased fraction of precipitation converted to runoff to suggest that the rate of drainage has increased in each catchment over time. There are several potential explanations for this. First, it is possible that the increased drainage rate reflects maturity of the forest. As the forest has aged, increased soil macropores may have developed, thus allowing infiltrated precipitation to rapidly transport to the stream network during and after storm events (Guebert & Gardner, 2001). This rapid transport of water through the unsaturated and root zones via macropores could be one reason that each catchment appears to be increasingly flashy with time. A second reason could be a shift in the intensity of precipitation over the period of record. Given increases in temperature, it is plausible that the intensity of precipitation may have shifted as well given increased water holding capacity of the atmosphere. If precipitation intensity increased over the record, it is possible that more runoff was generated during storms and less precipitation infiltrated into deeper groundwater stores, which may release water more slowly to stream networks.

Table 5. 1 Summary statistics of hydrologic signatures in Falling Rock. Values represent the magnitude of Sen's Slope. The color key is shown in Table 5.3, however green cells represent positive trends where orange cells represent negative trends.

Signature	Timescale																					Stream-flow regime
	Half-decadal	Yearly			Seasonal				Monthly													
		Calendar	Water	Climate	W	Sp	Sm	F	Jan	Feb	Mar	Apr	May	Jun	Jul	Aug	Sep	Oct	Nov	Dec		
Minimum Air Temperature	0.75	0.12	0.08	0.12	--	0.13	--	--	--	--	--	0.19	0.16	0.11	--	--	--	--	--	0.17		Climate
Mean Air Temperature	0.5	0.18	0.12	0.18	--	0.09	--	--	--	--	--	0.15	0.13	0.08	--	--	--	--	--	--		
Maximum Air Temperature	--	0.15	--	0.13	--	--	--	--	--	--	--	0.12	--	--	--	--	--	--	--	--		
Total Precipitation	--	--	--	--	--	--	--	--	--	1.47	--	--	--	--	--	--	--	--	1.28	--		
Minimum flow	--	--	--	--	--	--	0.00	--	--	--	--	--	--	--	0.00	0.02	0.00	--	--	--		Magnitude
Minimum flow (logarithmic scale)	--	--	--	--	--	--	0.00	--	--	--	--	--	--	--	0.00	0.02	0.00	--	--	--		
Mean flow	--	0.00	0.01	--	0.01	--	0.00	--	--	--	--	--	--	--	0.00	0.00	--	0.00	--	0.01		
Mean flow (logarithmic scale)	--	0.00	0.01	--	0.01	--	0.00	--	--	--	--	--	--	--	0.00	0.00	--	0.00	--	0.01		
Maximum flow	--	--	0.03	--	0.04	0.04	--	--	0.06	--	0.03	0.05	--	--	0.06	--	--	--	--	0.04		
Maximum flow (logarithmic scale)	--	--	0.03	--	0.04	0.04	--	--	0.06	--	0.03	0.05	--	--	0.06	--	--	--	--	0.04		
No flow days	--	--	--	--	--	--	0.31	0.09	--	--	--	--	--	0.00	0.00	0.11	0.00	0.00	--	0.00		Frequency
Days with < 90% exceeded flow	--	2.15	2.39	1.75	--	--	1.57	1.04	--	--	--	--	--	0.04	0.52	0.67	0.38	0.30	0.00	--		
Days with < 75% exceeded flow	--	2.13	2.22	--	1.40	1.36	--	0.00	--	--	--	--	--	--	0.48	0.33	0.25	--	0.00	--		
Days with < 50% exceeded flow	--	1.86	1.81	--	0.7	0.43	--	--	--	--	--	--	0.33	--	0.15	--	--	--	--	0.29		

Days with > 25% exceeded flow	39.5	1.21	--	1.15	--	0.63	0.15	--	0.25	--	--	--	0.28	--	0.09	--	--	--	--	0.29	
Days with > 5% exceeded flow	13	0.18	--	--	--	--	--	--	0.08	--	--	--	--	--	--	--	--	--	--	0.00	
Days with > 1% exceeded flow	3.67	0.09	0.1	0.11	0.04	--	--	--	0.00	--	--	--	--	--	--	--	0.00	--	--	--	
Longest consecutive no flow period	--	0.32	0.33	--	--	--	0.24	--	--	--	--	--	--	0.00	0.00	0.11	0.00	--	--	0.00	Duration
First no-flow day	NA	--	--	--	NA	NA	NA	NA	NA	NA	NA	NA	NA	NA	NA	NA	NA	NA	NA	NA	Timing
Slope of the FDC midpoint	--	0.0002	--	--	--	--	--	--	0.0004	0.0004	0.0005	--	--	--	0.0001	0.00003	--	--	--	0.005	Rate of Change
Water budget	**--**	**0.00**	**0.00**	**0.00**	**0.01**	**0.01**	**0.00**	**0.00**	**--**	**0.01**	**0.01**	**--**	**0.01**	**--**	**0.00**	**0.00**	**--**	**0.00**	**--**	**--**	

Table 5. 2 Summary statistics of hydrologic signatures in Little Millseat. Values represent the magnitude of Sen's Slope. The color key is shown in Table 5.3.

Signature	Timescale																				Stream-flow regime
	Half-decadal	Yearly			Seasonal				Monthly												
		Calendar	Water	Climate	W	Sp	Sm	F	Jan	Feb	Mar	Apr	May	Jun	Jul	Aug	Sep	Oct	Nov	Dec	
Minimum Air Temperature	0.75	0.12	0.08	0.12	--	0.13	--	--	--	--	--	0.19	0.16	0.11	--	--	--	--	--	0.17	Climate
Mean Air Temperature	0.5	0.18	0.12	0.18	--	0.09	--	--	--	--	--	0.15	0.13	0.08	--	--	--	--	--	--	
Maximum Air Temperature	--	0.15	--	0.13	--	--	--	--	--	--	--	0.12	--	--	--	--	--	--	--	--	
Total Precipitation	--	--	--	--	--	--	--	--	--	0.76	--	--	--	--	--	--	--	--	1.02	--	
Minimum flow	--	--	0.00	--	0.05	0.02	--	--	--	--	--	--	--	--	--	--	--	--	--	--	Magnitude
Minimum flow (log scale)	--	--	0.00	--	0.05	0.02	--	--	--	--	--	--	--	--	--	--	--	--	--	--	
Mean flow	0.12	0.01	0.01	0.01	0.02	--	--	--	0.03	--	--	--	--	--	--	0.03	0.03	--	--	0.03	
Mean flow (log scale)	0.12	0.01	0.01	0.01	0.02	--	--	--	0.03	--	--	--	--	--	--	0.03	0.03	--	--	0.03	
Maximum flow	0.3	0.03	0.03	0.05	0.04	0.04	--	--	0.04	--	--	--	--	--	--	--	0.04	0.04	--	0.06	
Maximum flow (log scale)	0.3	0.03	0.03	0.05	0.04	0.04	--	--	0.04	--	--	--	--	--	--	--	0.04	0.04	--	0.06	
No flow days	--	--	--	--	0.00	--	--	--	--	--	--	--	--	--	--	--	--	0.00	0.00	--	Frequency
Days with < 90% exceeded flow	--	--	--	--	0.00	--	--	--	--	--	--	--	0.00	--	--	0.19	--	--	--	0.00	
Days with < 75% exceeded flow	--	--	--	--	--	0.00	--	--	--	--	--	--	--	--	--	--	--	--	--	--	
Days with < 50% exceeded flow	--	0.93	--	--	--	--	--	--	--	--	--	--	--	--	--	0.00	--	--	--	--	
Days with > 25% exceeded flow	--	--	--	--	--	--	--	--	--	--	--	--	0.18	--	--	--	--	--	--	--	

Days with > 5% exceeded flow	--	--		--	0.22	--	--	--	--	--	--	--	--	--	--	--	--	--	--	--	--	--	--	--	--	
Days with > 1% exceeded flow	--	--	--	--	--	--	--	--	--	--	--	--	--	--	--	--	--	--	--	--	--	--				
Longest consecutive no flow period	--	--		0.08	0.00	0.00	0.00	--	0.04	0.00	0.00	--	--	0.00	0.00	--	--	--	0.00	0.00	--	Duration				
First no-flow day	--	--	--	--	--	--	--	--	--	--	--	--	--	--	--	--	--	--	--	--	--	Timing				
Slope of the FDC midpoint	--	0.0002	0.0002	--	0.0002	--	--	--	--	--	--	--	--	--	0.0001	0.0004	--	--	--	0.0004	Rate of Change					
Water budget	--	--	--	--	**0.00**	--	--	--	**0.04**	--	--	**0.03**	--	--	--	--	--	--	--	--						

Table 5. 3 Color key for Tables 5.1 and 5.2.

Key	
Negative trend	P < 0.05
Negative trend	0.05 < P < 0.1
No trend	P > 0.1
Positive trend	0.05 < P < 0.1
Positive trend	P < 0.05

Figure 5. 1 Quantile-Kendall plots for Falling Rock and Little Millseat. Figs. (a), (b), and (c) show plots for maximum, mean, and minimum daily flow for Little Millseat at the water year time scale. Figs (d), (e), and (f) show plots for maximum, mean, and minimum daily flow for Falling Rock at the water year time scale. Red points represent trends with significance of $\boldsymbol{\alpha} < 0.05$, green points represent trends with significance of $0.05 < \boldsymbol{\alpha} < 0.1$, and blue points represent trends with significance of $\boldsymbol{\alpha} > 0.1$. Plots generally indicate statistically significant increases in flow for flows exceeded less than 5% of the water year in Little Millseat. Plots indicate statistically significant increases in flow throughout the flow duration curve in Falling Rock, with significant increases in both high (exceeded less than 10% of the water year) and low flows (exceeded between 75% and 95% of the water year).

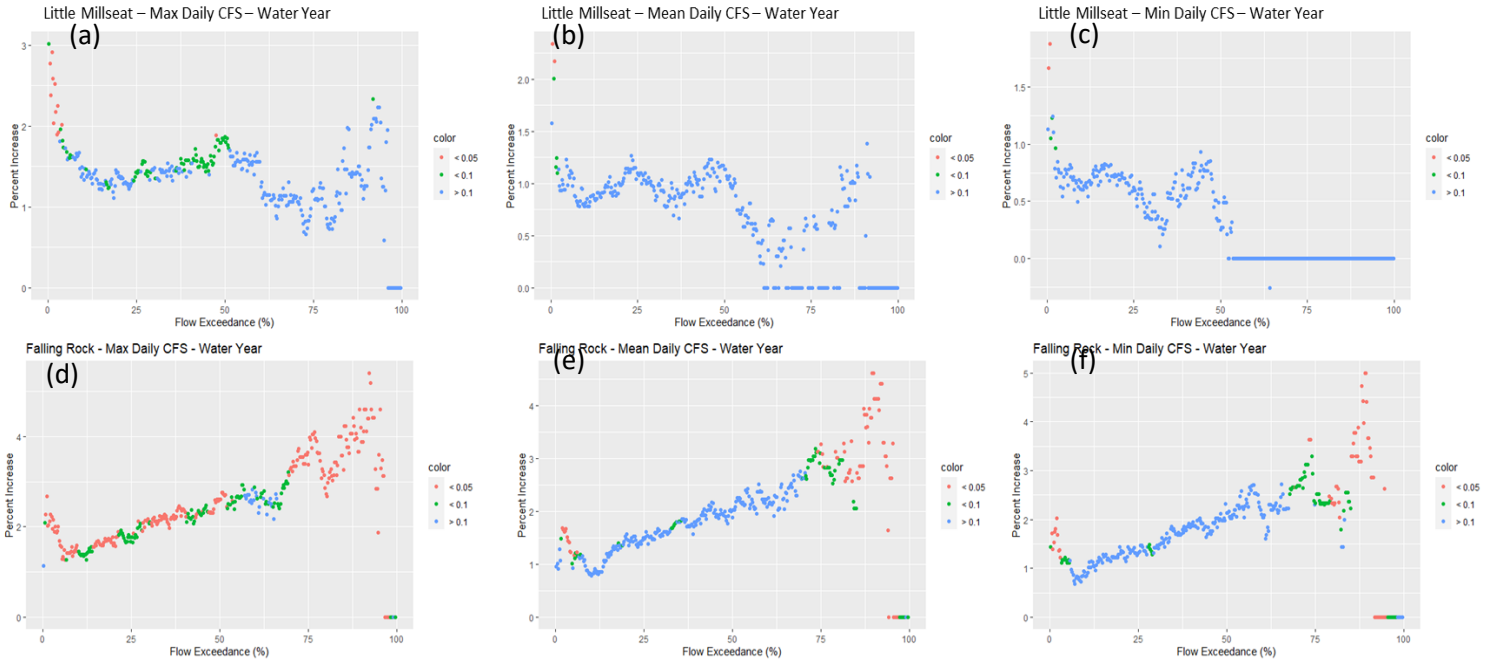

Figure 5. 2 Summary of changes in frequency, magnitude, duration, and rate of change in Falling Rock and Little Millseat. No changes in timing were observed. Frequency is represented by the number of no flow days occurring in a given time period. Trends in frequency are presented for the summer season. Duration is represented by the longest consecutive no flow period in a given time period. Trends in duration are presented for the water year. Magnitude is represented by shifts in minimum and maximum flows. Trends in minimum flows are presented for the winter season and trends in maximum flows are presented for the water year. Rate of change is represented by the slope of the midpoint of the flow duration curve. Trends in rate of change are presented for the calendar year.

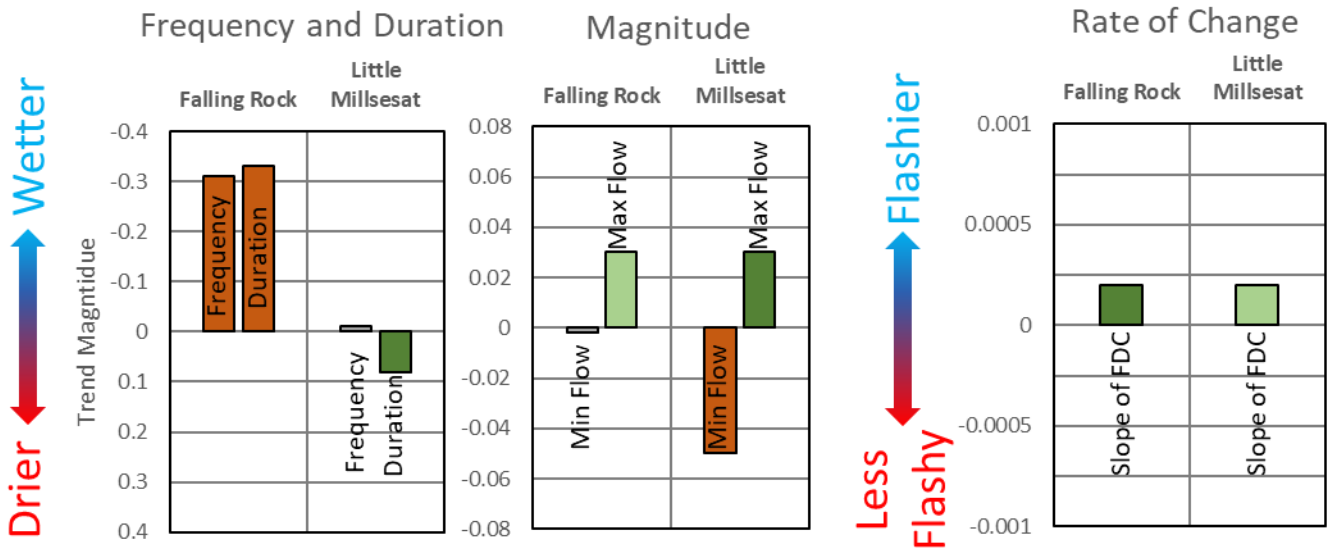

CHAPTER 6 DISCUSSION

6.1 Structural differences in discharge trends in Robinson Forest

We observed statistically significant decreasing trends in precipitation volume for both Falling Rock and Little Millseat during the months of February and November and no statistically significant values at the half-decadal, yearly, or seasonal scales. The decreasing trends indicate that both Falling Rock and Little Millseat are becoming drier during those two months from year to year but are not experiencing changes in precipitation at other timescales. Since there are generally no statistically significant yearly or half-decadal trends, we are unable to conclude that total precipitation shifted over the period of record in Robinson Forest. However, Robinson Forest exhibits statistically significant increases in minimum, mean, and maximum air temperature over most timesteps indicating warming of air temperatures in the forest. We did not observe significant differences in climate variables at Falling Rock and Little Millseat, which leads us to believe the structural properties of each watershed and the overall climate trends for Robinson Forest are the primary drivers of the differences in flow regime in each catchment.

Differences in the trends of streamflow regime in Falling Rock and Little Millseat may be attributed to differences in aspect, slope, or other structural properties of each catchment. Little Millseat's trellis-like structure is more steeply sloped than Falling Rock, which may drain runoff with higher velocities compared to Falling Rock. This could contribute to the decreasing magnitude of minimum flows that was observed in Little

Millseat over the study period as well as the increased duration of no flow. Additionally, the aspect of Falling Rock is split somewhat evenly between north, south, east, and westward facing slopes whereas the aspect of Little Millseat is split with mainly north and south facing slopes. Generally

within the northern hemisphere, solar radiation and ET are distributed asymmetrically with drier slopes occurring on south and southwest-facing slopes due to maximum air temperatures occurring during the afternoon ((Perring,1959);(Davis,1982).) within the northern hemisphere, solar radiation and ET are distributed asymmetrically with drier slopes occurring on south and southwest-facing slopes due to maximum air temperatures occurring during the afternoon ((Perring,1959); (Davis,1982)).Donaldson et al. (2023) determined that increased solar radiation correlated with a decrease in the presence of tree cover. This could in-turn dry out soils and contribute to higher ET of intermittent streams resulting in less streamflow permanence during low flow events from one catchment to another. Given that larger portions of Little Millseat have south and southwest facing aspects compared to Falling Rock, this could explain why Little Millseat may be experiencing drying trends in the lowest flow metrics while Falling Rock does not.

6.2 Shifts in streamflow regime in Robinson Forest

6.2.1 Shifts in streamflow frequency

No flow fraction

Both Falling Rock and Little Millseat have statistically significant values for the no flow fraction metric occurring at the seasonal and monthly scale, however the slope of the trendline for Falling Rock was negative and for Little Millseat was zero. This indicates

that the streamflow permanence in Falling Rock could be increasing whereas the streamflow permanence of Little Millseat may not be changing. With a decrease in the number of no flow days over time, Falling Rock is experiencing flow within the catchment at a higher ratio from year to year. The notable periods in which we observed changes in no flow fraction for Falling Rock include the summer and autumn which encompass the months of June to October, typically leaf-on periods. Since the forest remains undisturbed, the growth of trees and other foliage over time may become more effective at shading the stream and therefore preventing water loss from evaporation, however transpiration may also increase during this period. The statistically significant no flow trends occurring at Little Millseat happen during the winter season, including the months of October and November, which are typically leaf-off periods. The slopes of these trendlines are zero denoting no changes in no flow days over time. The statistically significant values occurring in different seasons for Falling Rock and Little Millseat may explain why we see variations in trends in one catchment over another as leaf-on and leaf-off periods impact ET and streamflow permanence differently (Warter et al., 2023).

Low-flow metrics

Both Falling Rock and Little Millseat experience statistically significant decreases in days with flow less than Q_{90}. Falling Rock experienced decreasing trends at the calendar year, water year, and climate year scales as well as during the summer and autumn seasons including the months from June to November whereas Little Millseat experienced statistically significant decreases in the month of August. The magnitude of the trends at Falling Rock are higher than the magnitude of trends at Little Millseat as well. Both catchments exhibit these trends during leaf-on periods corresponding to the timing of the

decrease in no flow days at Falling Rock. Decreases in low flow days would indicate that the streams are becoming wetter during the summer and autumn months at both sites and yearly for Falling Rock. This may be a result of increased cover and forest density during leaf-on periods preventing excess evaporation or may be a result of shifting precipitation intensities.

We observed statistically significant decreases in days with flow less than Q_{75} at the calendar year and water year scales as well as during the months of July, August, September, and November in Falling Rock. We simultaneously observed statistically significant increases in days with flow less than Q_{75} during the winter and spring seasons. Little Millseat observed a singular statistically significant value with a slope of zero during the spring season. These trends indicate that generally, Falling Rock is experiencing a decrease in low flows, specifically during the summer and autumn months but during the winter and spring there is an increase in low-flow days resulting in higher streamflow permanence in summer and autumn months and less permanence in the winter and spring. We draw no conclusions for Little Millseat as there were not notable trends.

We observed decreases in days with flow less than Q_{50} for both Falling Rock and Little Millseat at the calendar year scale, with Falling Rock experiencing higher magnitudes in trends. Falling Rock additionally experiences decreasing trends during the winter and spring seasons as well as the months of May, July, and December. These trends indicate that at the calendar year scale, both sites are experiencing an increase in median flow over time, coinciding with the decreases in minimum flow values as discussed above. Differences in statistically significant flow frequency trends in Falling Rock and Little Millseat may again be attributed to differences in structural properties including aspect or

slope. Little Millseat's smaller trellis-like drainage area has steeper slopes than Falling Rock which may drain runoff quicker and at higher velocities. Paired with south facing aspects which are generally drier and are correlated with higher runoff velocities (Bennie et al., 2008), quicker runoff times through the Little Millseat catchment may be observed.

High-flow metrics

Falling Rock experiences increasing trends in days with flow greater than Q_{25} at the half decadal, calendar and climate year scales as well as during the Spring and Summer and the months January, May, July, and December. Little Millseat experiences increasing trends in days with flow greater than Q_{25} during the month of May. These trends indicate that both Falling Rock and Little Millseat experience an increase in the frequency of days with high flows over time, with Falling Rock experiencing these trends at higher magnitudes.

Falling Rock and Little Millseat both experience increases in days with flow greater than Q_5 but the statistically significant values occur at different timescales. There are statistically significant positive values for Falling Rock at the half-decadal and calendar year scale as well as during the months of January and December whereas Little Millseat only experiences increasing trends at the Climate year scale. Both catchments experience the trend at similar magnitudes. It is important to note that the increasing trends of days with flow greater than Q_5 for both sites are occurring at smaller magnitudes than the increase in days with flow greater than Q_{25}. The smaller increasing magnitude from Q_{25} to Q_5 shows the extent of the magnitude change for both watersheds.

Falling Rock experiences statistically significant increases in the frequency of days with flow greater than Q_1 whereas Little Millseat experiences no statistically significant trends in days with flow greater than Q_1. We observe these statistically significant trends at the half-decadal, calendar, water, and climate year scales, during the winter and the months of January and September. The magnitude of these trends is similar to the magnitude of trend in days with flow greater than Q_5. From these results, we can conclude that Falling Rock is experiencing increases in the frequency of the highest flow events year to year throughout the study period. This may be attributed to the steeper slopes in Little Millseat, which may allow for water to quickly drain out of the catchment.

In sum, we find that the frequency of high flow events tended to increase in each catchment, although these were more pronounced in Falling Rock, which had a dendritic drainage pattern and slightly flatter slopes.

6.2.2 Duration

We observed statistically significant decreasing trends within the longest no-flow period at Falling Rock. These trends occurred at the calendar and water year scales as well as during the summer and the months June, July, August, September, and December. Conversely, we observed statistically significant increasing trends within the longest no-flow period in Little Millseat at the water year scale and during autumn. These trends indicate that Falling Rock's streamflow permanence may be increasing over time whereas Little Millseat's may be decreasing. The structural properties of each catchment may be contributing to these opposing trends as each catchment has differing stream configuration, shape, slopes, and opposing aspects. The more dendritic Falling Rock has milder slopes and a more prominent southwesterly facing aspect as well as a slightly larger drainage area.

These variables may cultivate slower moving runoff that takes longer to drain after storm events causing more permanent flow. Little Millseat, on the other hand, has steeper, more connected slopes that may drain more quickly with minimal changes to streamflow permanence. Furthermore, the enhanced ET that the catchment experiences due to its aspect may result in longer durations of no flow.

6.2.3 Timing

We did not observe statistically significant trends in the timing of the first no-flow day for Falling Rock or Little Millseat over the study period. Through this analysis we can conclude that there is no statistically significant linear trend in the timing of the first no-flow day at either catchment, and this indicates that drying does not occur earlier or later in the year over the period of record. Future studies might investigate the median date of no flow as opposed to the first no flow day to further assess shifts in the timing of no flow in the forest.

6.2.4 Magnitude

Minimum Discharge

We observed statistically significant slightly positive trends in minimum flow at Falling Rock and slightly negative trends in minimum flow at Little Millseat. These trends indicate that streamflow permanence om Falling Rock may be increasing over time whereas streamflow permanence in Little Millset may be decreasing over time. The structural properties of each watershed may be contributing to the opposing discharge trends at each catchment. As discussed previously, Falling Rock and Little Millseat have different shapes, slopes, and aspects which contribute to the way runoff accumulates. Increased ET in Little Millseat may be occurring due to the south facing aspect as opposed to the variation in

aspect of Falling Rock. We also observe from the other metrics, namely high-flow metrics, and the duration metric, that Little Millseat's streamflow permanence may be decreasing. A decreasing trend in minimum discharge corroborates this finding.

Maximum discharge

We observed statistically significant increases in maximum discharge at both Falling Rock and Little Millseat. These trends occurred at the climate year scale as well as in the spring for both catchments with Falling Rock also experiencing positive trends in Winter and during the month of January and with Little Millseat experiencing positive trends at the water year scale. These trends are particularly interesting as the statistically significant trends in temperature are positive across the board and the statistically significant trends in precipitation are negative in the months of February and November. Typically increases in temperature and decreases in precipitation can contribute to drought-like conditions as ET increases, however increases in temperature also increase water holding capacity of the atmosphere, and thus precipitation intensities may have shifted over the record. One explanation for the increase in peak discharge could be an increase in intensity of storm events in the catchments. Further research into changes in rainfall intensity could explain why peak discharge values are increasing over time for both catchments, however hourly data to facilitate this analysis is not currently available.

6.2.5 Rate of change

Slope of the Midpoint of the Flow Duration Curve

Both Falling Rock and Little Millseat returned statistically significant increasing values for the slope of the midpoint of their Flow Duration Curves at the yearly, seasonal,

and monthly scales. These trends indicate that over time, the catchments are becoming flashier. The time it takes for precipitation to drain out of a watershed is often a function of land use, land cover, soil type, slope, rainfall intensity, and watershed area. For Falling Rock and Little Millseat, few changes in the land use/land cover and slope have occurred over the study period as the site has been left relatively undisturbed for the purpose of research and reforestation and there are not definitive trends regarding the precipitation volume varying from year to year.

Water Budget

We observed statistically significant increases in the f_P ratio representing the fraction of precipitation becoming runoff over a period for both Falling Rock and Little Millseat. The trend was more pronounced in Falling Rock compared to Little Millseat, however, there is significance in Little Millseat in winter and several months. It is noteworthy that in general f_P trended positively in FR during many timescales. This may be related to the amount of ET that occurs in each catchment given that Falling Rock has aspects in all directions and Little Millseat is primarily south and north facing aspect.

We interpret the increased slope of the midpoint of the flow duration curve and the increased fraction of precipitation converted to runoff to suggest that the rate of drainage has increased in each catchment over time. There are several potential explanations for this. First, it is possible that the increased drainage rate reflects maturity of the forest. As the forest has aged, increased soil macropores may have developed, thus allowing infiltrated precipitation to rapidly transport to the stream network during and after storm events (Guebert and Gardner, 2001). This rapid transport of water through the unsaturated and root zones via macropores could be one reason that each catchment appears to be

increasingly flashy with time. A second reason could be a shift in the intensity of precipitation over the period of record. Given increases in temperature, it is plausible that the intensity of precipitation may have shifted as well, given the increased water holding capacity of the atmosphere due to temperature increases. If precipitation intensity increased over the record, it is possible that more runoff was generated during storms and less precipitation infiltrated into deeper groundwater stores, which may release water more slowly to stream networks.

6.3 Comparison of shifts in streamflow regime in Robinson Forest with other catchments

We compared the results from this study with similar assessments of streamflow regime completed at the CONUS and international scale. Previous studies suggest that the number of zero-flow days has increased across much of CONUS ((Jaeger et al., 2014); (Sauquet et al., 2021); (Zipper et al., 2023)). For example, Sauquet et al. (2021) generally found regional increases in the fraction of no-flow days in the eastern US. This finding is corroborated by Zipper et al. (2021) who found that drying trends emerged (as opposed to wetting trends) in the Eastern Forests region of the US. While this may be true at regional scales, our results suggest that trends in streamflow permanence and low flow regimes may vary catchment to catchment, and this may largely be due to structural configurations of the catchment. Future studies might further investigate the controls of intra-catchment variability in streamflow regime at regional scales.

A number of studies suggest that the ratio of precipitation to potential evapotranspiration is an important predictor of the number of no-flow days in a non-perennial stream, and the findings from our study corroborate this idea (e.g., (Hammond et al., 2021); (Sauquet et

al., 2021); (Zipper et al., 2021)). We found that structural differences in the two catchments analyzed herein may impact the rate of ET occurring in each catchment, and this explained the differences in the trend of low flow magnitude and duration in each catchment.

Our study is potentially unique for several reasons. First, most catchments analyzed in previous studies have contributing areas greater than 4-km^2 (e.g., (Sauquet et al., 2021); (Zipper et al., 2021)). Our catchments each have drainage areas of less than 1-km^2, yet have been previously classified as perennial (Mahoney et al., 2023). This suggests that in certain regions of the US, such as central Appalachia, the drainage area threshold required to maintain surface streamflow permanence may be lower than other regions of CONUS. Second, while the southern Appalachian region has been represented in previous studies ((Hammond et al., 2021); (Price et al., 2021); (Sauquet et al., 2021); (Zipper et al., 2021)), central Appalachia has seldom been included in such analyses. Taken together, our study characterizes shifts in streamflow regime at a relatively small spatial scale compared to other studies and in a relatively unstudied region of CONUS.

6.4 Limitations and opportunities

This study had several noteworthy limitations. We primarily used linear trend analysis methods to draw conclusions regarding the impacts of climate change on streamflow permanence given its prominence in the literature (Ward et al., 2020), however a more comprehensive analysis would also explore the use of non-linear trend tests. Within climate science, several researchers (e.g., Franzke, 2014) have also used nonlinear methods such as polynomial least squares regression models, exponential trendlines, and Monte Carlo methods to quantify climate change more robustly. However, it is noteworthy that we used

both the logarithmic and non-logarithmic scales for discharge data as a first attempt to quantify non-linear trends, however additional analyses could be completed.

We utilized one of the most comprehensive hydrologic datasets collected in headwater streams on the central Appalachian Plateau to conduct this analysis. However, there were still several periods of missing data, most notably the gap from 1994 to 1999 in Little Millseat discharge data. Furthermore, only daily precipitation amounts are currently publicly available. Analysis of shifts in precipitation intensity is required to corroborate several of the findings from this study. Additionally, discharge data analyzed herein was collected on streams classified as perennial (e.g., Mahoney et al., 2023). No analyses were performed on intermittent or ephemeral streams, and it is plausible that climate change may impact these low order stream more so than perennial reaches (Zipper et al., 2021). Taken together, this indicates that more data is required to better quantify shifts in streamflow regime on headwater reaches, and researchers should focus efforts on increasing hydrologic and climate monitoring in headwater catchments in coming years. We utilized one of the most comprehensive hydrologic datasets in headwater streams on the central Appalachian Plateau to conduct this analysis. However, there were still several periods of missing data, most notably the gap from 1994 to 1999 in Little Millseat discharge data. Additional data will be crucial to further corroborating the trends observed herein. While the dataset was used was very robust and allowed us to complete a thorough exploration of trends in Robinson Forest, there were still several limitations and lessons to be learned from this analysis. Namely, this study aimed to complete a basic trend analysis on several subsets of data for both catchments. Within this analysis, there is still room to complete a much more comprehensive analysis if the use of non-linear trends were to be explored. We

chose to use linear models as this is by far the most popular and approachable analysis that can be completed. Within climate science though, may researchers (Franzke, 2014) are also using nonlinear methods such as polynomial least squares regression models, exponential trendlines, Monte Carlo methodologies to quantify climate change more effectively. It is important to note that we used both the logarithmic and non-logarithmic scales for discharge data to mitigate error within the flow analysis. In terms of how the data was subset, we attempted to utilize the most comprehensive datasets and fill in missing values from other gauges to prevent as much error as possible, but there were still several periods missing data, most notably the gap from 1994 to 1999 in Little Millseat discharge data. A more accurate analysis might have been completed if we had that extra half-decade of data available.

Additional data and analysis are required to confirm if the trends observed in Robinson Forest extend to the rest of the Cumberland plateau. While the catchments analyzed herein have been relatively undisturbed over the last 100 years, the forests were clear cut in the early 1900s, and thus shifts in streamflow regime may also be attributed to forest maturity. While much of the region has been previously logged or mined, analysis of shifts in streamflow regime in old-growth forests would aid in this analysis.

Finally, given the scarcity of data and studies on headwater streams within this region, we emphasize the need for the establishment of additional long-term study sites and investigation of streamflow regime in headwater systems. While this study primarily focused on examining flow regimes through the lens of low flows, we have observed numerous shifts in the frequency and magnitude of high flows in Robinson Forest. This has important implications for flooding in the area. Future studies should better elucidate

the controls of flood generation throughout the region and focus on monitoring flow regime further up into the catchment on smaller streams.

CHAPTER 7 CONCLUSION

The objective of this study was to quantify shifts in frequency, magnitude, duration, and timing of streamflow regime in two headwater catchments with relatively little disturbance on the Cumberland Plateau using a suite of emerging hydrological statistics and trend analyses. This study determined that within second growth deciduous forests on the Cumberland Plateau, there are statistically significant increases in minimum, mean, and maximum air temperatures but not in precipitation depth over the period of record. While this should theoretically increase ET and subsequently decrease streamflow permanence, streamflow regime in each catchment differed in its response. In Falling Rock we observed an increase in the frequency, magnitude, and duration of streamflow permanence over the period of record as the trends denote fewer no-flow days each year, shorter periods of consecutive no-flow, increasing discharge magnitudes, and increasing runoff as discharge in water budgets. In Little Millseat, we observed a decrease in streamflow magnitude during low flow periods and an increasing the duration of no flow, suggesting that streamflow permanence has decreased in the catchment over the period of record. We also observed an increase in the frequency and magnitude of high flow events in Little Millseat over the period of record. This suggests that in Falling Rock, both low and high flows have increased over the period of record, whereas in Little Millseat, low flows have become lower and high flows have become higher. Climate and ET may have a significant impact on processes impacting streamflow permanence in each

catchment as the major structural differences between the two catchments are slope and aspect. Given that larger portions of Little Millseat have south and southwest facing aspects, which generally have increased ET and drying rates, this could explain why Little Millseat may be experiencing drying trends in the lowest flow metrics while Falling Rock does not. Additional analyses are required to determine if these trends extend to the remainder of the Cumberland Plateau. However, this study demonstrates several of the dominant processes impacting changes in streamflow regime on Cumberland Plateau, and this knowledge may aid in enhancing the protection of vulnerable headwater streams in the region in years to come.

REFERENCES

Abney, R., Gaur, N., Levi, M. R., and Hawkins, G. L. (2022). Forest land use and soil hydrology. *Soil Hydrology in a Changing Climate*, 157.

Addor, N., Nearing, G., Prieto, C., Newman, A. J., Le Vine, N., and Clark, M. P. (2018). A Ranking of Hydrological Signatures Based on Their Predictability in Space. *Water Resources Research*, *54*(11), 8792-8812. https://doi.org/https://doi.org/10.1029/2018WR022606

Al Aamery, N., Fox, J. F., and Mahoney, T. (2021). Variance decomposition of forecasted sediment transport in a lowland watershed using global climate model ensembles. *Journal of Hydrology*, *602*, 126760.

Alexander, R. B., Boyer, E. W., Smith, R. A., Schwarz, G. E., and Moore, R. B. (2007). The role of headwater streams in downstream water quality 1. *JAWRA Journal of the American Water Resources Association*, *43*(1), 41-59.

Arthur, M., Coltharp, G., and Brown, D. (1998). EFFECTS OF BEST MANAGEMENT PRACTICES ON FOREST STREAMWATER QUALITY IN EASTERN KENTUCKY 1. *JAWRA Journal of the American Water Resources Association*, *34*(3), 481-495.

Bennie, J., Huntley, B., Wiltshire, A., Hill, M. O., & Baxter, R. (2008). Slope, aspect and climate: spatially explicit and implicit models of topographic microclimate in chalk grassland. Ecological Modelling, 216(1), 47–59. https://doi.org/10.1016/j.ecolmodel.2008.04.010

Birgand, F., Skaggs, R. W., Chescheir, G. M., and Gilliam, J. W. (2007). Nitrogen removal in streams of agricultural catchments—a literature review. *Critical Reviews in Environmental Science and Technology*, *37*(5), 381-487.

Botter, G., Vingiani, F., Senatore, A., Jensen, C., Weiler, M., McGuire, K., Mendicino, G., and Durighetto, N. (2021). Hierarchical climate-driven dynamics of the active channel length in temporary streams. *Scientific reports*, *11*(1), 21503. https://doi.org/10.1038/s41598-021-00922-2

Bronaugh, D., Werner, A., and Bronaugh, M. D. (2009). Package 'zyp'. *CRAN Repository*.

Cherry, M. (2006). *Hydrochemical characterization of ten headwater catchments in eastern Kentucky (Master's Thesis, University of Kentucky, Lexington, KY).*

Christian, W. J., May, B., and Levy, J. E. (2023). Flood fatalities in eastern Kentucky and the public health legacy of mountaintop removal coal mining. *Journal of Maps*, *19*(1), 2214159. https://doi.org/10.1080/17445647.2023.2214159

Colvin, S. A., Sullivan, S. M. P., Shirey, P. D., Colvin, R. W., Winemiller, K. O., Hughes, R. M., Fausch, K. D., Infante, D. M., Olden, J. D., and Bestgen, K. R. (2019). Headwater streams and wetlands are critical for sustaining fish, fisheries, and ecosystem services. *Fisheries*, *44*(2), 73-91. https://doi.org/10.1002/fsh.10229

Costigan, K. H., Jaeger, K. L., Goss, C. W., Fritz, K. M., and Goebel, P. C. (2016). Understanding controls on flow permanence in intermittent rivers to aid ecological research: integrating meteorology, geology and land cover. *Ecohydrology*, *9*(7), 1141-1153. https://doi.org/https://doi.org/10.1002/eco.1712

Crysler, K. A., L. R. Hoxit, and R. A. Maddox, 1980: A climatology of the flash flood hazard in a four state region of Appalachia. Preprints, Conf. on Flash Floods: Hydrometeorological Aspects and Human Aspects, Boston, MA, Amer. Meteor. Soc., 62-68.

Donaldson, A. M., Zimmer, M., Huang, M.-H., Johnson, K. N., Hudson-Rasmussen, B., Finnegan, N., Barling, N., & Callahan, R. P. (2023). Symmetry in hillslope steepness and saprolite thickness between hillslopes with opposing aspects. Journal of Geophysical Research: Earth Surface, 128(7). https://doi.org/10.1029/2023JF007076

Datry, T., Boulton, A. J., Bonada, N., Fritz, K., Leigh, C., Sauquet, E., Tockner, K., Hugueny, B., and Dahm, C. N. (2018). Flow intermittence and ecosystem services in rivers of the Anthropocene. *Journal of Applied Ecology*, *55*(1), 353-364. https://doi.org/10.1111/1365-2664.12941

Davis,B.N.K., Lakhani,K.H.,1982.Multiple regression models of the distribution of Helianthemum chamaecistus in relation to aspect and slope at Barnack, England. Journal of Applied Ecology19,621–629.

Drayer, A. N., and Richter, S. C. (2016). Physical wetland characteristics influence amphibian community composition differently in constructed wetlands and natural wetlands. *Ecological Engineering*, *93*, 166-174. https://doi.org/10.1016/j.ecoleng.2016.05.028

Dyer, K. L., and Curtis, W. R. (1977). *Effect of strip mining on water quality in small streams in eastern Kentucky, 1967-1975* (Vol. 372). Department of Agriculture, Forest Service, Northeastern Forest Experiment ….

Eisner, S., Flörke, M., Chamorro, A., Daggupati, P., Donnelly, C., Huang, J., Hundecha, Y., Koch, H., Kalugin, A., Krylenko, I., Mishra, V., Piniewski, M., Samaniego, L., Seidou, O., Wallner, M., and Krysanova, V. (2017). An ensemble analysis of climate change impacts on streamflow seasonality across 11 large river basins. *Climatic Change*, *141*(3), 401-417. https://doi.org/10.1007/s10584-016-1844-5

Ekström, M., Gutmann, E. D., Wilby, R. L., Tye, M. R., and Kirono, D. G. C. (2018). Robustness of hydroclimate metrics for climate change impact research. *Wiley Interdisciplinary Reviews: Water*, *5*(4). https://doi.org/10.1002/wat2.1288

Falcone, J. A. (2011). *GAGES-II: Geospatial attributes of gages for evaluating streamflow*.

Franzke, C. L. E. (2014). Nonlinear climate change. *Nature Climate Change*, *4*(6), 423-424. https://doi.org/10.1038/nclimate2245

Fritz, K. M., Hagenbuch, E., D'Amico, E., Reif, M., Wigington Jr, P. J., Leibowitz, S. G., Comeleo, R. L., Ebersole, J. L., and Nadeau, T. L. (2013). Comparing the extent and permanence of headwater streams from two field surveys to values from hydrographic databases and maps. *JAWRA Journal of the American Water Resources Association*, *49*(4), 867-882. https://doi.org/10.1111/jawr.12040

Fritz, K. M., Johnson, B. R., and Walters, D. M. (2006). *Field Operations Manual for Assessing the Hydrologic Permanence and Ecological Condition of Headwater Streams (EPA/600/R-06/126)*.

Fritz, K. M., Johnson, B. R., and Walters, D. M. (2008). Physical indicators of hydrologic permanence in forested headwater streams. *Journal of the North American Benthological Society*, *27*(3), 690-704. https://doi.org/10.1899/07-117.1

Fritz, K. M., Nadeau, T.-L., Kelso, J. E., Beck, W. S., Mazor, R. D., Harrington, R. A., and Topping, B. J. (2020). Classifying streamflow duration: the scientific basis and an operational framework for method development. *Water*, *12*(9), 2545. https://doi.org/10.3390/w12092545

Godsey, S. E., and Kirchner, J. W. (2014). Dynamic, discontinuous stream networks: hydrologically driven variations in active drainage density, flowing channels and stream order. *Hydrological Processes*, *28*(23), 5791-5803. https://doi.org/10.1002/hyp.10310

Goulsbra, C., Evans, M., and Lindsay, J. (2014). Temporary streams in a peatland catchment: pattern, timing, and controls on stream network expansion and contraction. *Earth Surface Processes and Landforms*, *39*(6), 790-803. https://doi.org/10.1002/esp.3533

Guebert, M. D., and Gardner, T. W. (2001). Macropore flow on a reclaimed surface mine: infiltration and hillslope hydrology. *Geomorphology*, *39*(3), 151-169. https://doi.org/https://doi.org/10.1016/S0169-555X(00)00107-0

Guttman, N. B., and D. S. Ezell, 1980: Flash flood climatology for Appalachia. Preprints, Second Conf. on Flash Floods, Atlanta, GA, Amer. Meteor. Soc., 70-72.

Hammond, J. C., Simeone, C., Hecht, J. S., Hodgkins, G. A., Lombard, M., McCabe, G., Wolock, D., Wieczorek, M., Olson, C., Caldwell, T., Dudley, R., and Price, A. N. (2022). Going Beyond Low Flows: Streamflow Drought Deficit and Duration

Illuminate Distinct Spatiotemporal Drought Patterns and Trends in the U.S. During the Last Century. *Water Resources Research*, *58*(9), e2022WR031930. https://doi.org/https://doi.org/10.1029/2022WR031930

Hammond, J. C., Zimmer, M., Shanafield, M., Kaiser, K., Godsey, S. E., Mims, M. C., Zipper, S. C., Burrows, R. M., Kampf, S. K., and Dodds, W. (2021). Spatial patterns and drivers of nonperennial flow regimes in the contiguous United States. *Geophysical Research Letters*, *48*(2), e2020GL090794. https://doi.org/10.1029/2020GL090794

Hill, B. H., Kolka, R. K., McCormick, F. H., and Starry, M. A. (2014). A synoptic survey of ecosystem services from headwater catchments in the United States. *Ecosystem Services*, *7*, 106-115.

Hirsch, R. M., and De Cicco, L. A. (2015). *User guide to Exploration and Graphics for RivEr Trends (EGRET) and dataRetrieval: R packages for hydrologic data* (2328-7055).

Hodgkins, G., Dudley, R., Archfield, S. A., and Renard, B. (2019). Effects of climate, regulation, and urbanization on historical flood trends in the United States. *Journal of Hydrology*, *573*, 697-709. https://doi.org/10.1016/j.jhydrol.2019.03.102

Jaeger, K. L., Olden, J. D., and Pelland, N. A. (2014). Climate change poised to threaten hydrologic connectivity and endemic fishes in dryland streams. *Proceedings of the National Academy of Sciences*, *111*(38), 13894-13899. https://doi.org/10.1073/pnas.1320890111

Jensen, C. K., McGuire, K. J., McLaughlin, D. L., and Scott, D. T. (2019). Quantifying spatiotemporal variation in headwater stream length using flow intermittency sensors. *Environmental monitoring and assessment*, *191*(4), 1-19. https://doi.org/10.1007/s10661-019-7373-8

Jensen, C. K., McGuire, K. J., and Prince, P. S. (2017). Headwater stream length dynamics across four physiographic provinces of the Appalachian Highlands. *Hydrological Processes*, *31*(19), 3350-3363. https://doi.org/10.1002/hyp.11259

Jensen, C. K., McGuire, K. J., Shao, Y., and Andrew Dolloff, C. (2018). Modeling wet headwater stream networks across multiple flow conditions in the Appalachian Highlands. *Earth Surface Processes and Landforms*, *43*(13), 2762-2778. https://doi.org/10.1002/esp.4431

Jones, J. B. (1992). The Development of Coal Mining on Tenessee's Cumberland Plateau, 1880-1930, . *Appalachian Cultural Resources Workshop Papers*.

Kendall, M. G. (1938). A New Measure of Rank Correlation. *Biometrika*, *30*(1/2), 81-93. https://doi.org/10.2307/2332226

Koundouri, P., Boulton, A. J., Datry, T., and Souliotis, I. (2017). Ecosystem services, values, and societal perceptions of intermittent rivers and ephemeral streams. In *Intermittent rivers and ephemeral streams* (pp. 455-476). Elsevier. https://doi.org/10.1016/B978-0-12-803835-2.00018-8

Lane, C. R., Creed, I. F., Golden, H. E., Leibowitz, S. G., Mushet, D. M., Rains, M. C., Wu, Q., D'Amico, E., Alexander, L. C., and Ali, G. A. (2022). Vulnerable waters are essential to watershed resilience. *Ecosystems*, 1-28.

Liang-Liang, L., Jian, L., and Ru-Cong, Y. (2022). Evaluation of CMIP6 HighResMIP models in simulating precipitation over Central Asia. *Advances in Climate Change Research*, *13*(1), 1-13. https://doi.org/https://doi.org/10.1016/j.accre.2021.09.009

Mahoney, D. T., Christensen, J. R., Golden, H. E., Lane, C. R., Evenson, G. R., White, E., Fritz, K. M., D'Amico, E., Barton, C. D., Williamson, T. N., Sena, K. L., and Agouridis, C. T. (2023). Dynamics of streamflow permanence in a headwater network: Insights from catchment-scale model simulations. *Journal of Hydrology*, *620*, 129422. https://doi.org/https://doi.org/10.1016/j.jhydrol.2023.129422

Mann, H. B. (1945). Nonparametric Tests Against Trend. *Econometrica, 13*(3), 245-259. https://doi.org/10.2307/1907187

McMillan, H. (2020). Linking hydrologic signatures to hydrologic processes: A review. *Hydrological Processes*, *34*(6), 1393-1409.

McMillan, H., Westerberg, I., and Branger, F. (2017). Five guidelines for selecting hydrological signatures. *Hydrological Processes*, *31*(26), 4757-4761. https://doi.org/10.1002/hyp.11300

McMillan, H. K. (2021). A review of hydrologic signatures and their applications. *Wiley Interdisciplinary Reviews: Water*, *8*(1). https://doi.org/10.1002/wat2.1499

Meyer, J., Kaplan, L., Newbold, J., Strayer, D., Woltemade, C., Zelder, J., Beilfuss, R., Carpenter, Q., Semlitsch, R., and Watzin, M. (2003). Where rivers are born: the scientific imperative for defending small streams and wetlands. Special Publication of American Rivers and the Sierra Club. In.

Montgomery, W. L., McCormick, S. D., Naiman, R. J., Whoriskey Jr, F. G., and Black, G. A. (1983). Spring migratory synchrony of salmonid, catostomid, and cyprinid fishes in Riviere a la Truite, Quebec. *Canadian Journal of Zoology*, *61*(11), 2495-2502.

Nadeau, T. L., and Rains, M. C. (2007). Hydrological connectivity between headwater streams and downstream waters: how science can inform policy. *JAWRA Journal of the American Water Resources Association*, *43*(1), 118-133. https://doi.org/10.1111/j.1752-1688.2007.00010.x

NASA. (2022, December 23). Educator guide: Modeling the water budget. NASA. https://www.jpl.nasa.gov/edu/teach/activity/modeling-the-water-budget/#:~:text=A%20water%20budget%20is%20an,in%20water%20storage%2C%20and%20evapotranspiration.

O'Gorman, P., and Muller, C. J. (2010). How closely do changes in surface and column water vapor follow Clausius–Clapeyron scaling in climate change simulations? *Environmental Research Letters*, *5*(2), 025207.

Perring,F.,1959.Topographical gradients of chalk grassland. Journal of Ecology 47,447–481.

Poff, N. L., Allan, J. D., Bain, M. B., Karr, J. R., Prestegaard, K. L., Richter, B. D., Sparks, R. E., and Stromberg, J. C. (1997). The Natural Flow Regime. *BioScience*, *47*(11), 769-784. https://doi.org/10.2307/1313099

Poff, N. L., and Ward, J. V. (1989). Implications of Streamflow Variability and Predictability for Lotic Community Structure: A Regional Analysis of Streamflow Patterns. *Canadian Journal of Fisheries and Aquatic Sciences*, *46*(10), 1805-1818. https://doi.org/10.1139/f89-228

Prancevic, J. P., and Kirchner, J. W. (2019). Topographic controls on the extension and retraction of flowing streams. *Geophysical Research Letters*, *46*(4), 2084-2092. https://doi.org/10.1029/2018GL081799

Price, A. N., Jones, C. N., Hammond, J. C., Zimmer, M. A., and Zipper, S. C. (2021). The Drying Regimes of Non-Perennial Rivers and Streams. *Geophysical Research Letters*, *48*(14), e2021GL093298. https://doi.org/https://doi.org/10.1029/2021GL093298

Price, S. J., Browne, R. A., and Dorcas, M. E. (2012). Resistance and resilience of a stream salamander to supraseasonal drought. *Herpetologica*, *68*(3), 312-323.

Rosburg, T. T., Nelson, P. A., and Bledsoe, B. P. (2017). Effects of Urbanization on Flow Duration and Stream Flashiness: A Case Study of Puget Sound Streams, Western Washington, USA. *JAWRA Journal of the American Water Resources Association*, *53*(2), 493-507. https://doi.org/10.1111/1752-1688.12511

Sauquet, E., Shanafield, M., Hammond, J. C., Sefton, C., Leigh, C., and Datry, T. (2021). Classification and trends in intermittent river flow regimes in Australia, northwestern Europe and USA: A global perspective. *Journal of Hydrology*, *597*, 126170.

Sen, P. K. (1968). Estimates of the regression coefficient based on Kendall's tau. *Journal of the American statistical association*, *63*(324), 1379-1389.

Sena, K., Barton, C., Angel, P., Agouridis, C., and Warner, R. (2014). Influence of spoil type on chemistry and hydrology of interflow on a surface coal mine in the eastern US coalfield. *Water, Air, & Soil Pollution*, *225*, 1-14.

Sena, K. L., Barton, C.D, and Williamson, T.N. (2020). *Precipitation and Precipitation Chemistry in Robinson Forest, Breathitt County, Kentucky (1971-2018)* U.S. Geological Survey. https://doi.org/ https://doi.org/10.5066/P9FPLG1O.

Senatore, A., Micieli, M., Liotti, A., Durighetto, N., Mendicino, G., and Botter, G. (2021). Monitoring and modeling drainage network contraction and dry down in Mediterranean headwater catchments. *Water Resources Research*, *57*(6), e2020WR028741. https://doi.org/10.1029/2020WR028741

Shanafield, M., Bourke, S. A., Zimmer, M. A., and Costigan, K. H. (2021). An overview of the hydrology of non-perennial rivers and streams. *Wiley Interdisciplinary Reviews: Water*, *8*(2), e1504. https://doi.org/10.1002/wat2.1504

Simpson, L. C., and Florea, L. J. (2009). The Cumberland Plateau of Eastern Kentucky. *Caves and Karst of America*, *2009*, 70.

Sloan, P. G., Moore, I. D., Coltharp, G. B., and Eigel, J. D. (1983). Modeling surface and subsurface stormflow on steeply-sloping forested watersheds. *Water Resources Research, 20(12),* 1815-1822. https://doi.org/10.1029/WR020i012p01815

Stadnyk, T., Delavau, C., Kouwen, N., and Edwards, T. (2013). Towards hydrological model calibration and validation: Simulation of stable water isotopes using the isoWATFLOOD model. *Hydrological Processes*, *27*(25), 3791-3810. https://doi.org/10.1002/hyp.9695

Strahler, A. N. (1957). Quantitative analysis of watershed geomorphology. *Eos, Transactions American Geophysical Union*, *38*(6), 913-920. https://doi.org/10.1029/TR038i006p00913

Tramblay, Y., Rutkowska, A., Sauquet, E., Sefton, C., Laaha, G., Osuch, M., Albuquerque, T., Alves, M. H., Banasik, K., Beaufort, A., Brocca, L., Camici, S., Csabai, Z., Dakhlaoui, H., DeGirolamo, A. M., Dörflinger, G., Gallart, F., Gauster, T., Hanich, L., Kohnová, S., Mediero, L., Plamen, N., Parry, S., Quintana-Seguí, P., Tzoraki, O., and Datry, T. (2021). Trends in flow intermittence for European rivers. *Hydrological Sciences Journal*, *66*(1), 37-49. https://doi.org/10.1080/02626667.2020.1849708

U.S. EPA. (2011). The effects of mountaintop mines and valley fills on aquatic ecosystems of the central Appalachian coalfields. *Washington, DC*.

U.S. Geological Survey. (2019). *NHDPlusV2 high resolution: National Hydrography Dataset (ver. USGS National Hydrography Dataset (NHD) plus version 2 for the contiguous U.S.)*. https://www.usgs.gov/core-science-systems/ngp/national-hydrography/access-national-hydrography-products

Villines, J. A., Agouridis, C. T., Warner, R. C., and Barton, C. D. (2015). Using GIS to Delineate Headwater Stream Origins in the Appalachian Coalfields of Kentucky. *JAWRA Journal of the American Water Resources Association*, *51*(6), 1667-1687. https://doi.org/10.1111/1752-1688.12350

Ward, A. S., Schmadel, N. M., and Wondzell, S. M. (2018). Simulation of dynamic expansion, contraction, and connectivity in a mountain stream network. *Advances in Water Resources*, *114*, 64-82. https://doi.org/10.1016/j.advwatres.2018.01.018

Ward, A. S., Wondzell, S. M., Schmadel, N. M., and Herzog, S. P. (2020). Climate change causes river network contraction and disconnection in the HJ Andrews Experimental Forest, Oregon, USA. *Frontiers in Water*, *2*, 7. https://doi.org/10.3389/frwa.2020.00007

Warter, M. M., Singer, M. B., Cuthbert, M. O., Roberts, D., Caylor, K. K., Sabathier, R., and Stella, J. (2023). Modeling seasonal vegetation phenology from hydroclimatic drivers for contrasting plant functional groups within drylands of the Southwestern USA. *Environmental Research: Ecology*, *2*(2), 025001.

Whiting, J. A., and Godsey, S. E. (2016). Discontinuous headwater stream networks with stable flowheads, Salmon River basin, Idaho. *Hydrological Processes*, *30*(13), 2305-2316. https://doi.org/10.1002/hyp.10790

Williamson, T. N., Agouridis, C. T., Barton, C. D., Villines, J. A., and Lant, J. G. (2015). Classification of Ephemeral, Intermittent, and Perennial Stream Reaches Using a TOPMODEL-Based Approach. *JAWRA Journal of the American Water Resources Association*, *51*(6), 1739-1759. https://doi.org/10.1111/1752-1688.12352

Williamson, T. N., and Barton, C. D. (2020). Hydrologic modeling to examine the influence of the forestry reclamation approach and climate change on mineland hydrology. *Science of The Total Environment*, *743*, 140605. https://doi.org/https://doi.org/10.1016/j.scitotenv.2020.140605

Witt, E. L., Barton, C. D., Stringer, J. W., Kolka, R. K., and Cherry, M. A. (2016). Influence of variable streamside management zone configurations on water quality after forest harvest. *Journal of Forestry*, *114*(1), 41-51. https://doi.org/10.5849/jof.14-099

Wohl, E. (2018). *The Upstream Extent of a River Network: A Review of Scientific Knowledge of Channel Heads*. U.S. Army Engineer Research and Development Center

Woods, A.J., Omernik, J.M., Martin, W.H., Pond, G.J., Andrews, W.M., Call, S.M., Comstock, J.A. and Taylor, D.D., 2002, Ecoregions of Kentucky (color poster with map, descriptive text, summary tables, and photographs): Reston, VA., U.S. Geological Survey (map scale 1:1,000,000).

World Meteorological Organization. (1989). Calculation of monthly and annual 30-year standard normals. *WCDP 10, WMO-TD 341*.

Zégre, N. P., Maxwell, A., and Lamont, S. (2013). Characterizing streamflow response of a mountaintop-mined watershed to changing land use. *Applied Geography*, *39*, 5-15. https://doi.org/10.1016/j.apgeog.2012.11.008

Zimmer, M. A., and McGlynn, B. L. (2017). Ephemeral and intermittent runoff generation processes in a low relief, highly weathered catchment. *Water Resources Research*, *53*(8), 7055-7077. https://doi.org/10.1002/2016WR019742

Zipper, S. C., Hammond, J. C., Shanafield, M., Zimmer, M., Datry, T., Jones, C. N., Kaiser, K. E., Godsey, S. E., Burrows, R. M., Blaszczak, J. R., Busch, M. H., Price, A. N., Boersma, K. S., Ward, A. S., Costigan, K., Allen, G. H., Krabbenhoft, C. A., Dodds, W. K., Mims, M. C., Olden, J. D., Kampf, S. K., Burgin, A. J., and Allen, D. C. (2021). Pervasive changes in stream intermittency across the United States. *Environmental Research Letters*, *16*(8), 084033. https://doi.org/10.1088/1748-9326/ac14ec

SUPPLEMENTARY INFORMATION:

Supplementary Tables:

Table S.1 Falling Rock Precipitation Statistical Summary Table

Slope	Intercept	P Value	P Value (zyp)	Half Decade	Year	Season	Month
263.40	4213.35	0.26	0.46	Half Decade			
-0.72	2470.15	0.80	0.41		Calendar Year		
-2.53	6110.16	0.57	0.57		Water Year		
-0.30	1632.84	0.92	0.58		Climate Year		
-0.12	469.21	0.93	0.50			Winter	
-0.32	916.11	0.82	0.59			Spring	
0.76	-1242.06	0.60	1.00			Summer	
-1.02	2252.47	0.39	0.38			Autumn	
0.61	-1148.84	0.28	0.28				January
-1.47	3006.46	0.03	0.03				February
-0.90	1893.40	0.24	0.24				March
0.85	-1614.70	0.13	0.13				April
-0.60	1302.89	0.37	0.18				May
0.48	-860.85	0.66	0.66				June
0.71	-1324.53	0.29	0.29				July
-0.04	163.53	0.95	0.67				August
-0.25	588.77	0.81	0.81				September
0.08	-78.87	0.87	0.88				October
-1.28	2635.98	0.09	0.26				November
0.75	-1410.45	0.17	0.38				December

Table S.2 Little Millseat Precipitation Statistical Summary

Slope	Intercept	P Value	P Value (zyp)	Half Decade	Year	Season	Month
20.57	5463.79	0.90	0.90	Half Decade			
2.44	-3753.16	0.41	0.41		Calendar Year		
0.73	-360.00	0.82	0.82		Water Year		
3.49	-5895.32	0.33	0.33		Climate Year		
0.71	-1173.70	0.73	0.39			Winter	
0.71	-1111.98	0.82	0.46			Spring	
0.41	-531.92	0.92	0.55			Summer	
-0.10	426.91	0.57	0.94			Autumn	
0.82	-1564.78	0.29	0.11				January
-0.76	1611.12	0.10	0.22				February
-0.11	304.37	0.55	0.90				March
0.85	-1609.19	0.32	0.12				April
0.64	-1177.56	0.76	0.40				May
0.34	-579.63	0.92	0.71				June
0.55	-991.62	0.87	0.49				July
-0.24	562.83	0.35	0.25				August
0.55	-1011.49	0.95	0.57				September
0.22	-358.75	0.93	0.55				October
-1.02	2112.01	0.09	0.17				November
0.55	-1011.27	0.62	0.91				December

Table S.3 Robinson Forest Minimum Air Temperature Statistical Summary

Slope	Intercept	P Value	P Value (zyp)	Half Decade	Year	Season	Month
0.75	38.45	0.03	0.29	Half Decade			
0.12	-192.39	0.01	0.05		Calendar Year		
0.08	-123.92	0.05	0.05		Water Year		
0.12	-188.30	0.01	0.08		Climate Year		
0.08	-124.70	0.16	0.58			Winter	
0.13	-208.88	0.01	0.04			Spring	
0.06	-62.94	0.21	0.30			Summer	
0.06	-67.72	0.36	0.75			Autumn	
0.06	-86.17	0.50	0.68				January
0.02	-21.52	0.71	0.98				February
0.09	-150.41	0.16	0.24				March
0.19	-333.94	0.00	0.01				April
0.16	-262.22	0.07	0.13				May
0.11	-162.00	0.08	0.21				June
0.00	64.00	0.81	0.65				July
0.06	-57.80	0.17	0.24				August
0.11	-159.41	0.22	0.09				September
0.11	-179.96	0.16	0.37				October
0.03	-27.88	0.77	0.83				November
0.17	-306.50	0.01	0.01				December

Table S.4 Robinson Forest Mean Air Temperature Statistical Summary

Slope	Intercept	P Value	P Value (zyp)	Half Decade	Year	Season	Month
0.50	53.50	0.05	0.55	Half Decade			
0.18	-301.75	0.00	0.05		Calendar Year		
0.12	-175.06	0.08	0.02		Water Year		
0.18	-301.18	0.00	0.03		Climate Year		
0.07	-97.90	0.23	0.78			Winter	
0.09	-125.01	0.03	0.15			Spring	
0.02	29.71	0.59	0.68			Summer	
0.02	20.27	0.62	0.85			Autumn	
0.07	-112.46	0.31	0.67				January
-0.03	105.64	0.73	0.43				February
0.01	26.02	0.78	0.78				March
0.15	-244.30	0.02	0.05				April
0.13	-186.38	0.09	0.09				May
0.08	-95.08	0.05	0.23				June
0.00	74.50	0.86	0.88				July
0.00	73.50	0.87	0.87				August
0.02	29.52	0.73	0.53				September
0.00	55.00	0.86	0.85				October
-0.01	56.14	0.92	0.75				November
0.11	-182.73	0.18	0.18				December

Table S.5 Robinson Forest Maximum Air Temperature Statistical Summary

Slope	Intercept	P Value	P Value (zyp)	Half Decade	Year	Season	Month
0.33	68.67	0.37	0.09	Half Decade			
0.15	-230.50	0.03	0.15		Calendar Year		
0.09	-117.69	0.22	0.08		Water Year		
0.13	-180.63	0.03	0.29		Climate Year		
0.00	45.00	0.95	0.65			Winter	
0.08	-96.75	0.15	0.44			Spring	
0.00	85.00	0.97	0.97			Summer	
0.00	68.80	0.75	0.75			Autumn	
0.00	42.00	0.73	0.83				January
-0.05	149.25	0.58	0.58				February
-0.07	196.20	0.45	0.45				March
0.12	-158.73	0.10	0.32				April
0.09	-101.02	0.16	0.16				May
0.07	-64.24	0.14	0.31				June
-0.02	118.05	0.57	0.57				July
0.00	86.00	0.82	0.60				August
-0.02	117.33	0.68	0.68				September
-0.07	200.36	0.32	0.28				October
-0.04	131.90	0.68	0.68				November
0.08	-117.47	0.31	0.31				December

Table S.6 Falling Rock Minimum Discharge (log transformed) statistical summary Table

Slope	Intercept	P Value	P Value (zyp)	Half Decade	Year	Season	Month
0.00	-9.21	NA	NA	Half Decade			
0.00	-9.21	0.37	0.64		Calendar Year		
0.00	-9.21	0.50	0.65		Water Year		
0.00	-9.21	0.50	0.65		Climate Year		
0.02	-36.32	0.37	0.73			Winter	
0.01	-27.98	0.47	0.36			Spring	
0.00	-9.21	0.06	0.32			Summer	
0.00	-9.21	0.20	0.73			Autumn	
0.04	-73.12	0.14	0.10				January
0.01	-26.75	0.31	0.59				February
0.00	-1.31	0.92	0.29				March
0.01	-28.87	0.16	0.15				April
0.02	-41.53	0.31	0.31				May
0.00	-4.60	0.15	0.49				June
0.00	-4.60	0.04	0.27				July
0.02	-39.94	0.01	0.09				August
0.00	-9.21	0.07	0.41				September
0.00	-4.60	0.17	0.38				October
0.04	-74.34	0.14	0.14				November
0.02	-48.55	0.35	0.70				December

Table S.7 Little Millseat Minimum Flow (Log Transformed) statistical summary table

Slope	Intercept	P Value	P Value (zyp)	Half Decade	Year	Season	Month
0.00	-9.21	0.88	0.67	Half.Decade			
0.00	-9.21	0.26	0.54		Calendar Year		
0.00	-9.21	0.08	0.12		Water Year		
0.00	-9.21	0.11	0.86		Climate Year		
-0.05	95.88	0.06	0.20			Winter	
-0.02	30.98	0.05	0.10			Spring	
0.00	-4.60	0.87	0.54			Summer	
0.00	-9.21	0.15	0.25			Autumn	
0.00	-1.97	0.98	0.98				January
-0.01	21.77	0.17	0.38				February
0.01	-23.27	--	--				March
0.00	-1.08	0.77	0.77				April
-0.01	21.21	0.27	0.58				May
-0.01	12.20	0.46	0.51				June
0.00	-3.91	0.58	0.71				July
0.00	-3.91	0.54	0.81				August
0.00	-4.60	0.78	0.79				September
0.00	-4.60	0.25	0.67				October
-0.01	10.53	0.45	0.45				November
0.00	-2.21	0.82	0.82				December

Table S.8 Falling Rock Mean Flow (Log Transformed) Statistical Summary

Slope	Intercept	P Value	P Value (zyp)	Half Decade	Year	Season	Month
0.03	0.05	0.11	0.37	Half Decade			
0.00	-8.16	0.04	0.39		Calendar Year		
0.01	-24.79	0.10	0.15		Water Year		
0.01	-20.04	0.18	0.18		Climate Year		
0.01	-13.31	0.07	0.59			Winter	
0.01	-14.13	0.14	0.17			Spring	
0.00	-2.18	0.02	0.59			Summer	
0.00	-2.91	0.14	0.58			Autumn	
0.01	-15.36	0.23	0.20				January
0.00	7.49	0.43	0.55				February
0.01	-14.48	0.50	0.26				March
0.01	-18.36	0.27	0.27				April
0.01	-11.75	0.12	0.12				May
0.00	-2.11	0.33	1.00				June
0.00	-2.82	0.01	0.11				July
0.00	-2.47	0.02	0.20				August
0.00	-1.30	0.15	0.69				September
0.00	-3.11	0.09	0.61				October
0.00	-2.64	0.23	0.70				November
0.01	-17.63	0.07	0.37				December

Table S.9 Little Millseat Mean Flow (Log Transformed) Statistical Summary

Slope	Intercept	P Value	P Value (zyp_	Half Decade	Year	Season	Month
0.12	-1.02	0.03	0.00	Half Decade			
0.01	-24.97	0.05	0.05		Calendar Year		
0.01	-25.90	0.00	0.01		Water Year		
0.01	-26.45	0.07	0.07		Climate Year		
0.02	-37.74	0.02	0.04			Winter	
0.01	-16.63	0.31	0.31			Spring	
0.00	-1.77	0.99	0.99			Summer	
0.01	-31.59	0.47	0.57			Autumn	
0.03	-54.92	0.04	0.04				January
0.00	-1.60	0.96	0.96				February
0.01	-28.85	0.21	0.21				March
0.01	-17.08	0.39	0.39				April
0.02	-33.65	0.44	0.44				May
-0.01	23.32	0.49	0.49				June
0.03	-53.61	0.12	0.32				July
0.03	-53.38	0.06	0.06				August
0.03	-67.78	0.09	0.09				September
0.02	-47.54	0.26	0.26				October
0.00	0.37	0.96	0.95				November
0.03	-64.40	0.04	0.13				December

Table S.10 Falling Rock Maximum Flow (Log Transformed) Statistical Summary

Slope	Intercept	P Value	P Value (zyp)	Half Decade	Year	Season	Month
0.28	2.57	0.11	0.13	Half Decade			
0.01	-9.49	0.75	0.75		Calendar Year		
0.03	-51.83	0.04	0.04		Water Year		
0.00	-3.98	0.73	0.73		Climate Year		
0.04	-67.78	0.03	0.16			Winter	
0.04	-73.24	0.04	0.08			Spring	
0.01	-8.46	0.84	0.84			Summer	
0.00	6.12	0.95	0.95			Autumn	
0.06	-108.47	0.02	0.02				January
0.00	6.82	0.93	0.93				February
0.03	-63.44	0.06	0.06				March
0.05	-88.03	0.08	0.08				April
0.01	-10.52	0.79	0.72				May
0.01	-12.12	0.86	0.86				June
0.06	-125.08	0.05	0.05				July
0.02	-35.44	0.37	0.66				August
0.04	-82.43	0.49	0.55				September
0.02	-33.76	0.55	0.55				October
0.00	7.38	0.95	0.95				November
0.04	-87.78	0.10	0.10				December

Table S.11 Little Millseat Maximum Flow (Log Transformed) Statistical Summary

Slope	Intercept	P Value	P Value (zyp)	Half Decade	Year	Season	Month
0.30	2.74	0.03	0.04	Half.Decade			
0.03	-56.56	0.04	0.04		Calendar Year		
0.03	-62.93	0.02	0.02		Water Year		
0.05	-94.19	0.00	0.00		Climate Year		
0.04	-75.22	0.01	0.03			Winter	
0.04	-76.48	0.03	0.03			Spring	
0.01	-18.84	0.70	0.88			Summer	
0.01	-16.77	0.72	0.72			Autumn	
0.04	-83.80	0.02	0.01				January
0.02	-34.04	0.41	0.41				February
0.02	-42.50	0.17	0.17				March
0.03	-52.00	0.29	0.29				April
0.03	-62.82	0.22	0.22				May
0.02	-42.00	0.33	0.33				June
0.04	-71.08	0.26	0.26				July
0.03	-65.35	0.13	0.45				August
0.04	-77.99	0.08	0.08				September
0.04	-82.17	0.09	0.09				October
-0.01	14.89	0.72	0.76				November
0.06	-109.81	0.02	0.07				December

Table S.12 Falling Rock No Flow Days Statistical Summary

Slope	Intercept	P Value	P Value (zyp)	Half Decade	Year	Season	Month
-10.25	143.75	0.39	0.37	Half Decade			
0.00	1.00	0.53	0.62		Calendar Year		
0.00	1.00	0.33	0.97		Water Year		
0.00	1.00	0.33	0.97		Climate Year		
0.00	0.00	0.28	0.28			Winter	
0.00	0.00	0.64	--			Spring	
-0.31	628.44	0.00	0.10			Summer	
-0.09	183.00	0.02	0.04			Autumn	
0.00	0.00	0.88	--				January
0.00	0.00	--	--				February
0.00	0.00	--	--				March
0.00	0.00	--	--				April
0.00	0.00	0.64	--				May
0.00	0.00	0.02	0.02				June
0.00	0.00	0.01	0.26				July
-0.11	211.47	0.00	0.21				August
0.00	0.00	0.03	0.03				September
0.00	0.00	0.05	0.05				October
0.00	0.00	0.62	0.67				November
0.00	0.00	0.04	0.04				December

Table S.13 Little Millseat No Flow Days Statistical Summary

Slope	Intercept	P Value	P Value (zyp)	Half Decade	Year	Season	Month
0.00	5.00	1.00	1.00	Half Decade			
0.00	1.00	0.29	0.29		Calendar Year		
0.00	2.00	0.36	0.71		Water Year		
0.00	0.00	0.99	0.99		Climate Year		
0.00	0.00	0.08	--			Winter	
0.00	0.00	--	--			Spring	
0.00	0.00	0.37	0.37			Summer	
0.00	0.00	0.38	0.70			Autumn	
0.00	0.00	0.30	--				January
0.00	0.00	0.17	--				February
0.00	0.00	--	--				March
0.00	0.00	--	--				April
0.00	0.00	--	--				May
0.00	0.00	0.25	NA				June
0.00	0.00	0.41	0.41				July
0.00	0.00	0.41	0.41				August
0.00	0.00	0.86	0.81				September
0.00	0.00	0.02	0.84				October
0.00	0.00	0.08	--				November
0.00	0.00	--	--				December

Table S.14 Falling Rock: Days with Flow <Q90 Statistical Summary

Slope	Intercept	P Value	P Value (zyp)	Half Decade	Year	Season	Month
-31.25	466.75	0.39	0.39	Half Decade			
-2.15	4357.62	0.01	0.02		Calendar Year		
-2.39	4852.52	0.00	0.01		Water Year		
-1.75	3539.75	0.03	0.01		Climate Year		
0.00	0.00	1.00	1.00			Winter	
0.00	0.00	0.16	0.75			Spring	
-1.57	3164.14	0.00	0.02			Summer	
-1.04	2093.35	0.03	0.10			Autumn	
0.00	0.00	0.88	0.88				January
0.00	0.00	0.13	--				February
0.00	0.00	--	--				March
0.00	0.00	--	--				April
0.00	0.00	0.16	0.75				May
-0.04	71.89	0.05	0.14				June
-0.52	1051.04	0.01	0.03				July
-0.67	1341.67	0.00	0.02				August
-0.38	759.13	0.04	0.15				September
-0.30	596.93	0.04	0.06				October
0.00	0.00	0.04	0.04				November
0.00	0.00	0.83	0.66				December

Table S.15 Little Millseat Days with Flow <Q90 Statistical Summary

Slope	Intercept	P Value	P Value (zyp)	Half Decade	Year	Season	Month
5.40	90.20	0.75	1.00	Half Decade			
-0.07	183.57	0.80	0.92		Calendar Year		
0.00	7.00	--	--		Water Year		
0.00	32.00	0.91	0.91		Climate Year		
0.00	0.00	0.26	0.26			Winter	
0.00	0.00	0.07	--			Spring	
0.00	7.00	0.70	0.70			Summer	
0.00	9.00	0.90	0.78			Autumn	
0.00	0.00	0.83	0.83				January
0.00	0.00	0.56	0.56				February
0.00	0.00	--	--				March
0.00	0.00	0.13	--				April
0.00	0.00	0.02	0.02				May
0.00	0.00	0.89	0.89				June
0.00	2.00	0.42	1.00				July
-0.19	380.44	0.10	0.36				August
-0.16	328.16	0.19	0.37				September
0.00	6.00	0.63	0.36				October
0.00	0.00	0.40	0.40				November
0.00	0.00	0.08	0.08				December

Table S.16 Falling Rock Days with Flow <Q75 Statistical Summary

Slope	Intercept	P Value	P Value (zyp)	Half Decade	Year	Season	Month
-18.50	601.50	0.54	0.54	Half Decade			
-2.13	4372.67	0.05	0.31		Calendar Year		
-2.22	4549.11	0.02	0.12		Water Year		
-1.63	3345.38	0.17	0.14		Climate Year		
1.40	-2747.80	0.01	0.07			Winter	
1.36	-2665.27	0.05	0.17			Spring	
0.00	90.00	0.19	0.50			Summer	
0.00	92.00	0.06	0.49			Autumn	
0.00	0.00	0.38	0.18				January
0.00	0.00	0.13	--				February
0.00	0.00	--	--				March
0.00	0.00	0.64	--				April
0.00	0.00	0.40	0.70				May
-0.11	232.11	0.34	0.75				June
-0.48	970.62	0.01	0.05				July
-0.33	687.67	0.02	0.29				August
-0.25	521.75	0.03	0.45				September
-0.30	614.60	0.17	0.37				October
0.00	5.00	0.09	0.09				November
0.00	0.00	0.31	0.67				December

Table S.17 Little Millseat Days with Flow <Q75 Statistical Summary

Slope	Intercept	P Value	P Value (zyp)	Half Decade	Year	Season	Month
22.60	143.80	0.60	0.90	Half Decade			
-0.38	860.88	0.63	0.78		Calendar Year		
-0.50	1085.00	0.54	0.61		Water Year		
0.03	32.00	0.92	0.68		Climate Year		
0.00	0.00	0.87	1.00			Winter	
0.00	0.00	0.03	0.34			Spring	
-0.25	523.75	0.39	0.91			Summer	
-0.06	152.06	0.76	0.88			Autumn	
0.00	0.00	0.76	0.48				January
0.00	0.00	0.60	0.60				February
0.00	0.00	--	--				March
0.00	0.00	0.13	--				April
0.00	0.00	0.14	0.14				May
0.00	4.00	0.88	0.88				June
-0.09	195.00	0.45	0.65				July
-0.16	336.79	0.18	0.40				August
-0.10	219.60	0.52	0.78				September
0.00	15.00	1.00	0.67				October
0.00	7.00	0.87	0.63				November
0.00	0.00	0.68	0.98				December

Table S.18 Falling Rock Days with Flow <Q50 Statistical Summary

Slope	Intercept	P Value	P Value (zyp)	Half Decade	Year	Season	Month
-9.00	990.00	0.71	0.71	Half Decade			
-1.86	3916.00	0.02	0.21		Calendar Year		
-1.81	3796.65	0.06	0.11		Water Year		
-1.57	3322.91	0.11	0.07		Climate Year		
-0.70	1416.20	0.06	0.25			Winter	
-0.43	871.43	0.02	0.09			Spring	
-0.29	648.14	0.22	0.88			Summer	
-0.20	480.40	0.35	0.80			Autumn	
-0.07	154.81	0.15	0.08				January
0.00	0.00	0.11	0.11				February
0.00	0.00	0.44	0.82				March
0.00	0.00	0.25	0.52				April
-0.33	680.00	0.02	0.11				May
-0.05	123.15	0.58	0.90				June
-0.15	334.08	0.02	0.40				July
0.00	28.00	0.53	0.83				August
0.00	29.00	0.23	0.87				September
0.00	29.00	0.24	0.99				October
-0.09	204.18	0.26	0.46				November
-0.29	581.14	0.10	0.10				December

Table S.19 Little Millseat Days with Flow <Q50 Statistical Summary

Slope	Intercept	P Value	P Value (zyp)	Half Decade	Year	Season	Month
20.00	670.00	0.60	0.60	Half Decade			
-0.93	2065.80	0.10	0.25		Calendar Year		
-0.67	1517.33	0.32	0.20		Water Year		
-0.72	1645.14	0.35	0.35		Climate Year		
-0.52	1065.64	0.20	0.38			Winter	
-0.14	295.07	0.50	0.50			Spring	
-0.07	231.15	0.51	0.87			Summer	
0.00	87.00	0.79	0.79			Autumn	
0.00	3.00	0.13	0.13				January
0.00	0.00	0.94	0.94				February
0.00	0.00	0.81	0.81				March
0.00	0.00	0.74	0.74				April
-0.16	326.05	0.22	0.22				May
0.00	26.00	0.93	0.78				June
-0.06	150.18	0.12	0.60				July
0.00	31.00	0.04	0.18				August
0.00	30.00	0.13	0.13				September
0.00	30.00	0.46	0.46				October
0.00	24.00	0.84	0.71				November
-0.09	190.91	0.41	0.88				December

Table S.2 Falling Rock Days with Flow >Q25 Statistical Summary

Slope	Intercept	P Value	P Value (zyp)	Half Decade	Year	Season	Month
39.50	166.50	0.04	0.13	Half Decade			
1.21	-2341.00	0.04	0.42		Calendar Year		
1.00	-1919.00	0.12	0.45		Water Year		
1.15	-2229.54	0.06	0.54		Climate Year		
0.53	-1022.26	0.11	0.37			Winter	
0.63	-1220.32	0.07	0.09			Spring	
0.15	-300.15	0.09	0.55			Summer	
0.08	-150.00	0.25	0.67			Autumn	
0.25	-491.00	0.09	0.09				January
0.00	11.00	0.85	0.72				February
0.20	-382.00	0.24	0.33				March
0.18	-347.18	0.30	0.30				April
0.28	-546.72	0.03	0.10				May
0.03	-63.73	0.38	0.80				June
0.09	-178.82	0.02	0.02				July
0.00	1.00	0.39	1.00				August
0.00	1.00	0.16	0.72				September
0.00	1.00	0.32	0.32				October
0.00	2.00	0.42	0.91				November
0.29	-562.14	0.04	0.18				December

Table S.3 Little Millseat Days with Flow >Q25 Statistical Summary

Slope	Intercept	P Value	P Value (zyp)	Half Decade	Year	Season	Month
17.75	308.25	0.47	0.47	Half Decade			
0.35	-616.05	0.42	0.53		Calendar Year		
0.07	-63.79	0.86	1.00		Water Year		
0.38	-686.24	0.50	0.59		Climate Year		
0.28	-528.14	0.22	0.46			Winter	
0.19	-339.22	0.47	0.44			Spring	
0.00	1.00	0.30	0.30			Summer	
0.00	0.00	0.98	0.98			Autumn	
0.21	-405.38	0.16	0.16				January
-0.10	205.76	0.46	0.46				February
0.06	-100.24	0.67	0.67				March
-0.06	148.38	0.68	0.68				April
0.18	-346.82	0.07	0.18				May
0.00	1.00	0.70	0.69				June
0.00	0.00	0.14	0.14				July
0.00	0.00	0.17	0.40				August
0.00	0.00	0.21	0.21				September
0.00	0.00	0.55	0.55				October
0.00	1.00	0.62	0.62				November
0.19	-365.81	0.15	0.51				December

Table S.4 Falling Rock Days with Flow >Q5 Statistical Summary

Slope	Intercept	P Value	P Value (zyp)	Half Decade	Year	Season	Month
13.00	20.00	0.06	0.37	Half Decade			
0.18	-348.18	0.10	0.10		Calendar Year		
0.24	-454.12	0.11	0.11		Water Year		
0.23	-446.15	0.11	0.11		Climate Year		
0.13	-244.00	0.12	0.22			Winter	
0.04	-81.09	0.53	0.53			Spring	
0.00	2.00	0.35	0.35			Summer	
0.00	0.00	0.60	0.60			Autumn	
0.08	-152.00	0.02	0.02				January
0.00	2.00	0.34	0.34				February
0.00	2.00	0.66	0.59				March
0.00	2.00	0.43	0.43				April
0.00	1.00	0.78	0.78				May
0.00	0.00	0.78	0.78				June
0.00	0.00	0.19	0.19				July
0.00	0.00	0.47	0.80				August
0.00	0.00	0.84	1.00				September
0.00	0.00	0.51	0.51				October
0.00	0.00	0.58	0.58				November
0.00	1.00	0.09	0.34				December

Table S.5 Little Millseat Days with Flow >Q5 Statistical Summary

Slope	Intercept	P Value	P Value	Half Decade	Year	Season	Month
7.25	38.25	0.25	0.25	Half Decade			
0.17	-317.33	0.31	0.31		Calendar Year		
0.17	-332.09	0.22	0.31		Water Year		
0.22	-424.44	0.07	0.22		Climate Year		
0.00	0.00	0.89	0.79			Winter	
0.00	1.00	0.16	0.16			Spring	
0.00	0.00	1.00	1.00			Summer	
0.00	0.00	0.90	--			Autumn	
0.00	1.00	0.19	0.32				January
0.00	1.00	0.19	0.14				February
0.04	-84.26	0.22	0.22				March
0.00	3.00	0.61	0.61				April
0.00	0.00	0.98	0.98				May
0.00	0.00	0.98	0.98				June
0.00	0.00	0.43	0.43				July
0.00	0.00	0.12	--				August
0.00	0.00	0.93	--				September
0.00	0.00	0.92	0.92				October
0.00	0.00	0.61	0.72				November
0.00	1.00	0.20	0.20				December

Table S.6 Falling Rock Days with Flow >Q1 Statistical Summary

Slope	Intercept	P Value	P Value (zyp)	Half Decade	Year	Season	Month
3.67	-3.00	0.08	0.13	Half Decade			
0.09	-184.06	0.02	0.02		Calendar Year		
0.10	-196.30	0.02	0.05		Water Year		
0.11	-206.95	0.01	0.04		Climate Year		
0.04	-79.20	0.01	0.05			Winter	
0.00	1.00	0.14	0.14			Spring	
0.00	0.00	0.71	0.58			Summer	
0.00	0.00	0.74	0.91			Autumn	
0.00	0.00	0.00	0.05				January
0.00	0.00	0.30	0.59				February
0.00	0.00	0.20	0.20				March
0.00	0.00	0.41	0.41				April
0.00	0.00	0.58	0.58				May
0.00	0.00	0.41	0.41				June
0.00	0.00	0.22	0.21				July
0.00	0.00	--	--				August
0.00	0.00	0.10	0.76				September
0.00	0.00	0.49	--				October
0.00	0.00	0.87	0.64				November
0.00	0.00	0.35	0.85				December

Table S.7 Little Millseat Days with Flow >Q1 Statistical Summary

Slope	Intercept	P Value	P Value (zyp)	Half Decade	Year	Season	Month
3.00	-6.00	0.21	0.21	Half Decade			
0.00	1.00	0.24	0.24		Calendar Year		
0.00	1.00	0.32	0.32		Water Year		
0.03	-49.85	0.14	0.14		Climate Year		
0.00	0.00	0.82	--			Winter	
0.00	0.00	0.36	--			Spring	
0.00	0.00	--	--			Summer	
0.00	0.00	--	--			Autumn	
0.00	0.00	0.37	0.91				January
0.00	0.00	0.49	0.49				February
0.00	0.00	0.29	0.29				March
0.00	0.00	0.38	0.68				April
0.00	0.00	0.80	0.80				May
0.00	0.00	1.00	1.00				June
0.00	0.00	--	--				July
0.00	0.00	0.36	--				August
0.00	0.00	0.73	--				September
0.00	0.00	0.87	--				October
0.00	0.00	--	--				November
0.00	0.00	0.56	0.56				December

Table S.8 Falling Rock First No Flow Day Timing Statistical Summary

Slope	Intercept	P Value	P Value (zyp)	Year
0.88	-1574.96	0.44	0.44	Calendar Year
-0.65	1567.85	0.17	0.17	Water Year
0.29	-383.08	0.77	0.77	Climate Year

Table S.9 Falling Rock First No Flow Day Timing Statistical Summary

Slope	Intercept	P Value	P Value (zyp)	Year
-1.89	3978.21	0.25	0.25	Calendar Year
0.73	-1213.13	0.45	0.45	Water Year
-0.73	1670.31	0.62	0.62	Climate Year

Table S.10 Falling Rock Longest No-Flow Period Statistical Summary

Slope	intercept	P Value	P Value (zyp)	Half Decade	Year	Season	Month
-1.86	30.00	0.39	0.39	Half Decade			
-0.32	637.68	0.02	0.19		Calendar Year		
-0.33	675.67	0.02	0.20		Water Year		
-0.21	435.29	0.11	0.09		Climate Year		
0.00	0.00	0.23	0.23			Winter	
0.00	0.00	0.45	--			Spring	
-0.24	479.76	0.00	0.06			Summer	
-0.08	169.75	0.11	0.29			Autumn	
0.00	0.00	0.78	--				January
0.00	0.00	--	--				February
0.00	0.00	--	--				March
0.00	0.00	--	--				April
0.00	0.00	0.45	--				May
0.00	0.00	0.06	0.09				June
0.00	0.00	0.01	0.01				July
-0.11	211.68	0.00	0.17				August
0.00	1.00	0.08	0.16				September
0.00	0.00	0.20	0.50				October
0.00	0.00	0.58	0.58				November
0.00	0.00	0.03	0.03				December

Table S.11 Little Millseat Longest No-Flow Period Statistical Summary

Slope	Intercept	P Value	P Value (zyp)	Half Decade	Year	Season	Month
1.14	6.57	0.60	0.60	Half Decade			
0.03	-53.61	0.14	0.14		Calendar Year		
0.08	-152.00	0.05	0.24		Water Year		
0.00	2.00	0.08	0.08		Climate Year		
0.00	0.00	0.00	0.06			Winter	
0.00	0.00	0.01	0.01			Spring	
0.00	0.00	0.55	0.55			Summer	
0.04	-73.37	0.02	0.07			Autumn	
0.00	0.00	0.02	0.02				January
0.00	0.00	0.03	0.59				February
0.00	0.00	--	--				March
0.00	0.00	0.11	--				April
0.00	0.00	0.05	0.05				May
0.00	0.00	0.02	0.02				June
0.00	0.00	0.46	0.46				July
0.00	0.00	0.49	0.49				August
0.00	0.00	0.21	0.39				September
0.00	0.00	0.00	0.13				October
0.00	0.00	0.00	0.00				November
0.00	0.00	0.43	--				December

Table S.12 Falling Rock Slope of Midpoint of Flow Duration Curve Statistical Summary

Slope	Intercept	P Value	P Value (zyp)	Half Decade	Year	Season	Month
0.00068	0.01	0.21	0.55	Half Decade			
0.00022	-0.42	0.05	0.05		Calendar Year		
0.00013	-0.25	0.20	0.19		Water Year		
0.00013	-0.25	0.35	0.35		Climate Year		
0.00013	-0.24	0.33	0.33			Winter	
0.00011	-0.20	0.71	0.70			Spring	
0.00004	-0.08	0.25	0.24			Summer	
0.00004	-0.07	0.28	0.27			Autumn	
0.00039	-0.75	0.06	0.06				January
-0.00041	0.84	0.03	0.09				February
0.00045	-0.87	0.10	0.24				March
0.00030	-0.58	0.25	0.26				April
0.00022	-0.42	0.16	0.16				May
0.00000	0.00	0.95	0.93				June
0.00009	-0.18	0.03	0.06				July
0.00003	-0.06	0.06	0.06				August
0.00001	-0.03	0.46	0.44				September
0.00002	-0.04	0.33	0.35				October
-0.00002	0.05	0.63	0.64				November
0.00053	-1.04	0.01	0.07				December

Table S.13 Little Millseat Slope of Midpoint of Flow Duration Curve Statistical Summary

Slope	Intercept	P Value	P Value (zyp)	Half Decade	Year	Season	Month
0.00060	0.01	0.29	0.29	Half Decade			
0.00016	-0.31	0.06	0.07		Calendar Year		
0.00016	-0.31	0.03	0.01		Water Year		
0.00009	-0.18	0.24	0.15		Climate Year		
0.00021	-0.40	0.08	0.08			Winter	
-0.00001	0.03	0.85	0.88			Spring	
0.00002	-0.03	0.60	0.62			Summer	
0.00005	-0.09	0.16	0.17			Autumn	
0.00030	-0.58	0.16	0.09				January
-0.00020	0.42	0.33	0.32				February
0.00024	-0.46	0.19	0.19				March
0.00017	-0.33	0.36	0.39				April
0.00021	-0.40	0.15	0.14				May
-0.00001	0.02	0.77	0.79				June
0.00009	-0.18	0.04	0.11				July
0.00004	-0.07	0.08	0.07				August
0.00005	-0.10	0.09	0.12				September
0.00003	-0.06	0.27	0.26				October
0.00000	0.00	0.99	0.97				November
0.00039	-0.76	0.03	0.04				December

Table S.14 Falling Rock Water Budget Statistical Summary

Slope	Intercept	P Value	P Value (zyp)	Half Decade	Year	Season	Month
0.05	-0.11	0.46	0.46	Half Decade			
0.00	-6.14	0.02	0.59		Calendar Year		
0.00	-6.74	0.07	0.22		Water Year		
0.00	-5.25	0.08	0.65		Climate Year		
0.01	-14.86	0.03	0.19			Winter	
0.01	-13.06	0.03	0.02			Spring	
0.00	-1.40	0.02	0.39			Summer	
0.00	-2.79	0.10	0.64			Autumn	
0.01	-12.98	0.16	0.19				January
0.01	-29.16	0.04	0.03				February
0.01	-25.67	0.00	0.00				March
0.00	4.03	0.78	0.98				April
0.01	-15.07	0.01	0.02				May
0.00	-0.98	0.64	0.77				June
0.00	-1.91	0.00	0.13				July
0.00	-2.05	0.01	0.46				August
0.00	-1.04	0.14	0.59				September
0.00	-2.71	0.10	0.24				October
0.00	-5.54	0.12	0.44				November
0.00	-8.31	0.13	0.59				December

Table S.15 Little Millseat Water Budget Statistical Summary

Slope	Intercept	P Value	P Value (zyp)	Half Decade	Year	Season	Month
0.00	0.16	0.92	0.92	Half Decade			
0.00	-1.43	0.36	0.50		Calendar Year		
0.00	-2.16	0.50	0.50		Water Year		
0.00	-1.52	0.39	0.76		Climate Year		
0.00	-9.25	0.05	0.12			Winter	
0.00	4.79	0.41	0.61			Spring	
0.00	-0.17	0.81	0.55			Summer	
0.00	-1.68	0.22	0.31			Autumn	
0.04	-75.12	0.04	0.04				January
0.01	-19.25	0.21	0.21				February
0.01	-8.27	0.57	0.57				March
-0.03	53.81	0.01	0.01				April
0.00	-4.64	0.76	0.76				May
0.00	9.63	0.12	0.32				June
0.00	-2.59	0.37	0.63				July
0.00	-2.99	0.29	0.43				August
0.00	-3.56	0.31	0.59				September
0.00	0.46	0.99	0.99				October
0.02	-37.99	--	--				November
0.01	-18.25	--	--				December

Supplementary Figures

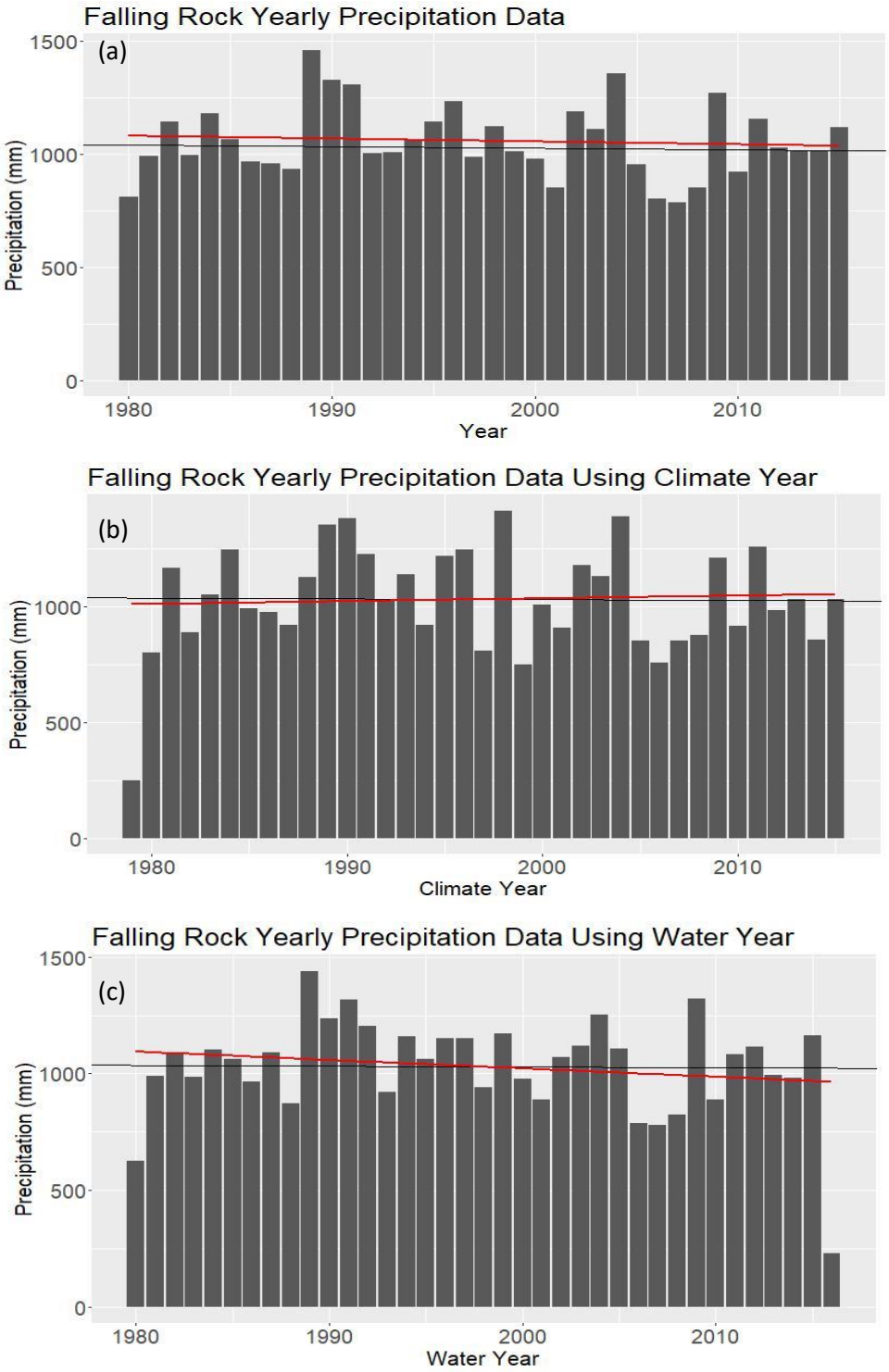

Figure S.1 Yearly Falling Rock precipitation plots.

The sum of the precipitation collected at Falling Rock for each year is plotted with the Sen's Slope trendline (black) and a linear fit trendline. (red). There are no statistically significant trends at the yearly scale.

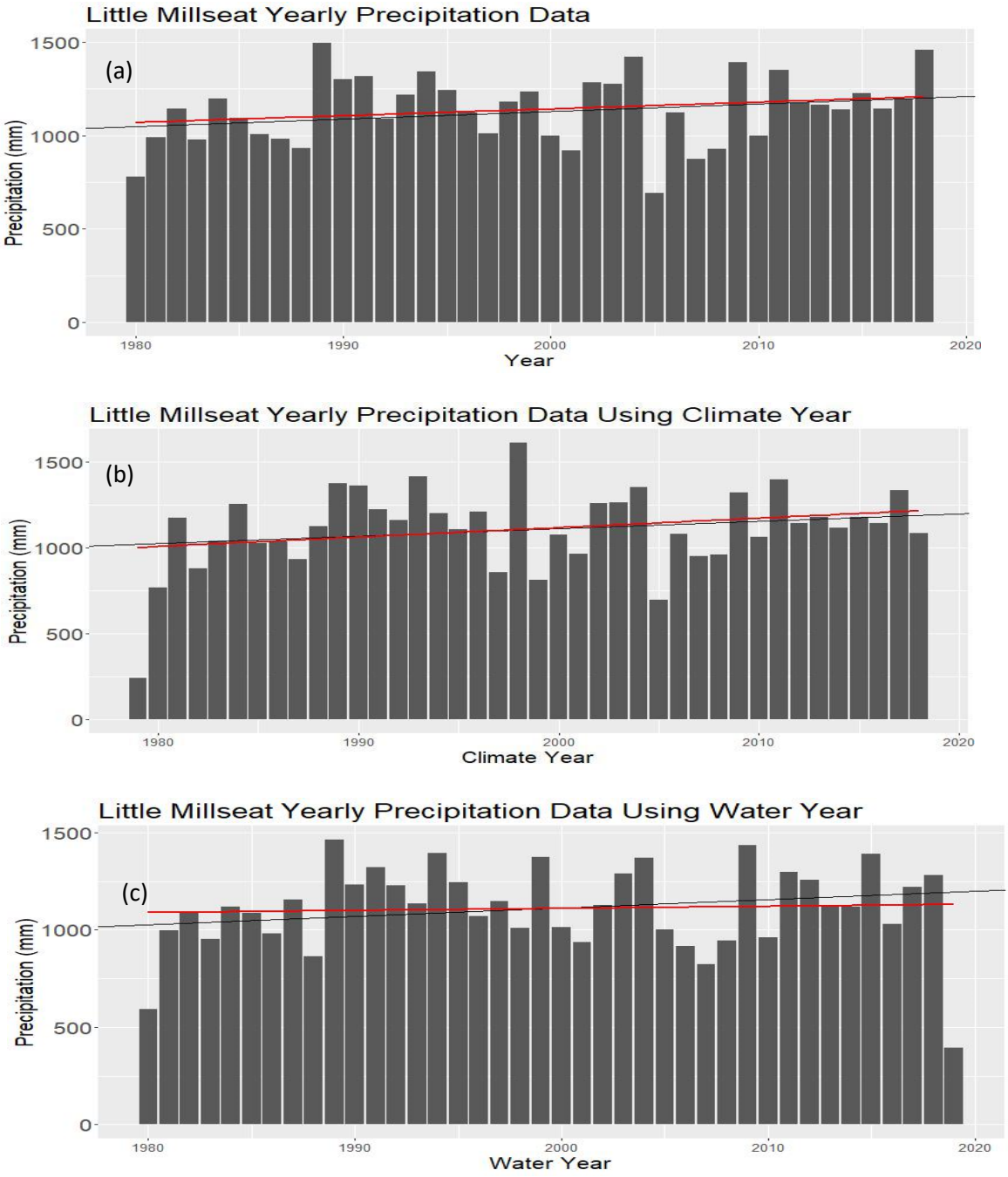

Figure S.2 Yearly Little Millseat precipitation plots.

The sum of the precipitation collected at Little Millseat for each year is plotted with the Sen's Slope trendline (black) and a linear fit trendline (red).. There are no statistically significant trends at the yearly scale.

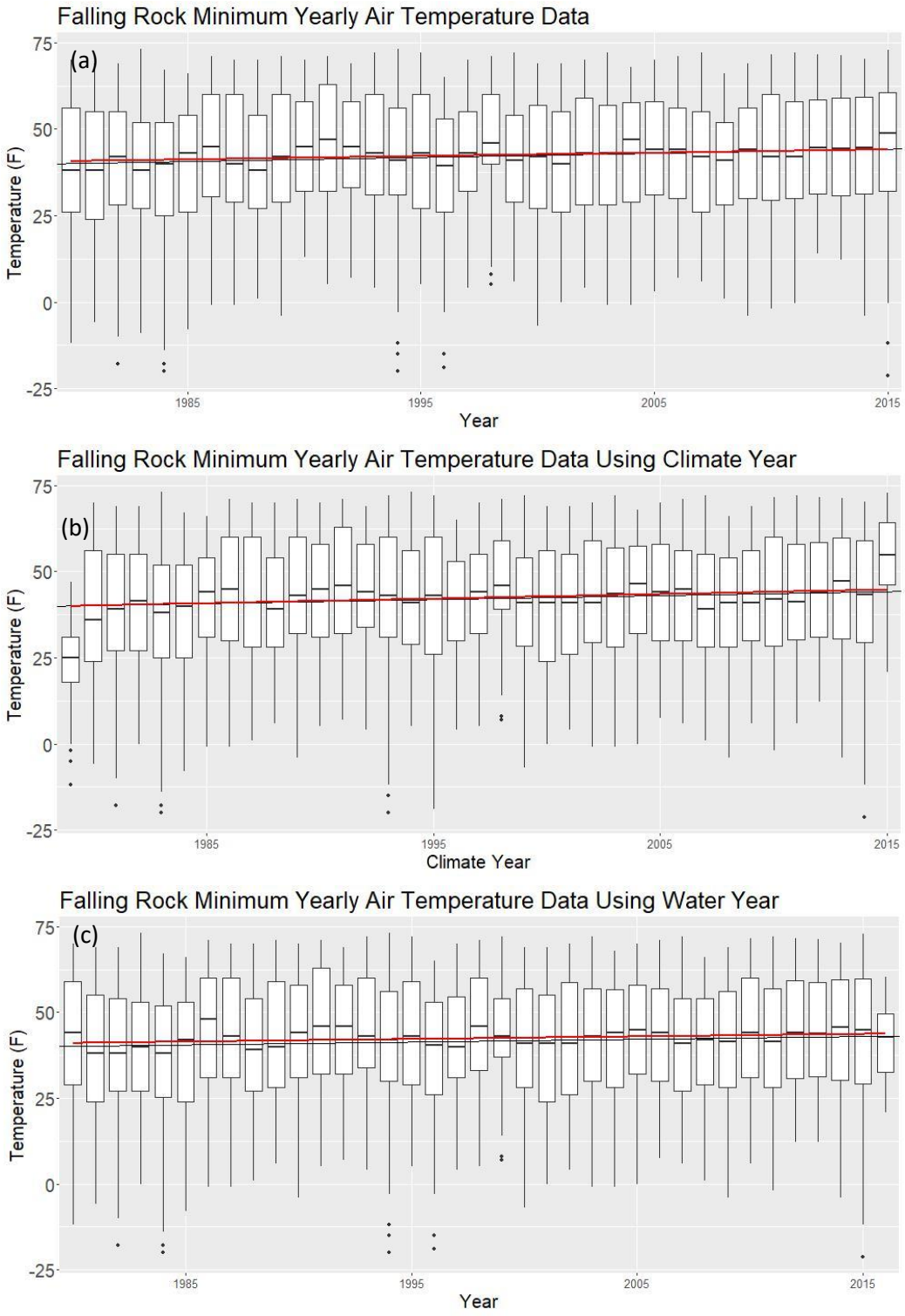

Figure S.3 Robinson Forest minimum air temperature plots.

A boxplot of daily minimum air temperature for each year is plotted with the Sen's Slope trendline (black) and a linear fit trendline (red).. There are statistically significant positive trends for calendar year, climate year, and water year.

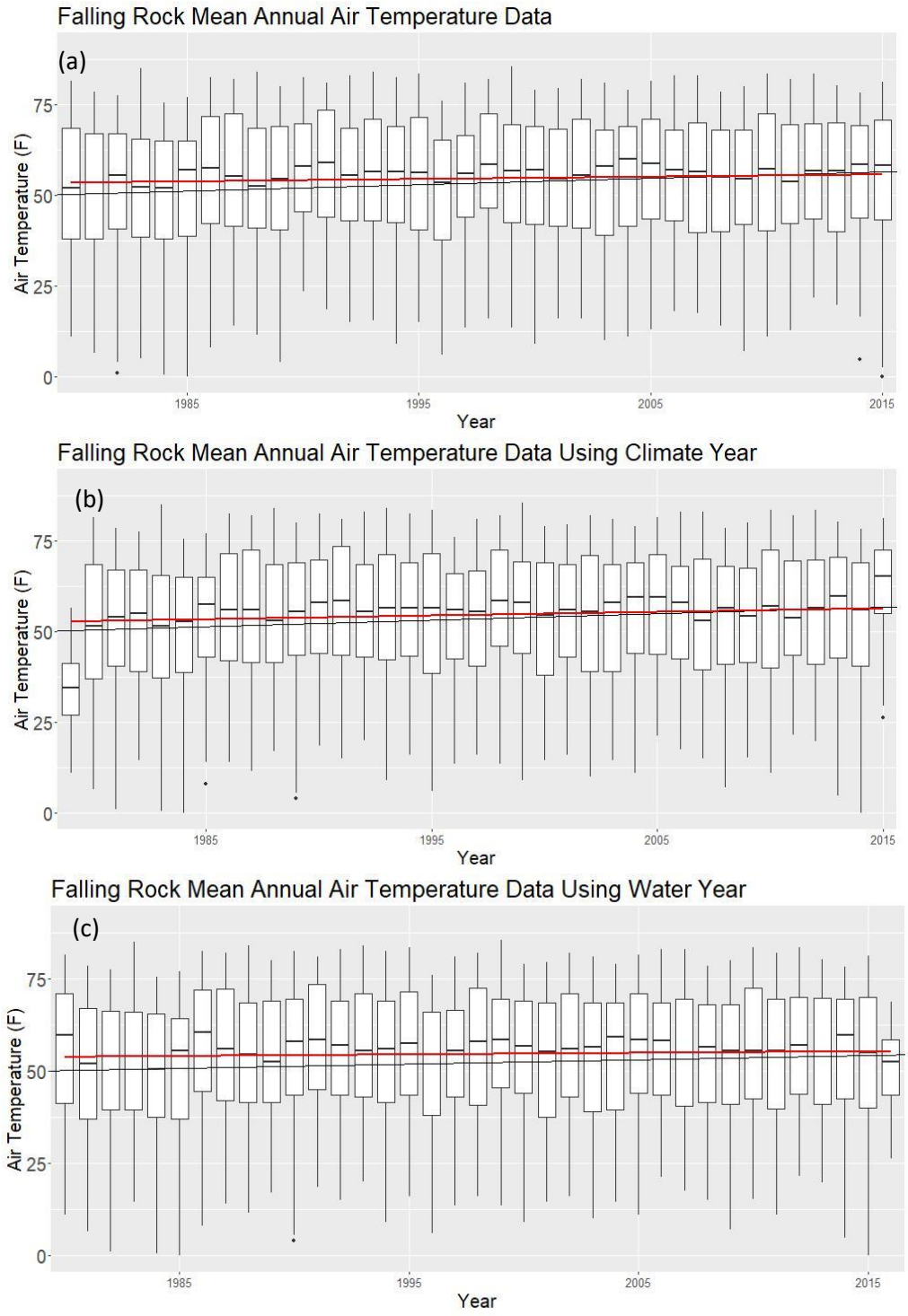

Figure S.4 Robinson Forest mean air temperature plots.

A boxplot of daily mean air temperature for each year is plotted with the Sen's Slope trendline (black) and a linear fit trendline (red).. There are statistically significant positive trends for calendar year, climate year, and water year.

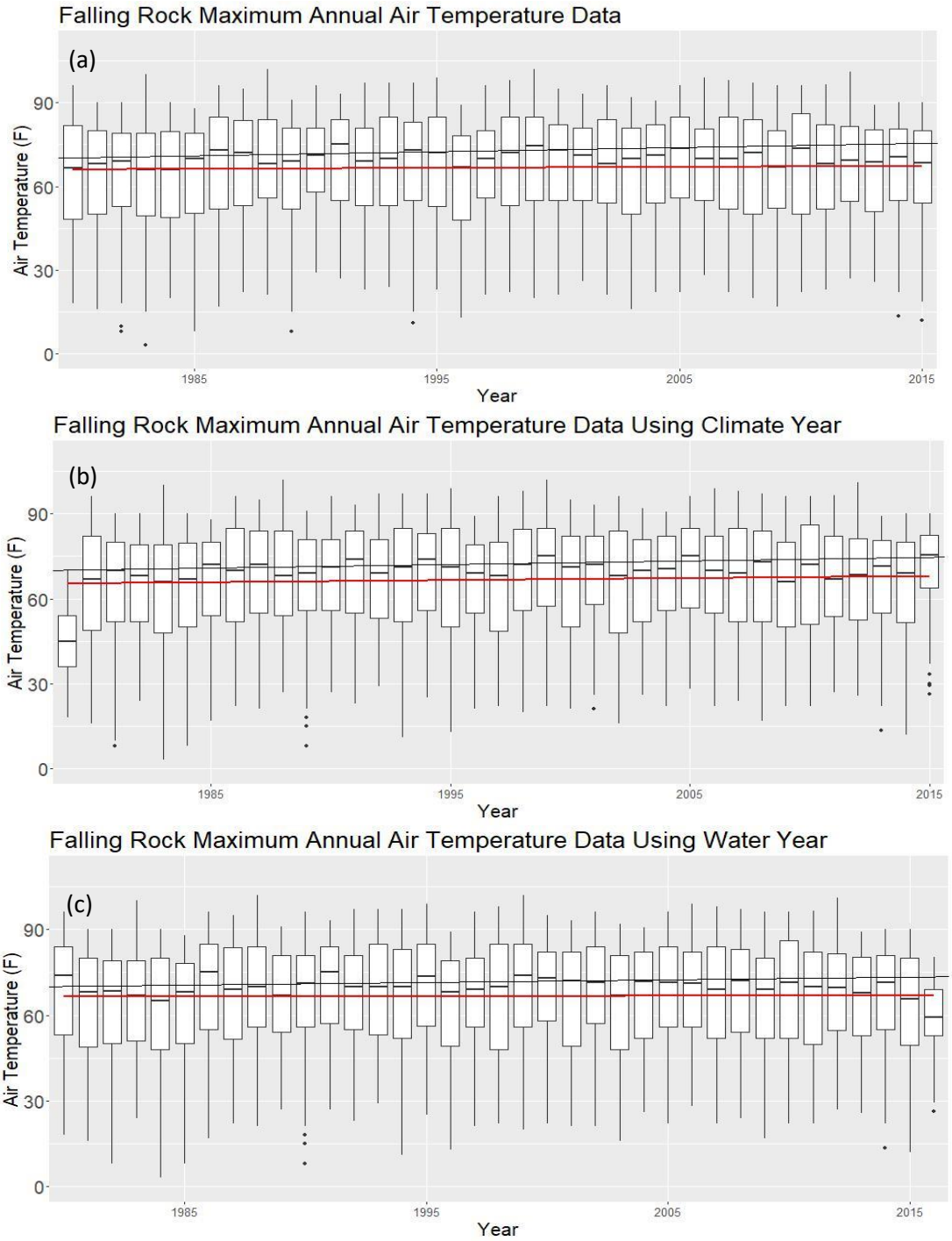

Figure S.5 Robinson Forest maximum air temperature plots.

A boxplot of daily maximum air temperature for each year is plotted with the Sen's Slope trendline (black) and a linear fit trendline (red). There are statistically significant positive trends for calendar year, climate year, and water year.

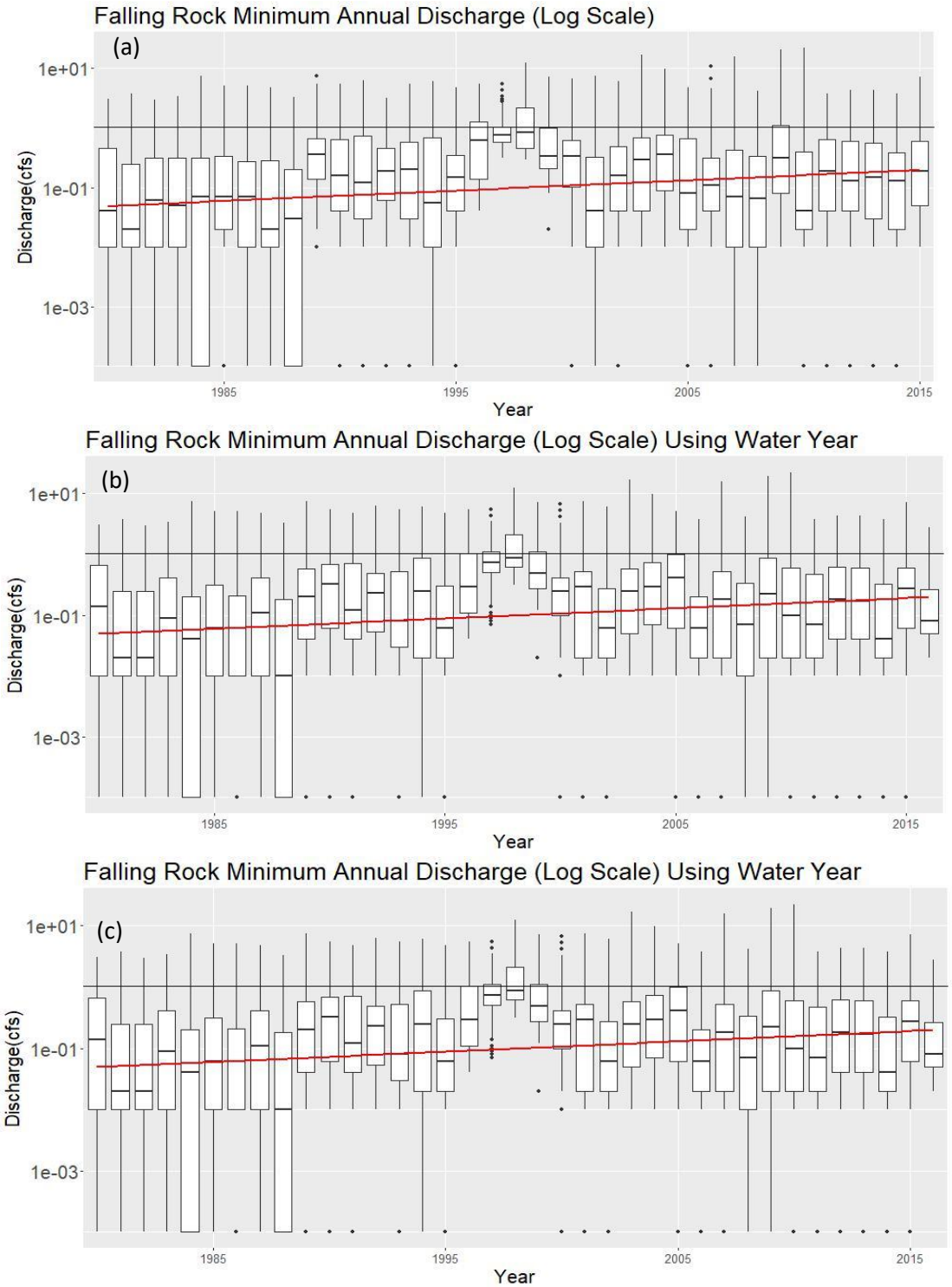

Figure S.6 Falling Rock minimum flow (log transformed) plots.

A boxplot of daily minimum discharge for each year is plotted with the Sen's Slope trendline (black) and a linear fit trendline (red).. There no statistically significant trends at the yearly scale.

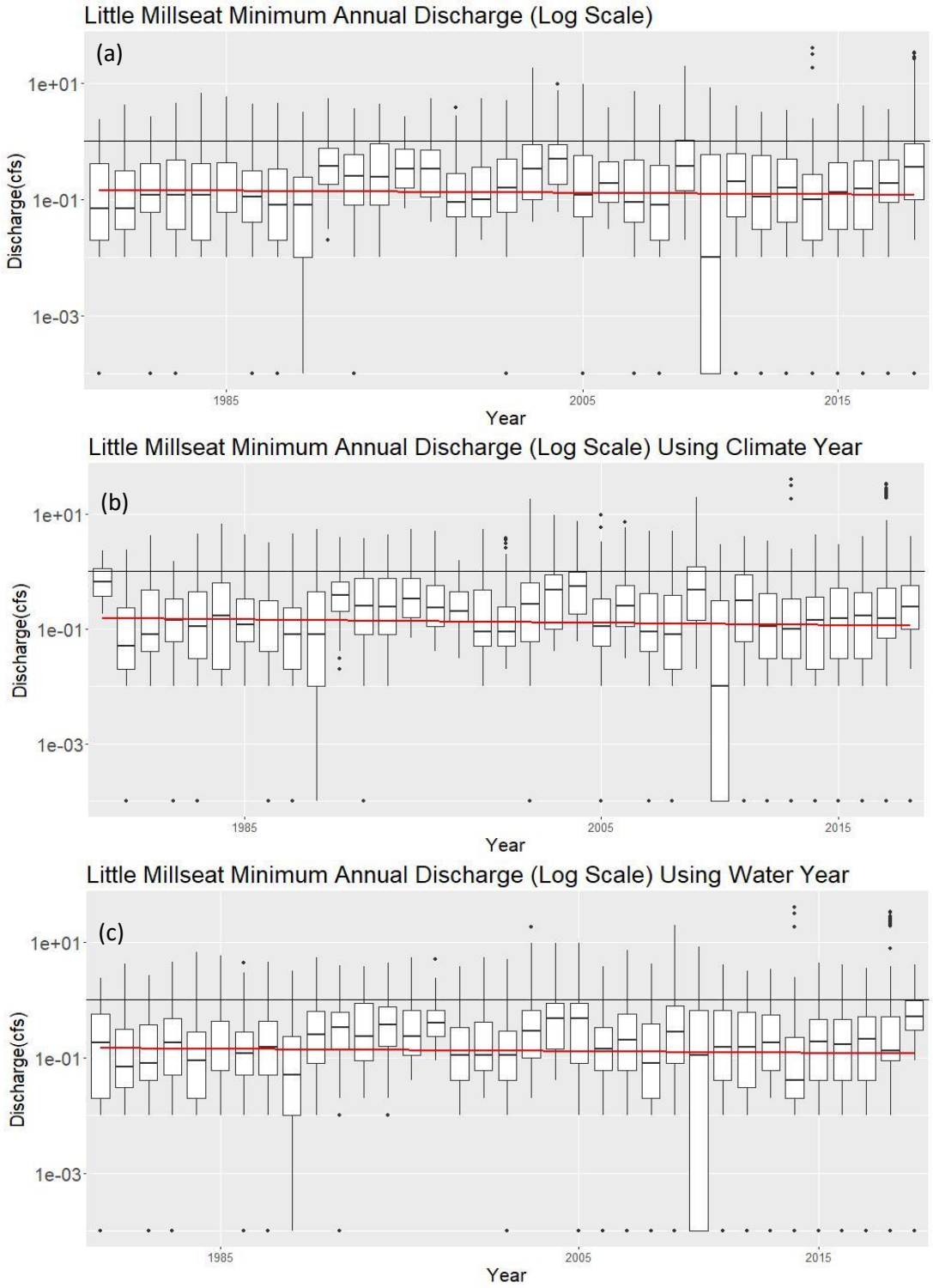

Figure S.7 Little Millseat minimum flow (log transformed) plots.

A boxplot of daily minimum discharge for each year is plotted with the Sen's Slope trendline (black) and a linear fit trendline (red)..There are no statistically significant trends at the yearly scale.

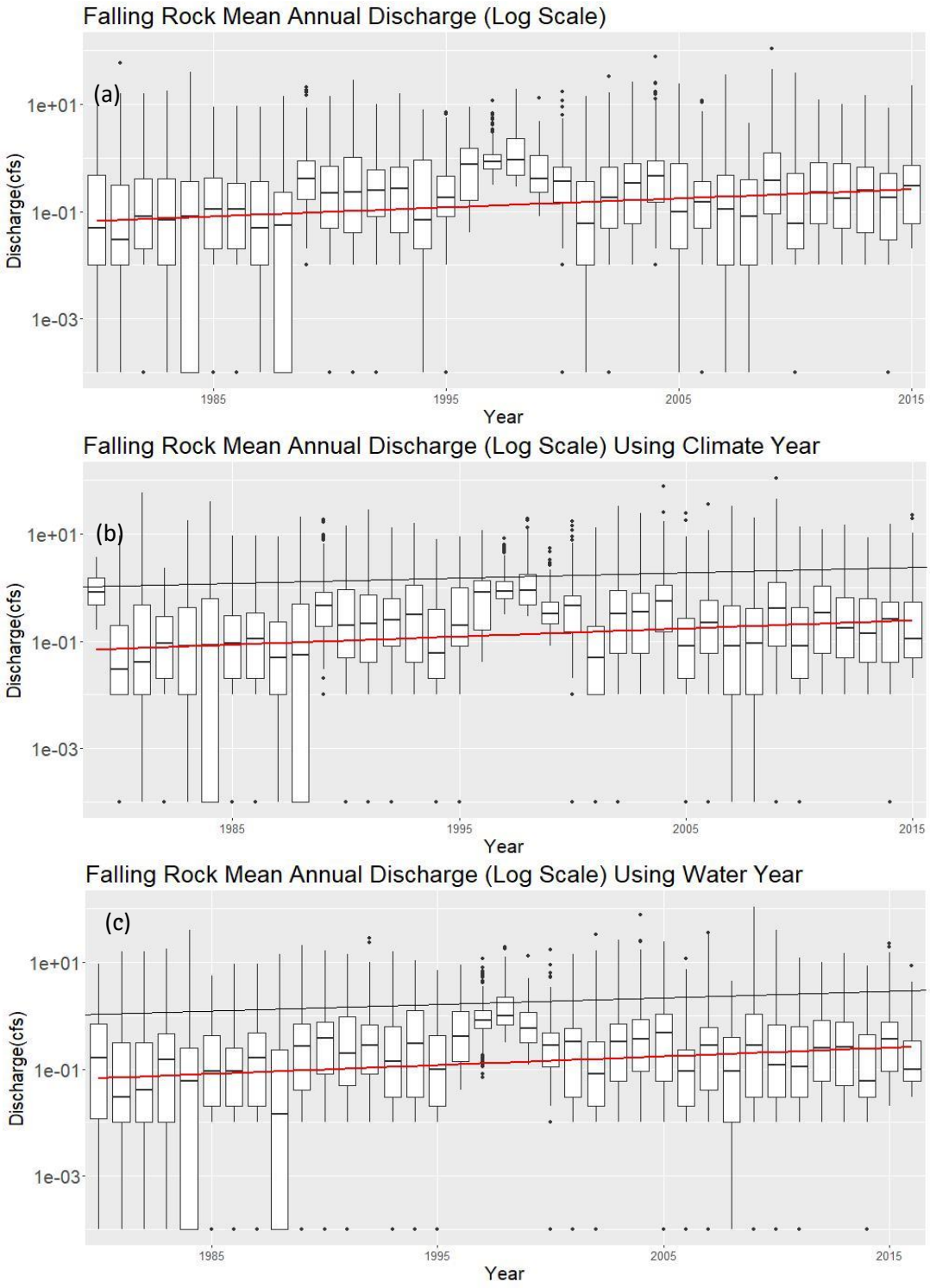

Figure S.8 Falling Rock mean flow (log transformed) plots.

A boxplot of daily minimum discharge for each year is plotted with the Sen's Slope trendline (black) and a linear fit trendline (red). There are statistically significant positive trends at the water year scale.

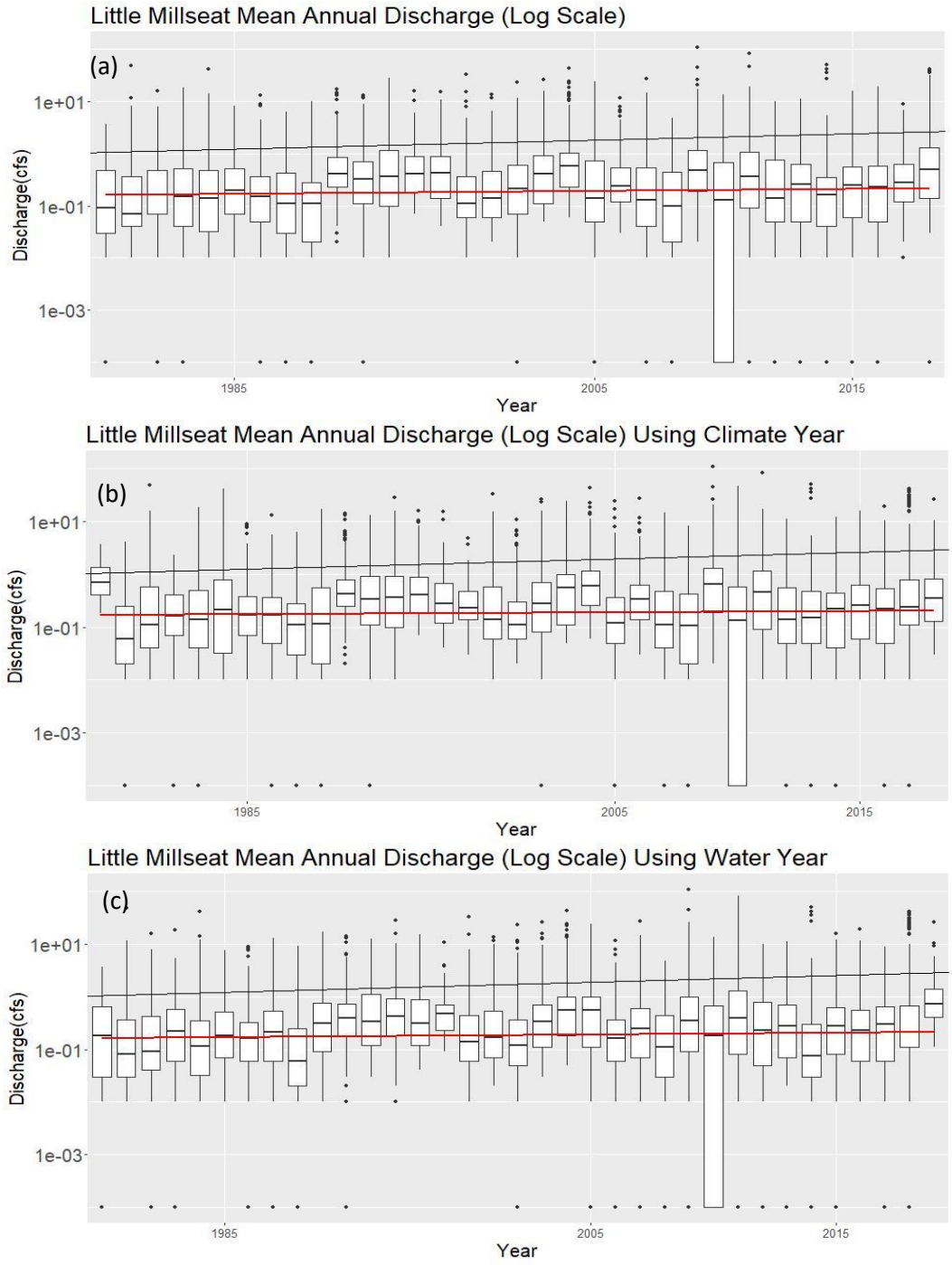

Figure S.9 Little Millseat mean flow (log transformed) plots.

A boxplot of daily mean discharge for each year is plotted with the Sen's Slope trendline (black) and a linear fit trendline (red). There are statistically significant positive trends at the yearly scale.

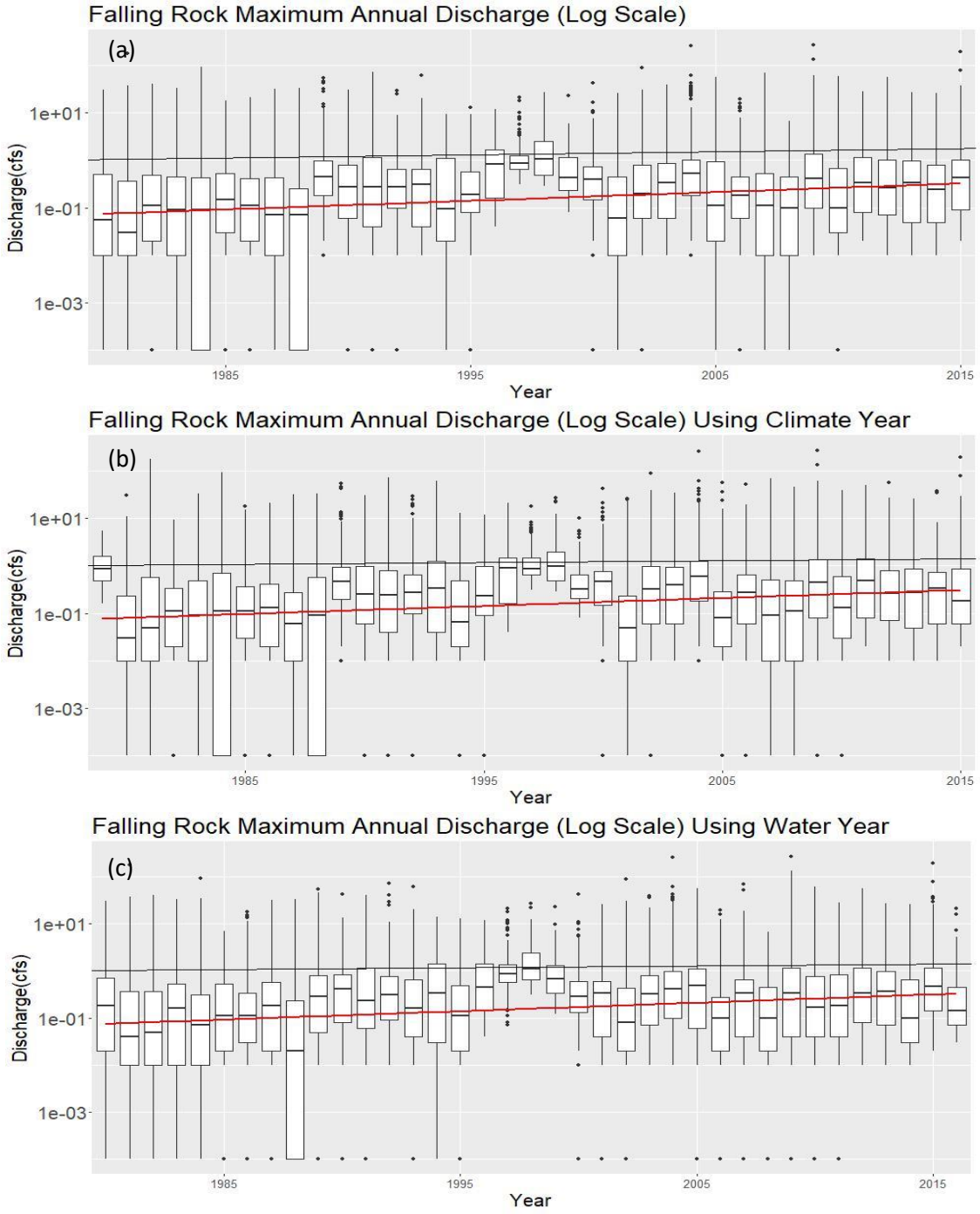

Figure S.10 Falling Rock maximum flow (log transformed) plots for (a) calendar, (b) climate year,), and (c) water year.

A boxplot of daily maximum discharge for each year is plotted with the Sen's Slope trendline (black) and a linear fit trendline (red). There are statistically significant positive trends at the water year scale.

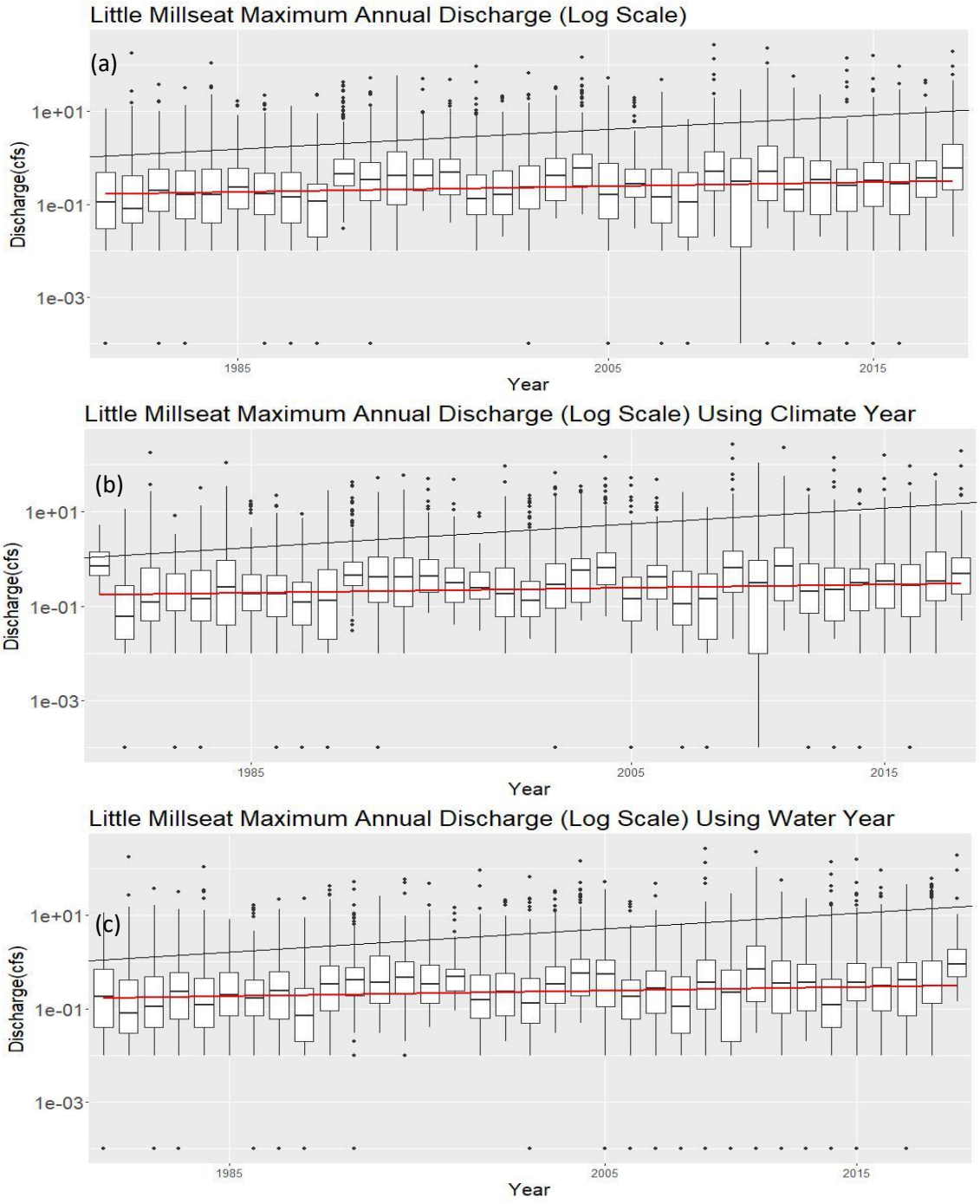

Figure S.11 Little Millseat maximum flow (log transformed) plots.

A boxplot of daily maximum discharge for each year is plotted with the Sen's Slope trendline (black) and a linear fit trendline (red).There are statistically significant positive trends at the yearly scale.

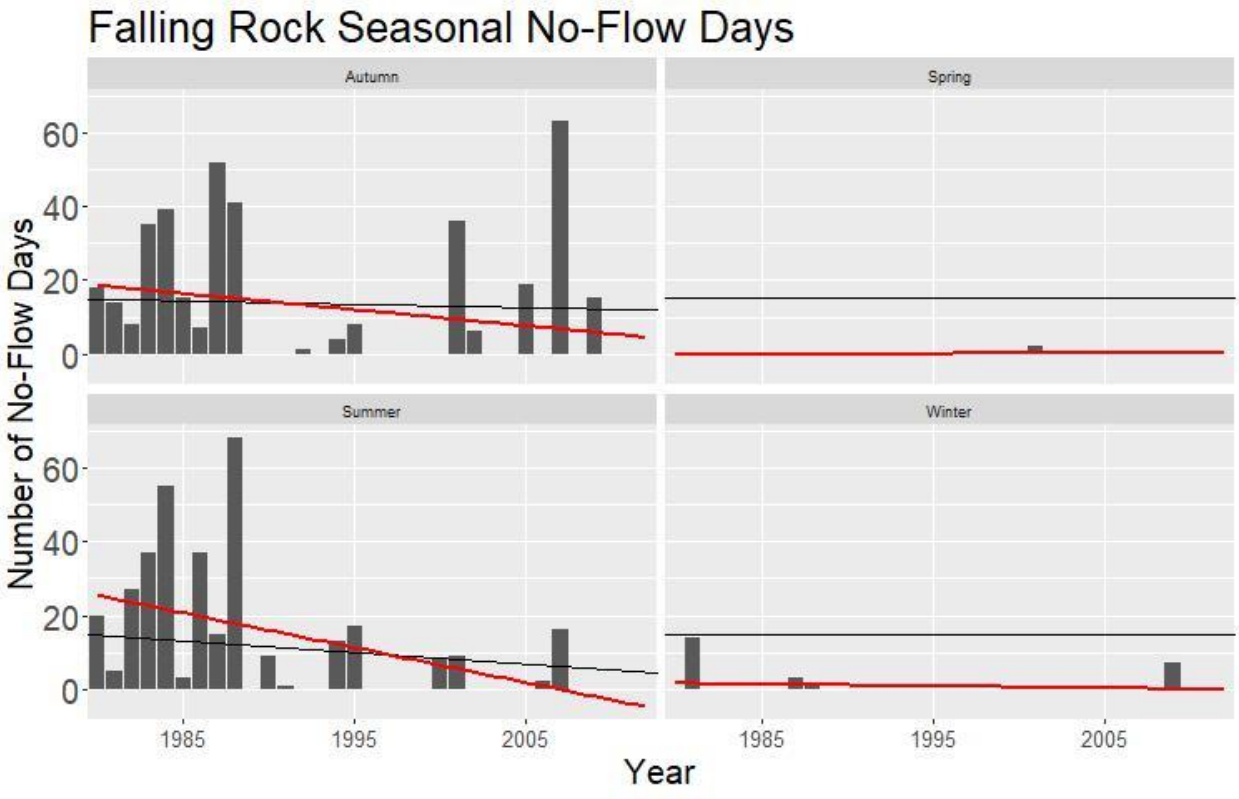

Figure S.12 Falling Rock seasonal no flow plots.

A bargraph of seasonal no flow days for each year is plotted with the Sen's Slope trendline (black) and a linear fit trendline (red). There are statistically significant negative trends during the Summer and Autumn seasons.

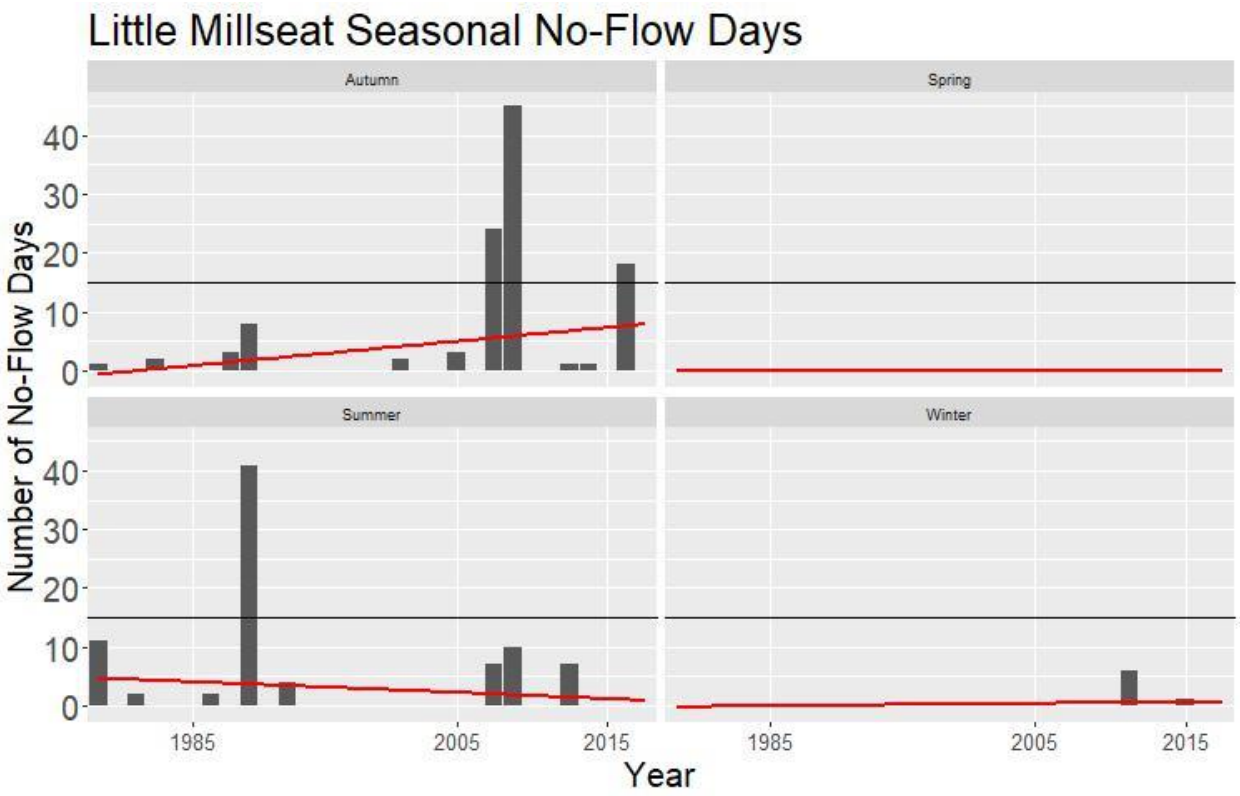

Figure S.13 Little Millseat seasonal no flow plots.

A bar graph of seasonal no flow days for each year is plotted with the Sen's Slope trendline (black) and a linear fit trendline (red). There are no statistically significant negative trends at the seasonal scale.

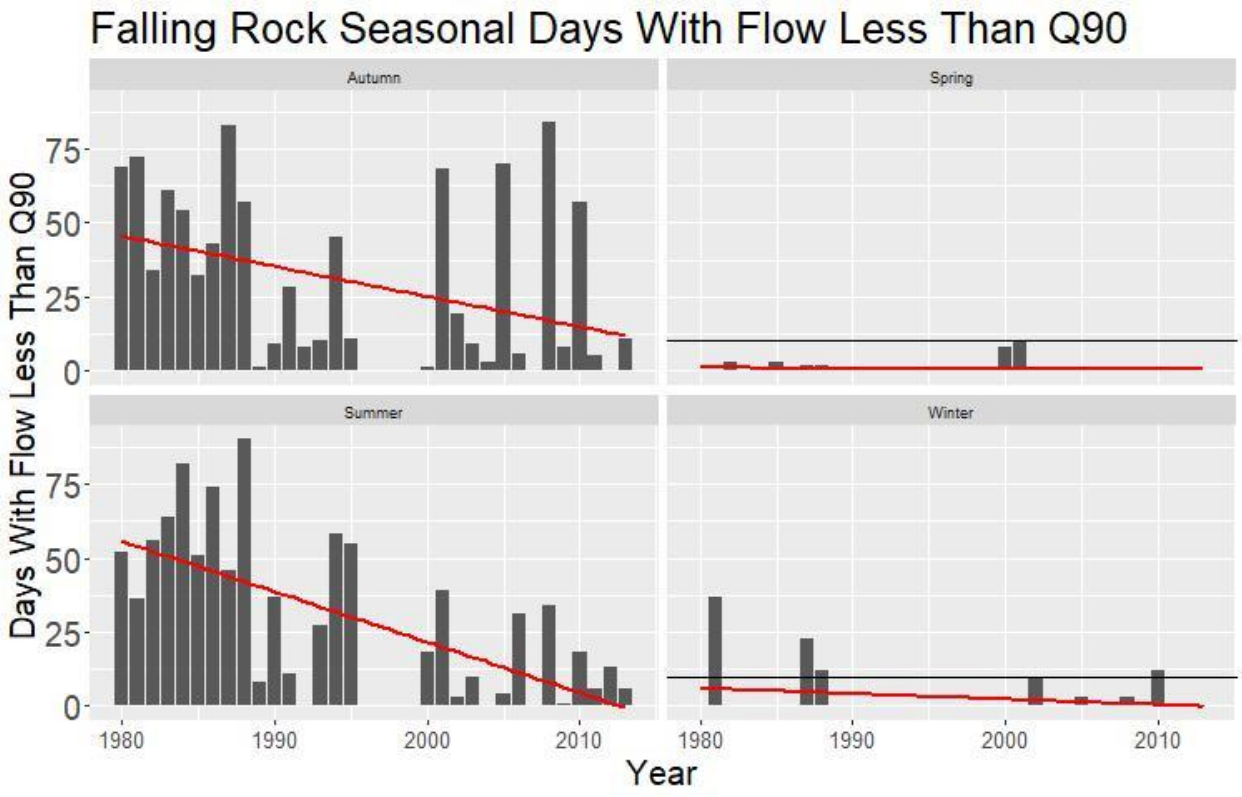

Figure S.14 Falling Rock seasonal days with flow less than Q90 plots.

A bargraph of days with flow less than Q90 for each year is plotted with the Sen's Slope trendline (black) and a linear fit trendline (red). There are statistically significant negative trends during the Summer and Autumn seasons.

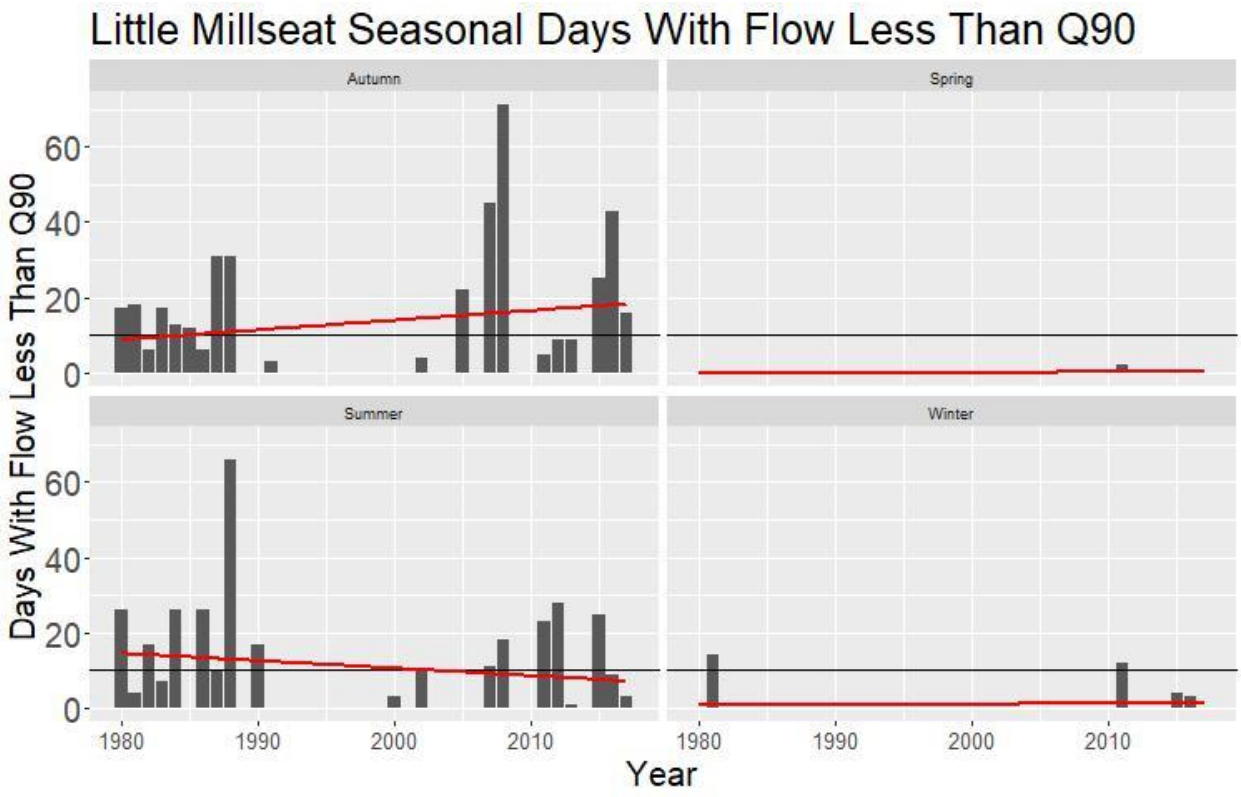

Figure S.15 Little Millseat seasonal days with flow less than Q90 plots.

A bar graph of days with flow less than Q90 for each year is plotted with the Sen's Slope trendline (black) and a linear fit trendline (red). There are no statistically significant trends at the seasonal scale.

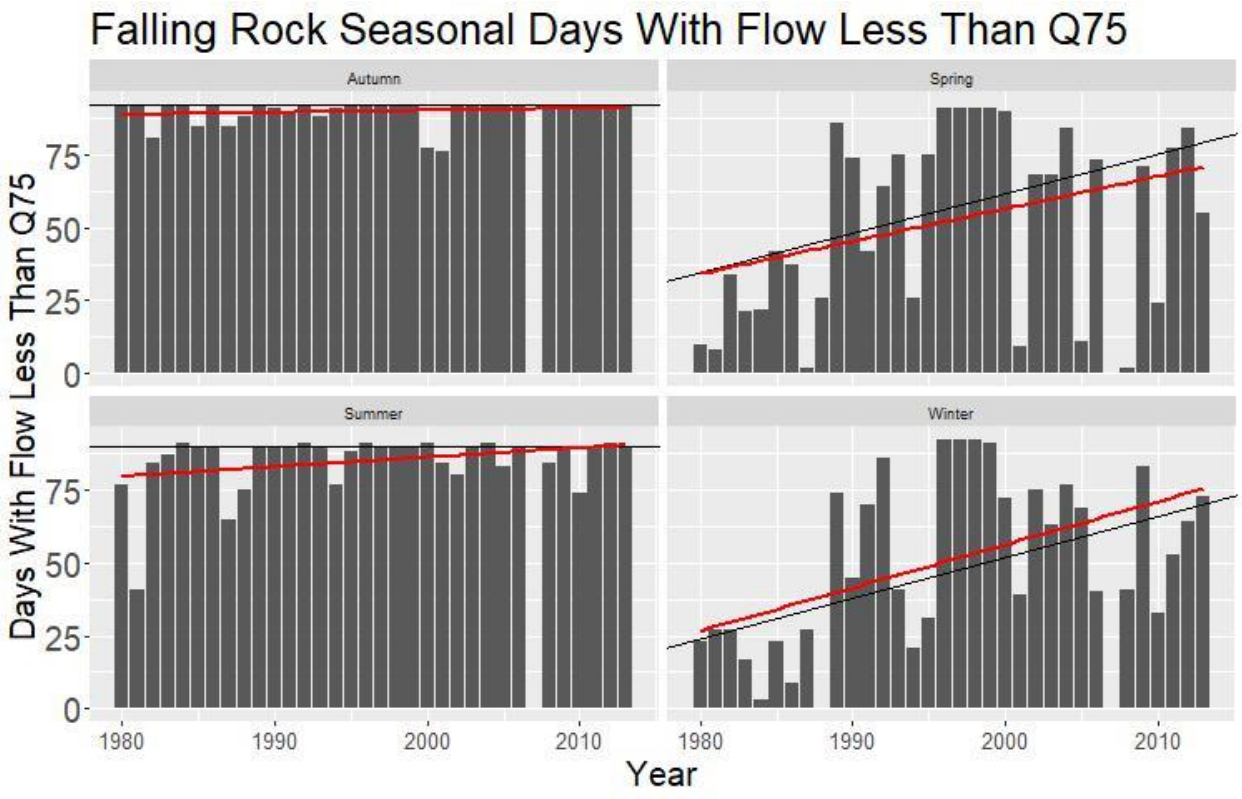

Figure S.16 Falling Rock seasonal days with flow less than Q75 plots.

A bar graph of days with flow less than Q75 for each year is plotted with the Sen's Slope trendline (black) and a linear fit trendline (red). There are statistically significant positive trends during the Winter, Spring, and Autumn seasons.

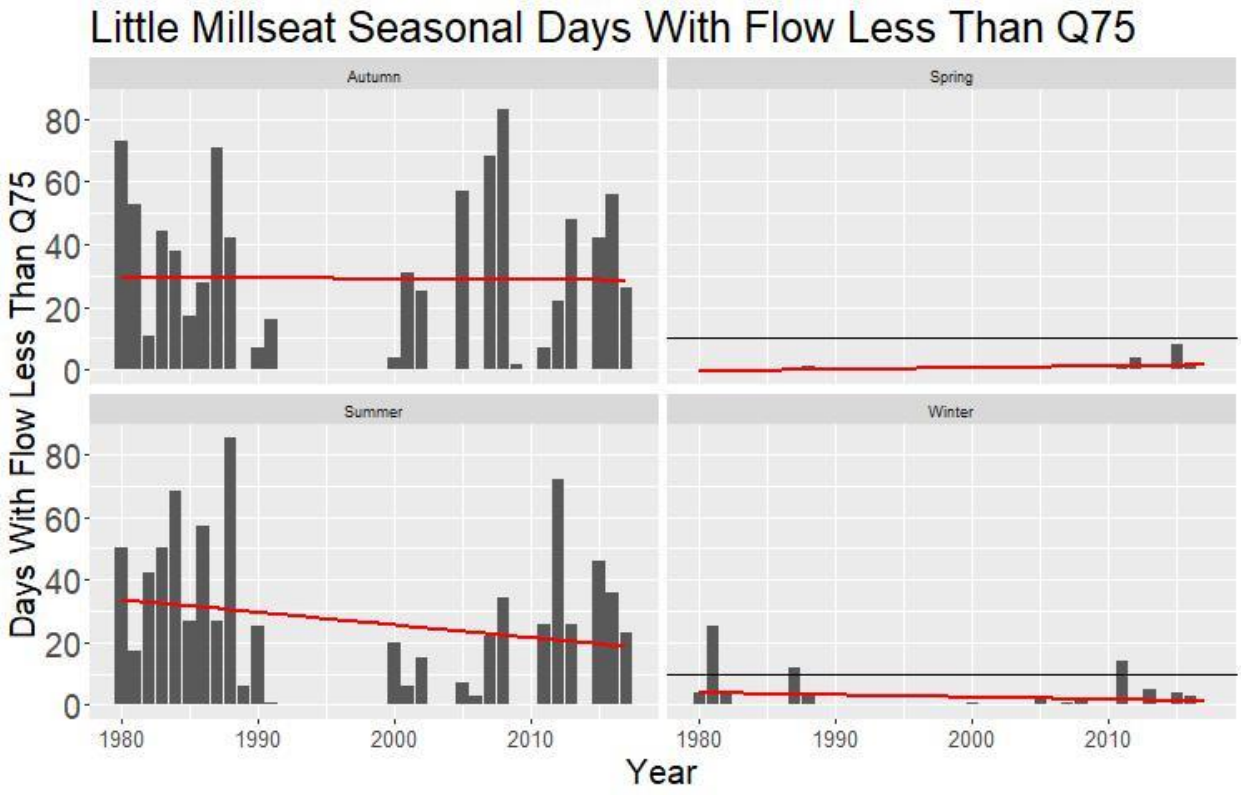

Figure S.17 Falling Little Millseat seasonal days with flow less than Q75 plots.

A bar graph of days with flow less than Q75 for each year is plotted with the Sen's Slope trendline (black) and a linear fit trendline (red). There are no statistically significant trends during at the seasonal scale.

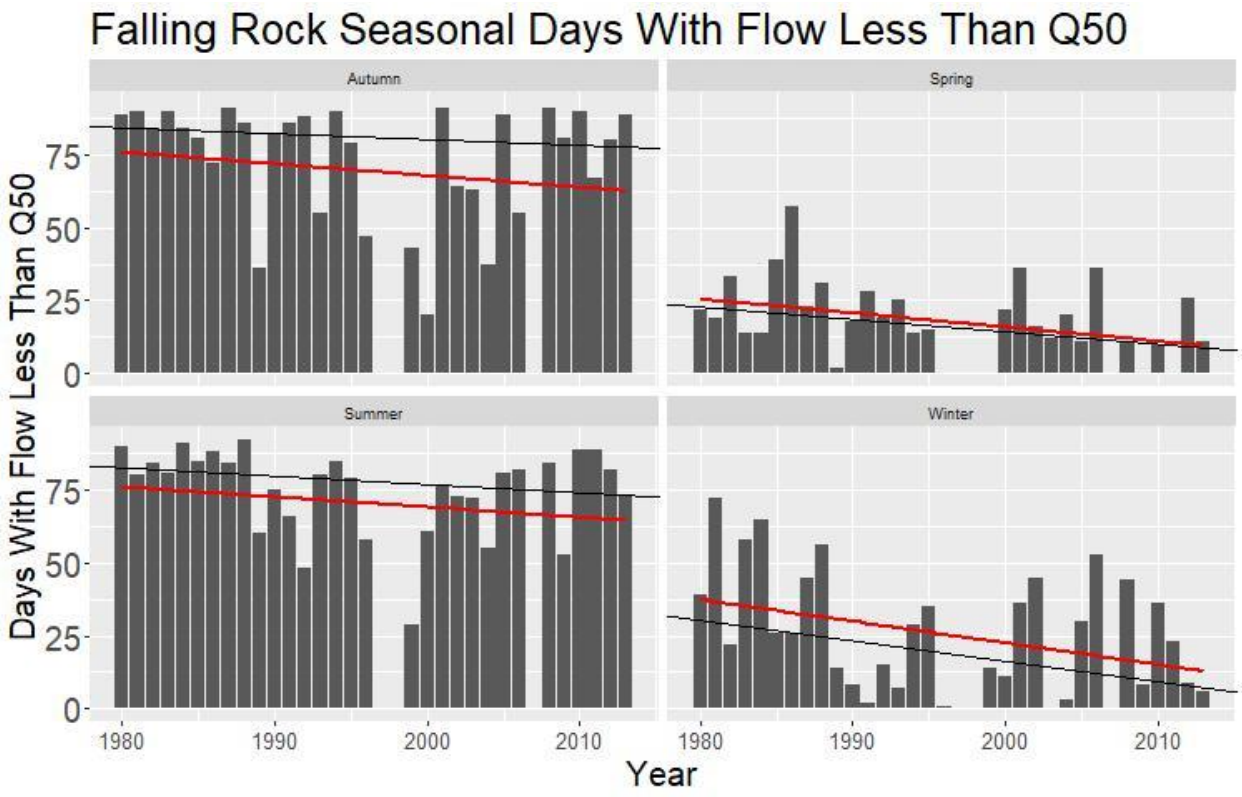

Figure S.18 Falling Rock seasonal days with flow less than Q50 plots.

A bar graph of days with flow less than Q50 for each year is plotted with the Sen's Slope trendline (black) and a linear fit trendline (red). There are statistically significant negative trends during the Winter and Spring, seasons.

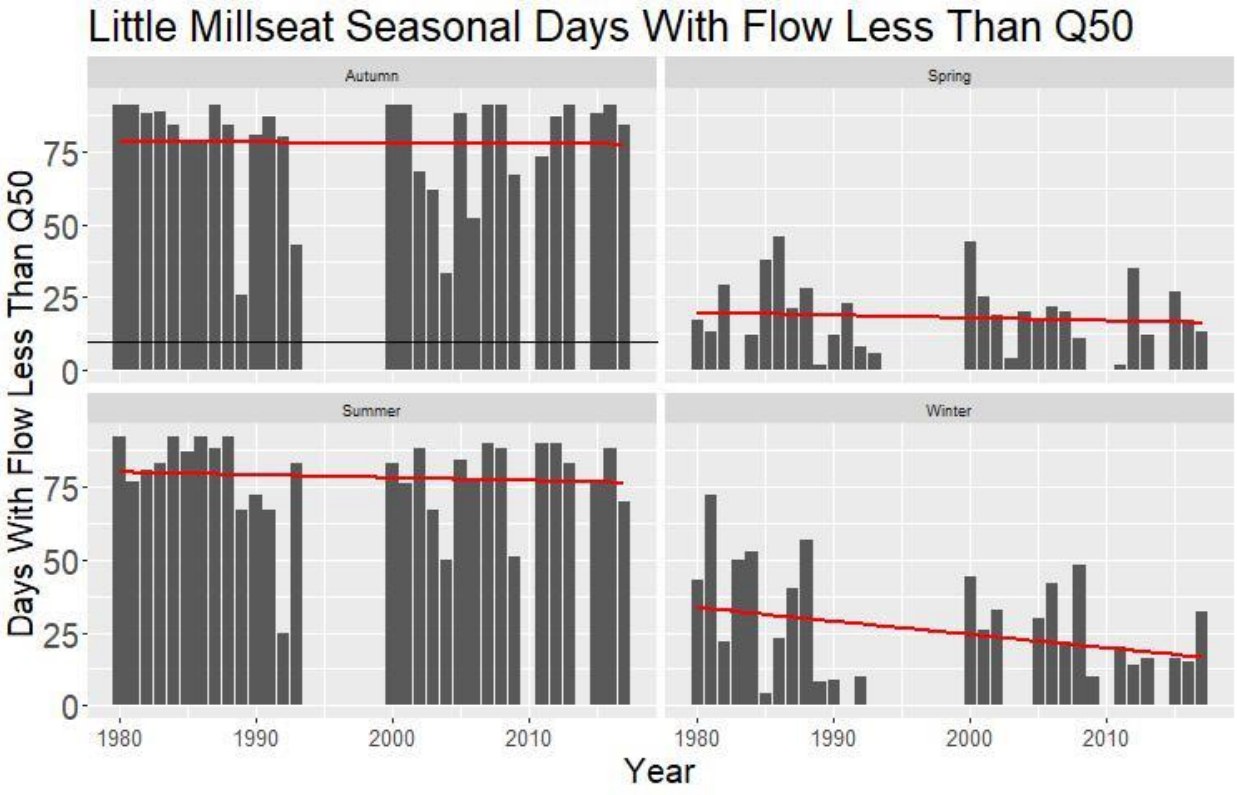

Figure S.19 Little Millseat seasonal days with flow less than Q50 plots.

A bar graph of days with flow less than Q50 for each year is plotted with the Sen's Slope trendline (black) and a linear fit trendline (red). There are no statistically significant trends at the seasonal scale.

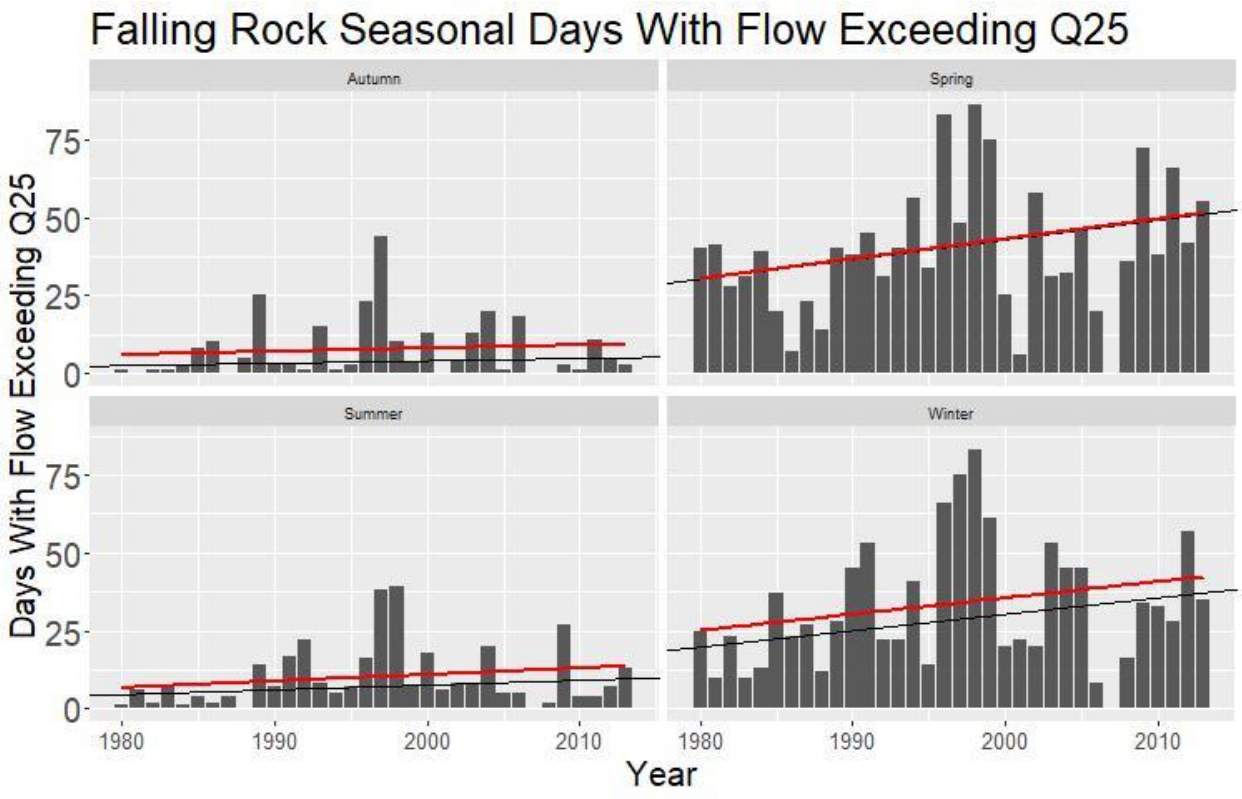

Figure S.20 Falling Rock seasonal days with flow greater than Q25 plots.

A bar graph of days with flow greater than Q25 for each year is plotted with the Sen's Slope trendline (black) and a linear fit trendline (red). There are statistically significant positive trends during the Spring and Summer seasons.

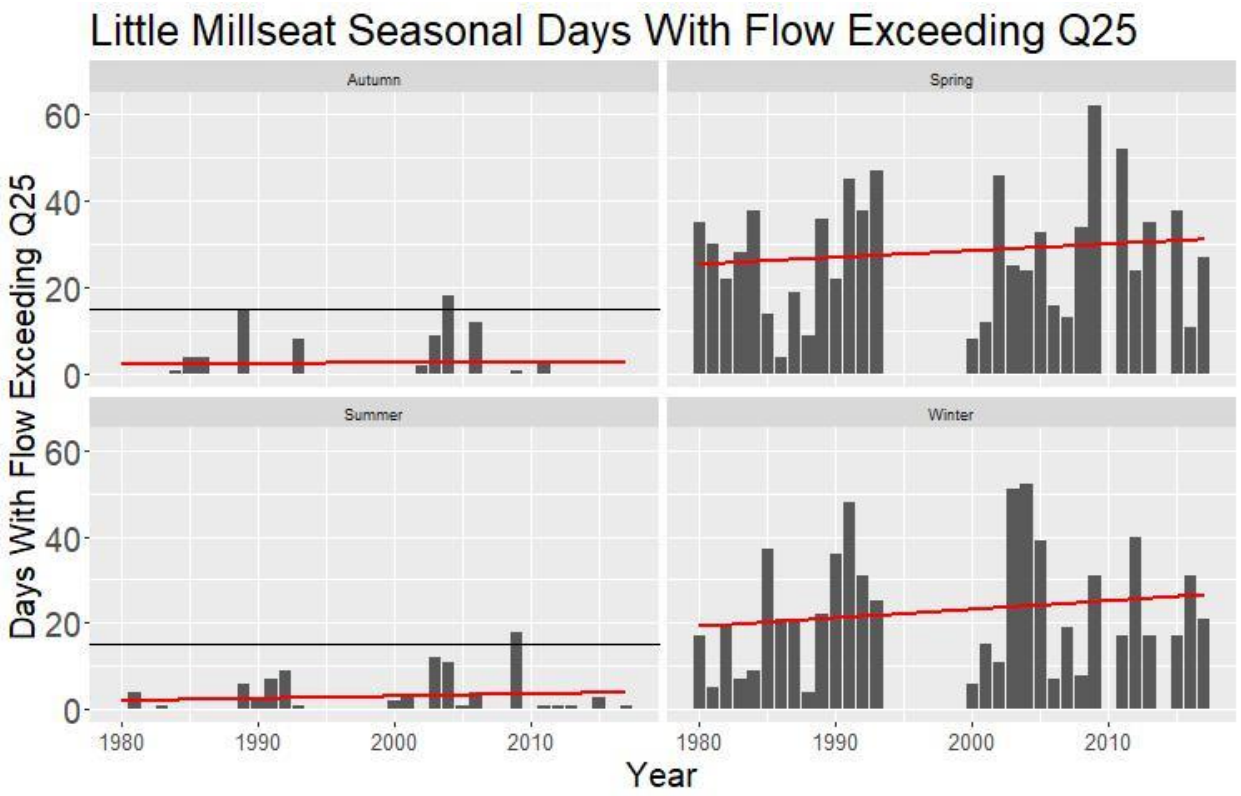

Figure S.21 Little Millseat seasonal days with flow greater than Q25 plots.

A bar graph of days with flow greater than Q25 for each year is plotted with the Sen's Slope trendline (black) and a linear fit trendline (red). There are no statistically significant trends at the seasonal scale.

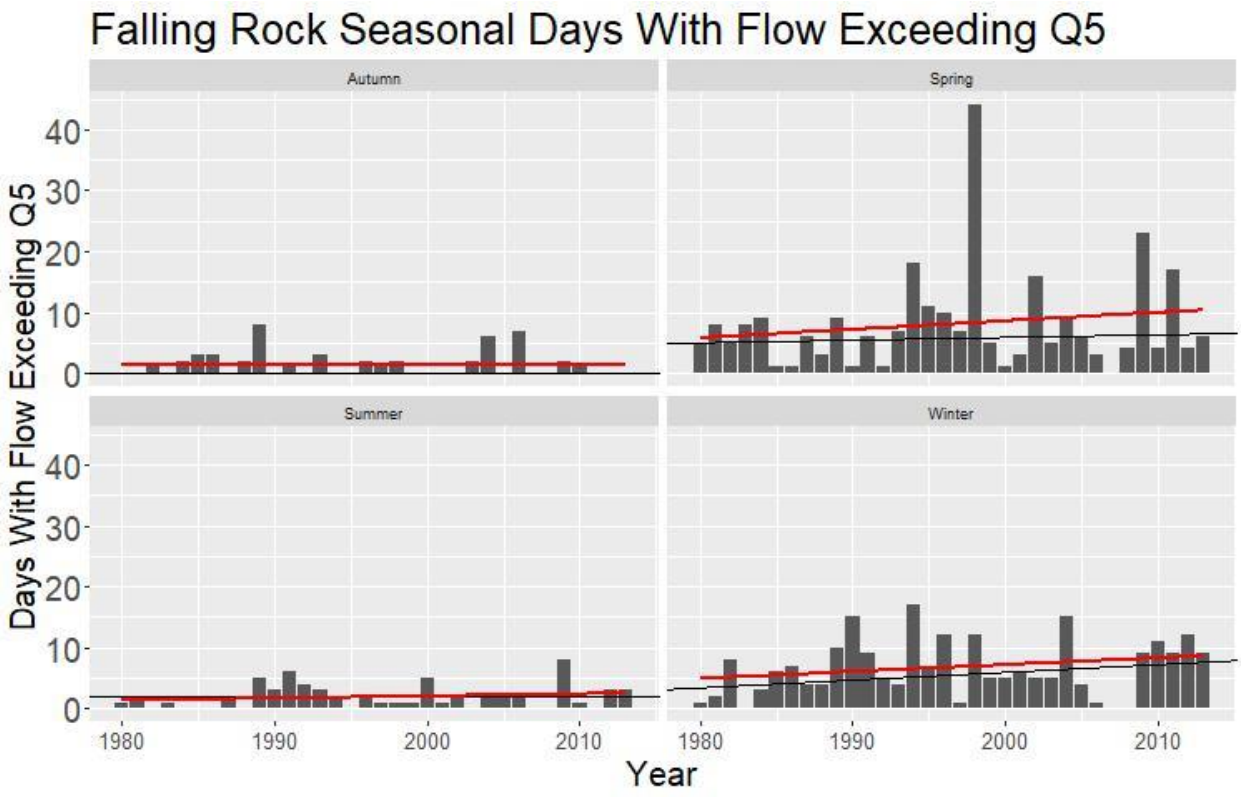

Figure S.22 Falling Rock seasonal days with flow greater than Q5 plots.

A bar graph of days with flow greater than Q5 for each year is plotted with the Sen's Slope trendline (black) and a linear fit trendline (red). There are no statistically significant trends at the seasonal scale.

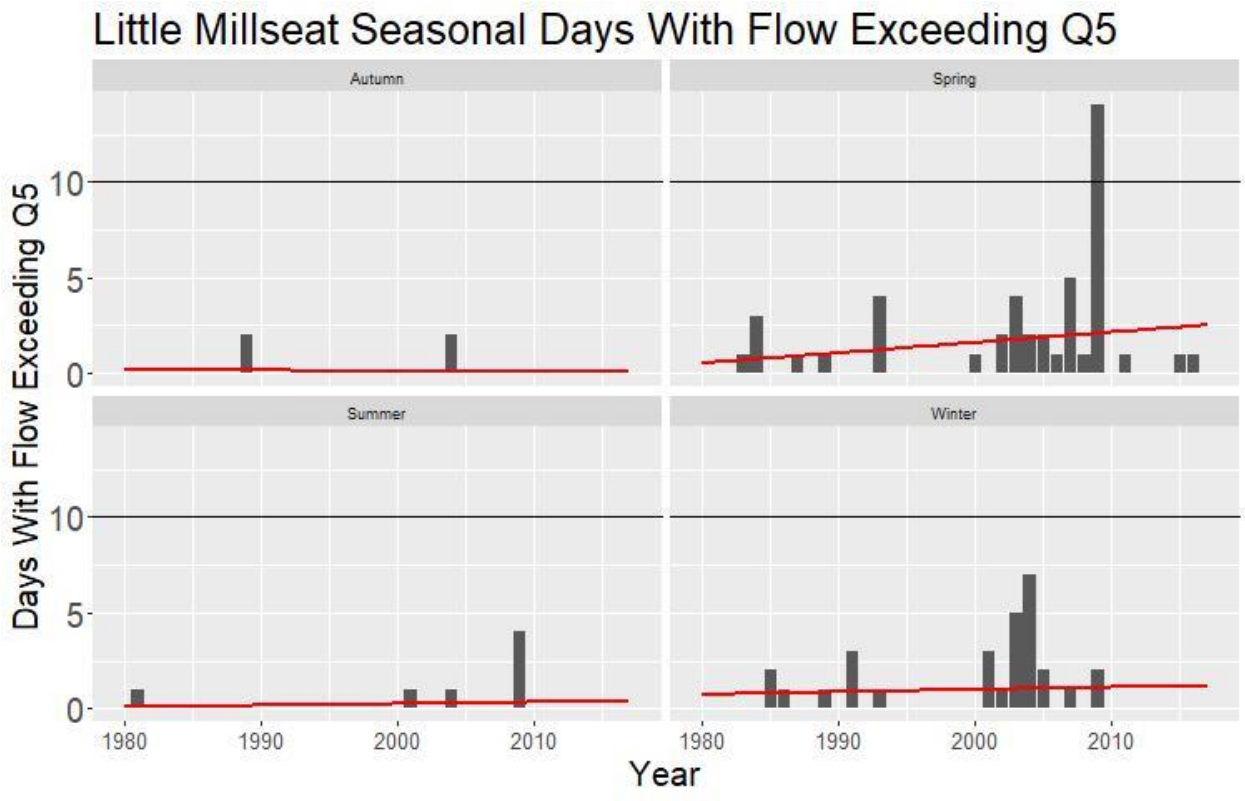

Figure S.23 Little Millseat seasonal days with flow greater than Q5 plots.

A bar graph of days with flow greater than Q5 for each year is plotted with the Sen's Slope trendline (black) and a linear fit trendline (red). There are no statistically significant trends at the seasonal scale.

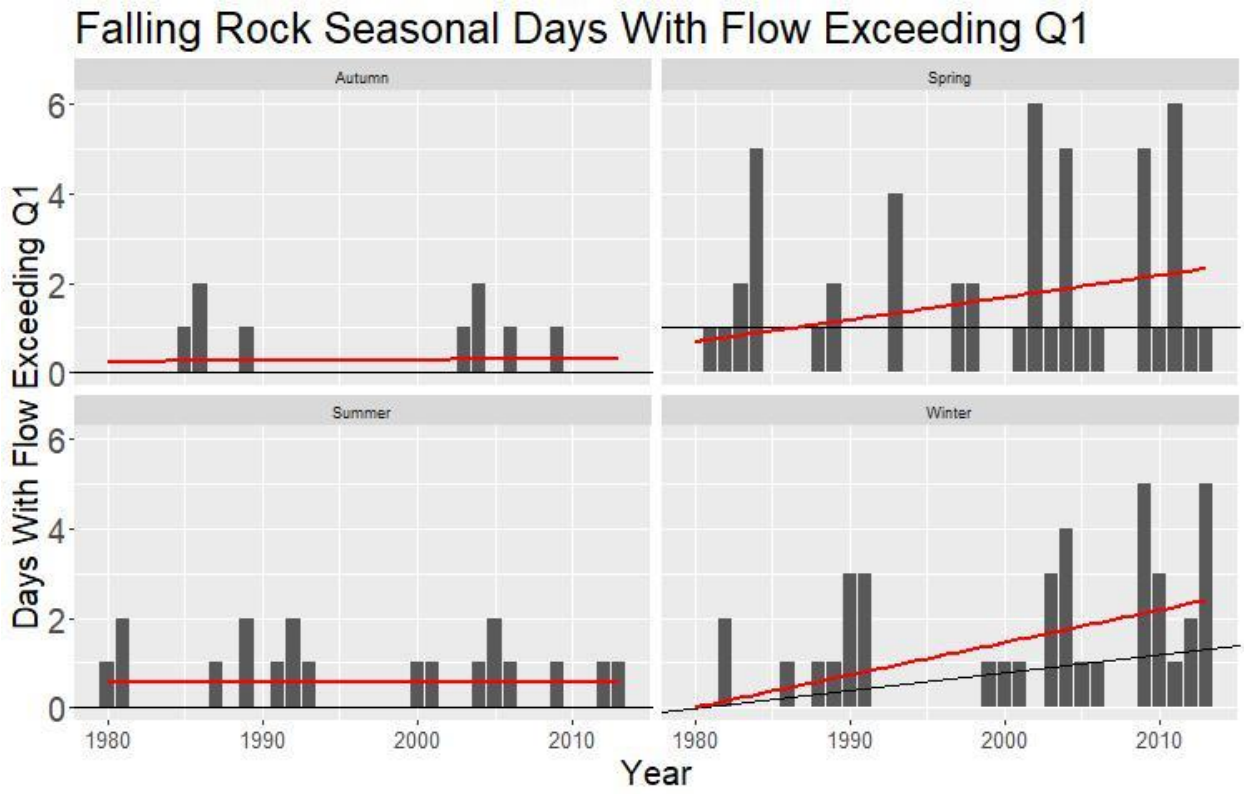

Figure S.24 Falling Rock seasonal days with flow greater than Q1 plots.

A bar graph of days with flow greater than Q1 for each year is plotted with the Sen's Slope trendline (black) and a linear fit trendline (red). There are no statistically significant trends at the seasonal scale.

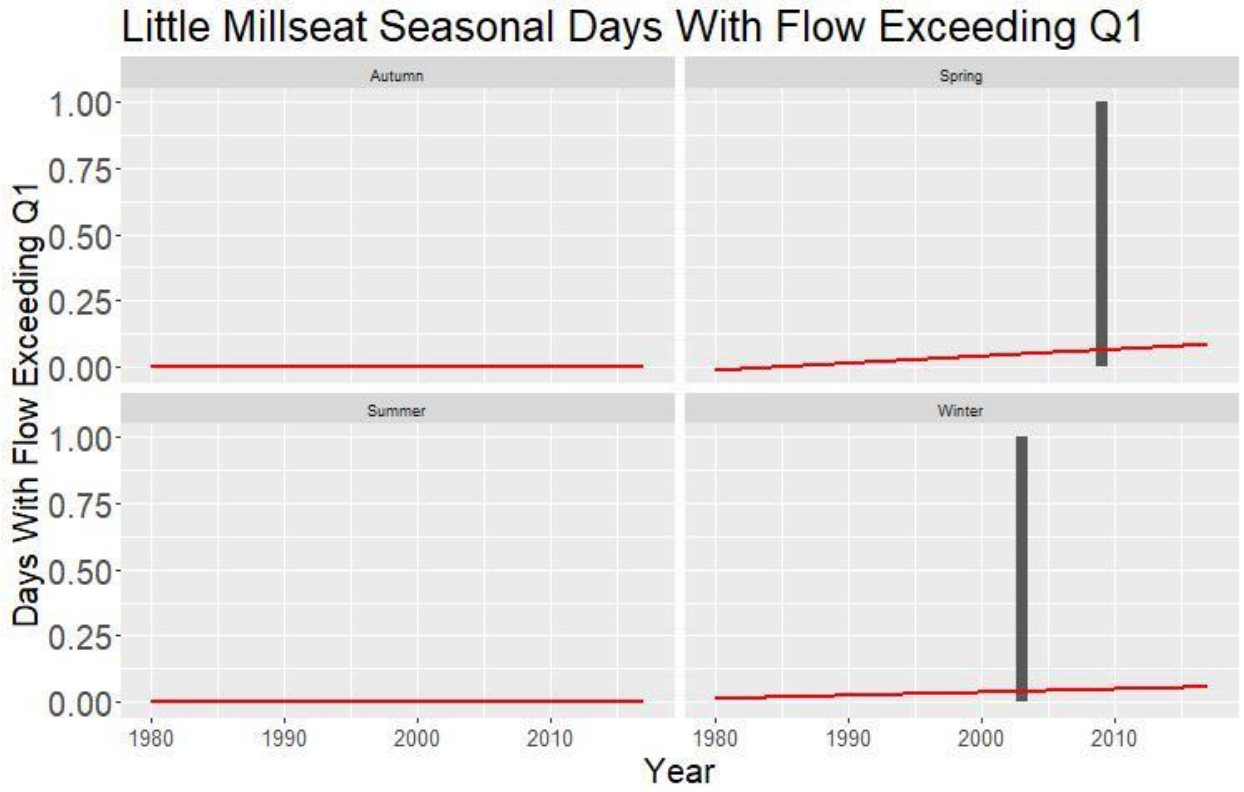

Figure S.25 Little Millseat seasonal days with flow greater than Q1 plots.

A bar graph of days with flow greater than Q1 for each year is plotted with the Sen's Slope trendline (black) and a linear fit trendline (red). There are no statistically significant trends at the seasonal scale.

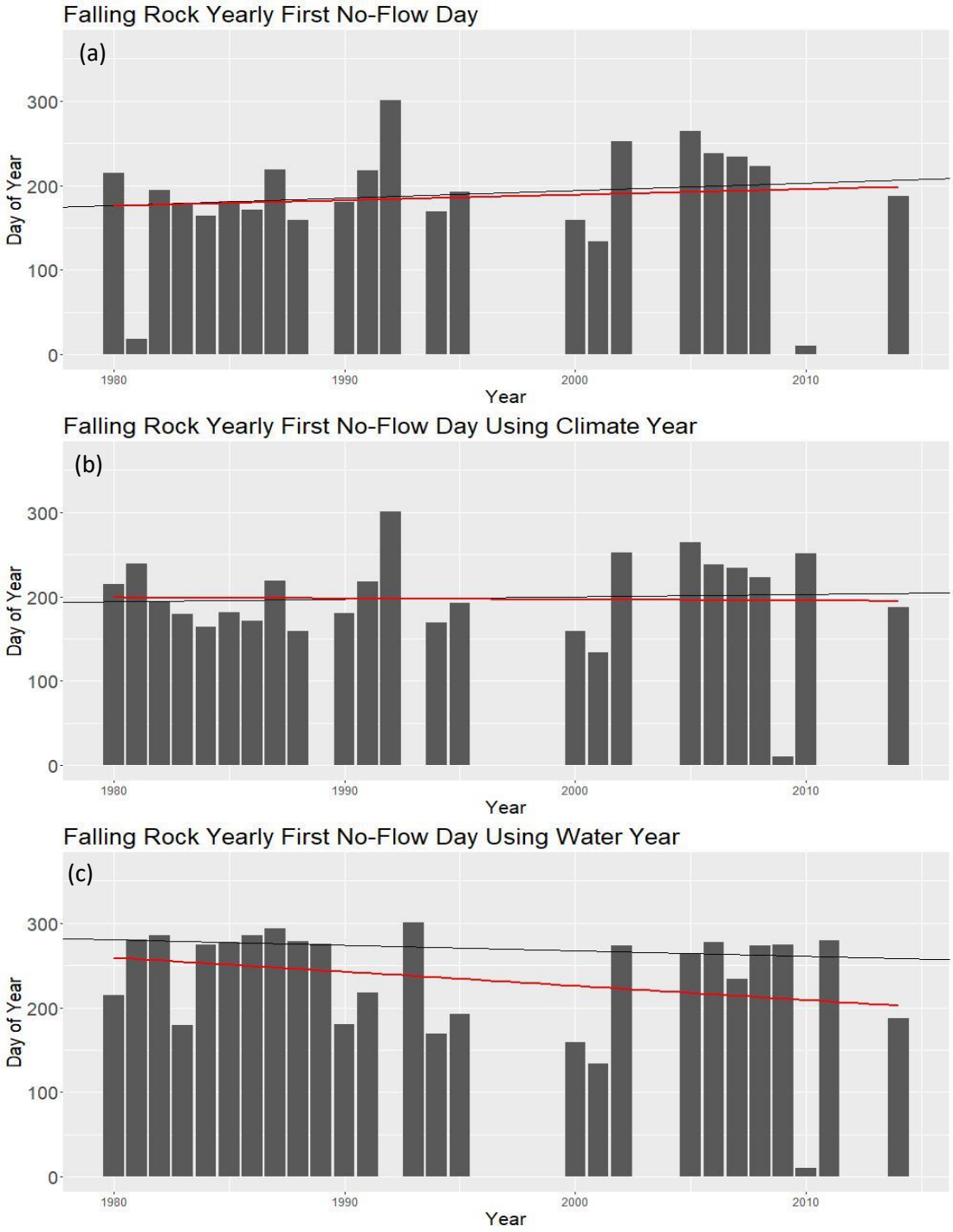

Figure S.26 Falling Rock timing of first no flow plots.

A bar graph denoting the first no flow day for each year is plotted with the Sen's Slope trendline (black) and a linear fit trendline (red). There are no statistically significant trends.

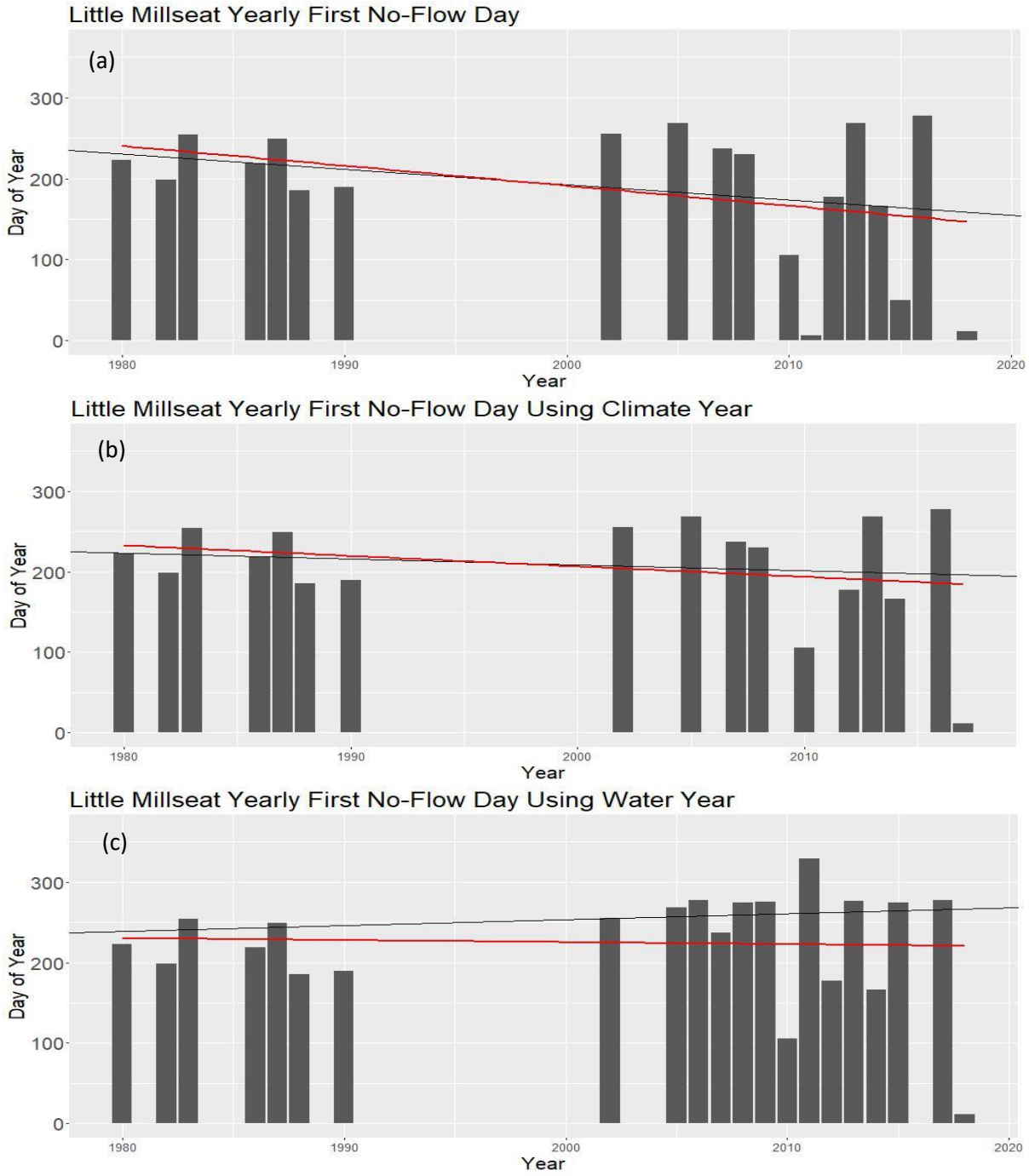

Figure S.27 Little Millseat timing of first no flow plots.

A bar graph denoting the first no flow day for each year is plotted with the Sen's Slope trendline (black) and a linear fit trendline (red). There are no statistically significant trends

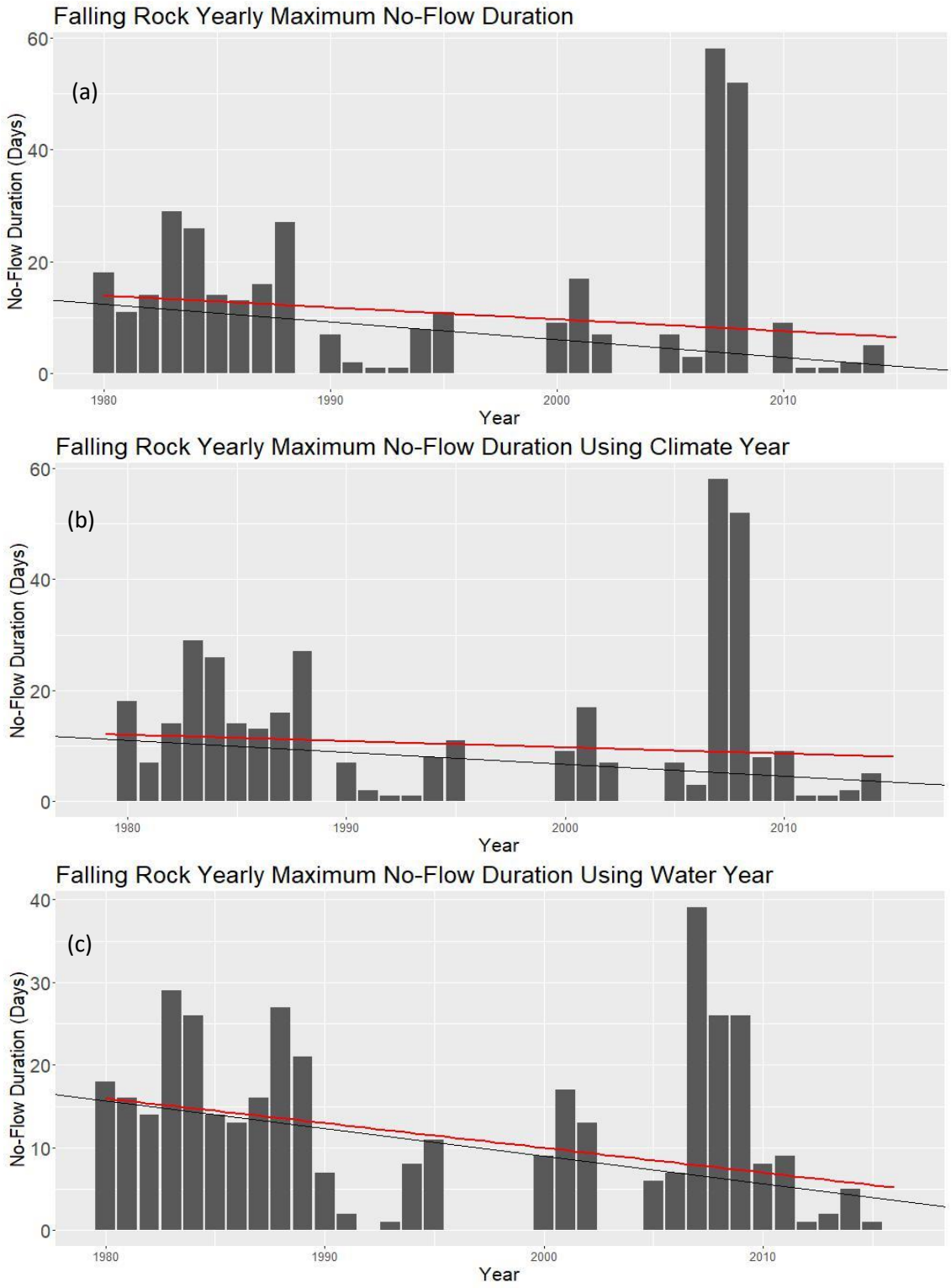

Figure S.28 Falling Rock maximum no flow duration.

A bar graph denoting the length of the longest no flow period for each year is plotted with the Sen's Slope trendline (black) and a linear fit trendline (red). There are statistically significant decreasing trends at the calendar year and water year scales.

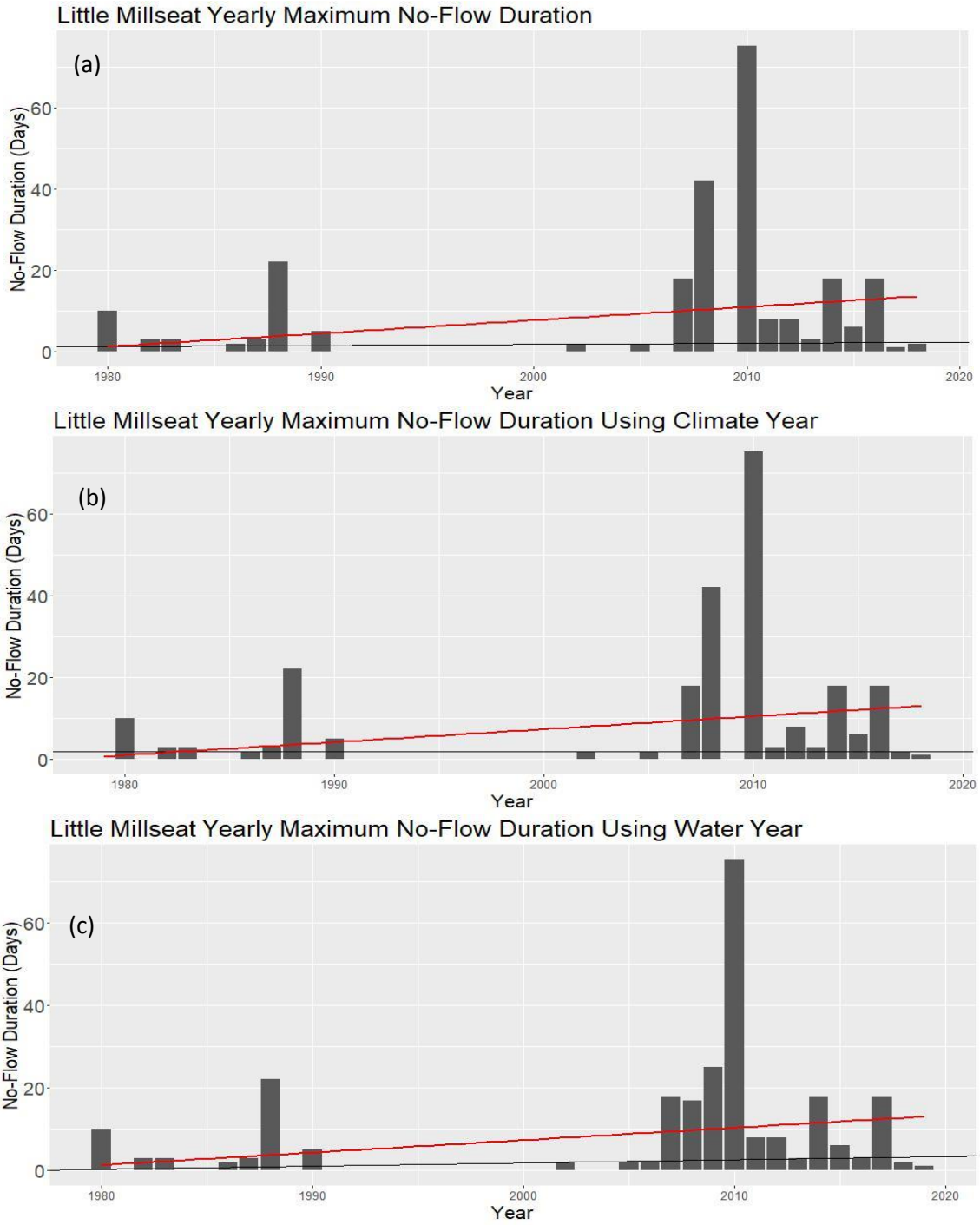

Figure S.29 Little Millseat maximum no flow duration.

A bar graph denoting the length of the longest no flow period for each year is plotted with the Sen's Slope trendline (black) and a linear fit trendline (red). There is a statistically significant positive trend at the water year scale.

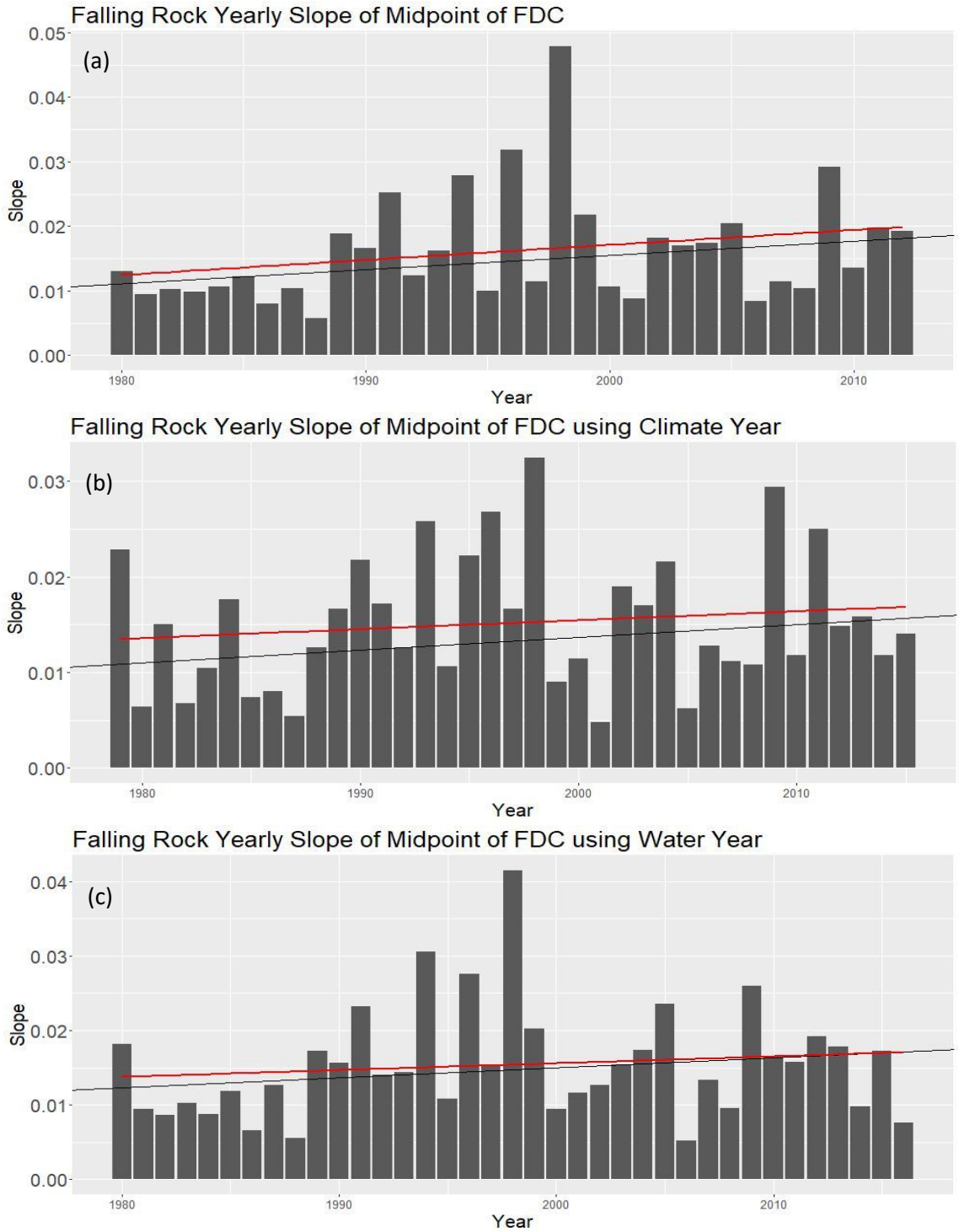

Figure S.30 Falling Rock slope of midpoint of FDC.

A bar graph denoting the slope of the flow duration curve for each year is plotted with the Sen's Slope trendline (black) and a linear fit trendline (red). There is a statistically significant positive trend at the calendar year scale.

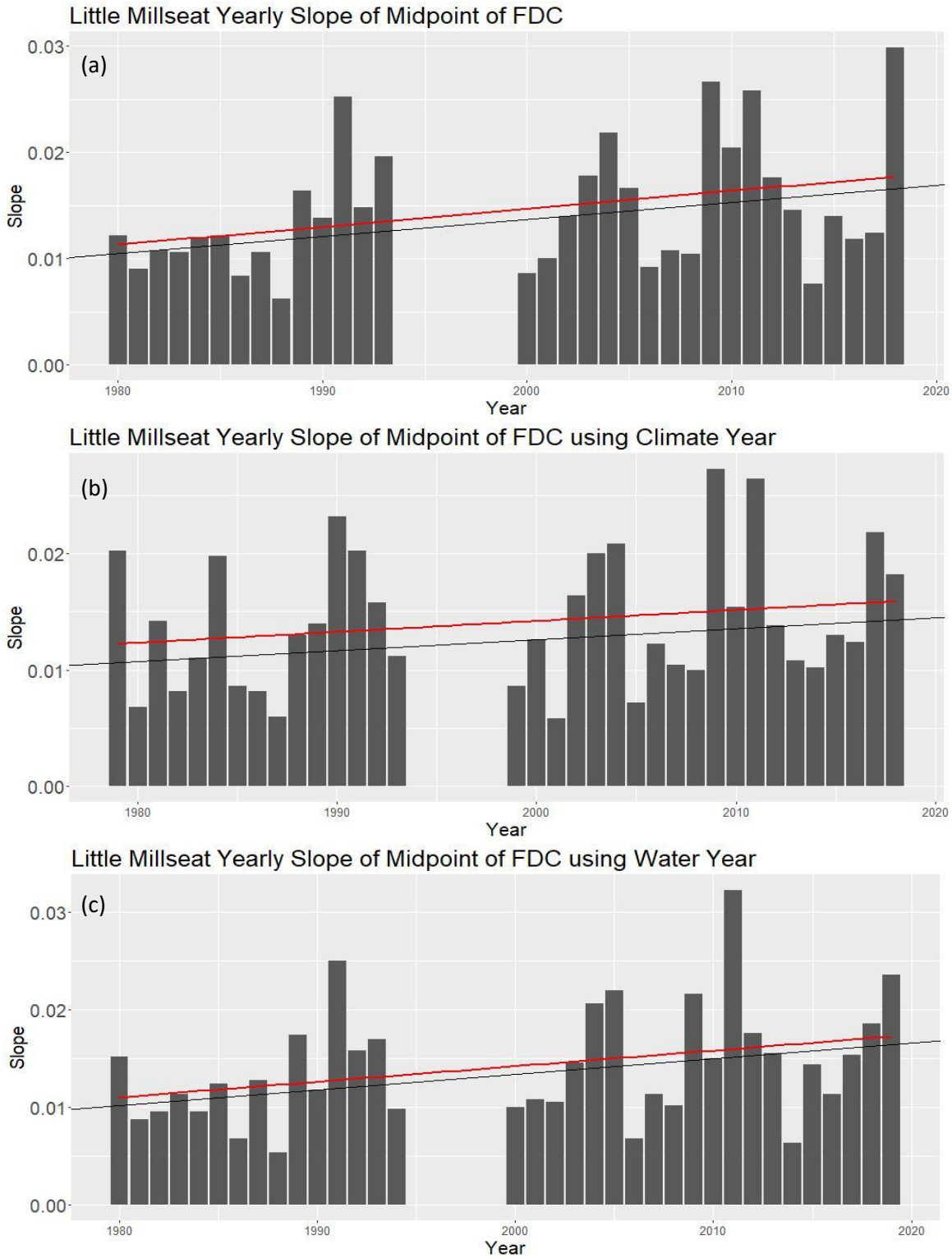

Figure S.31 Little Millseat slope of midpoint of FDC.

A bar graph denoting the slope of the flow duration curve for each year is plotted with the Sen's Slope trendline (black) and a linear fit trendline (red). There is a statistically significant positive trend at the calendar year and water year scales.

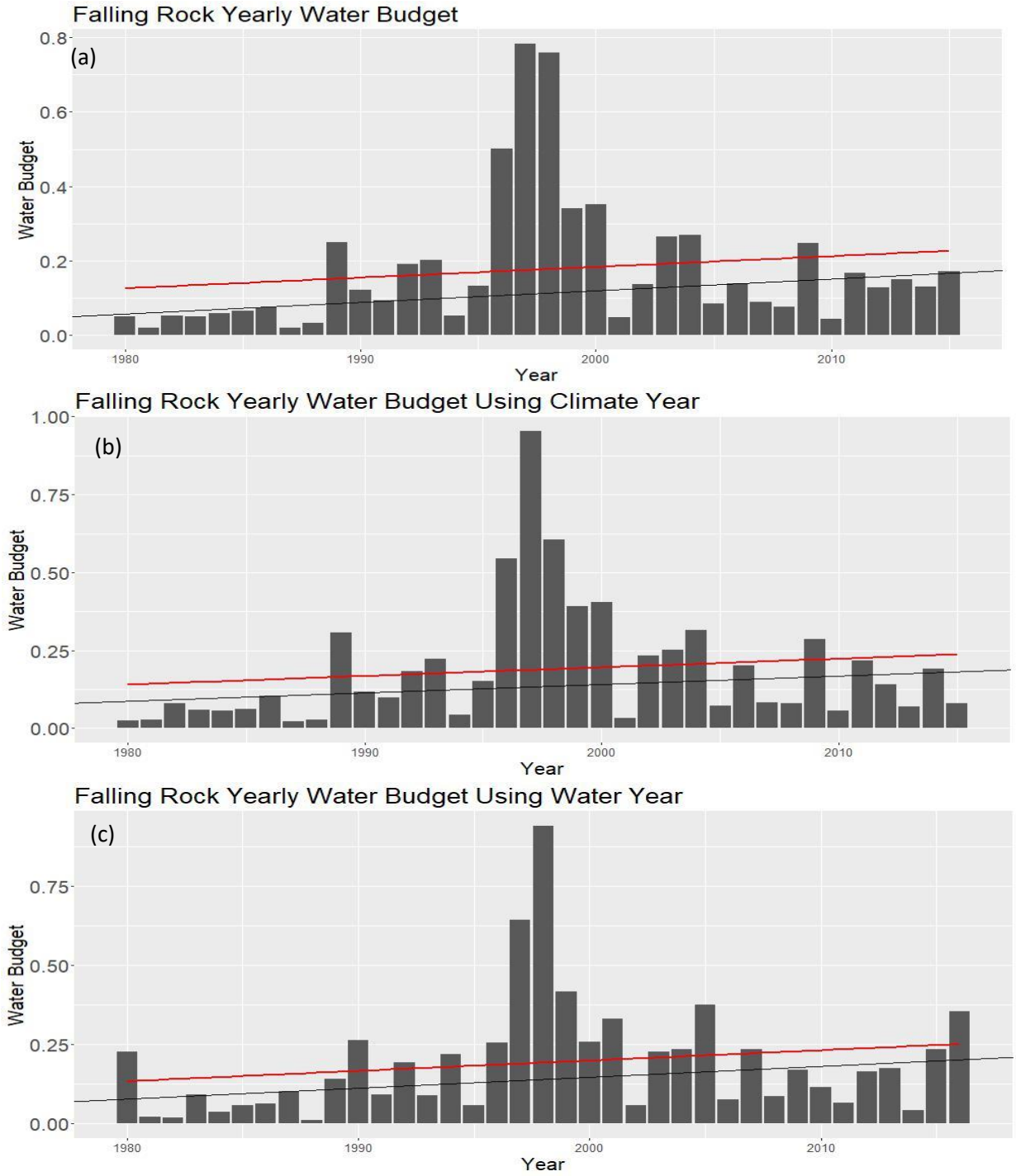

Figure S.32 Falling Rock Water Budget.

A bar graph denoting the water budget for each year is plotted with the Sen's slope trendline (black) and a linear fit trendline (red). There are statistically significant values at the yearly, seasonal, and monthly scales.

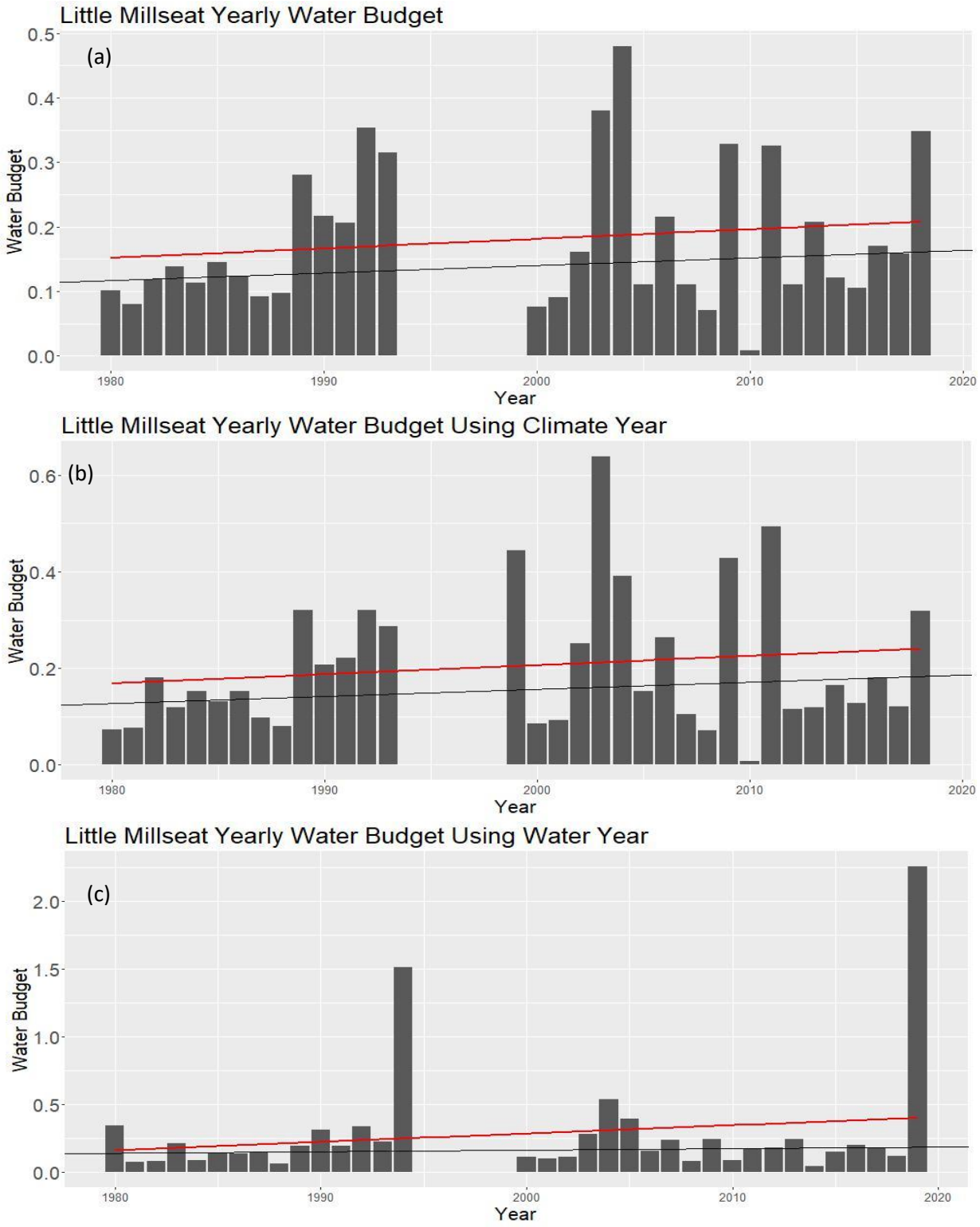

Figure S.33 Millseat Water Budget.

A bar graph denoting the water budget for each year is plotted with the Sen's Slope trendline (black) and a linear fit trendline (red). There are statistically significant trends in the winter and in the months January and April.